

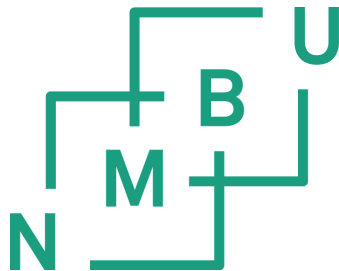
The novel A/J Min/+ mouse as a model for colorectal cancer, and the effects of hemin on intestinal tumorigenesis

Philosophiae Doctor (PhD) Thesis

Marianne Sødning

Department of Food Safety and Infection Biology
Faculty of Veterinary Medicine and Biosciences
Norwegian University of Life Sciences

Adamstuen 2016



Thesis number 2016:41
ISSN 1894-6402
ISBN 978-82-575-1970-4

© Marianne Sødning, 2016

Series of dissertation at the
Norwegian University of Life Sciences

Thesis number 2016: 41

ISSN 1894-6402

ISBN 978-82-575-1970-4

All rights reserved.

Printed in: Andvord Grafisk AS

Table of contents

ACKNOWLEDGEMENTS	I
ABBREVIATIONS	II
LIST OF PAPERS	III
SUMMARY	IV
SAMMENDRAG (SUMMARY IN NORWEGIAN)	VI
INTRODUCTION	1
COLORECTAL CANCER	1
Intestinal anatomy	1
Colorectal carcinogenesis.....	4
The canonical Wnt pathway and APC	7
Familial adenomatous polyposis (FAP)	8
Preneoplastic lesions	9
Flat ACF and MDF	10
ANIMAL MODELS FOR COLORECTAL CANCER	11
Murine models for Apc-driven tumorigenesis	12
The APC Min/+ mouse.....	12
Modifiers of Min.....	14
The A/J Min/+ mouse.....	15
DIET AND COLORECTAL CANCER	15
Red and processed meat	16
Animal studies on the link between meat and colorectal cancer	17
Potential mechanisms linking red meat and CRC	17
Heme iron and the N-nitroso pathway	18
AIMS OF THE STUDY	20
SUMMARY OF PAPERS	21
DISCUSSION	23
THE A/J MIN/+ MOUSE AS A MODEL FOR CRC	23
The importance of genetic background	24
Tumor progression and the importance of age.....	25

Colonic turnover.....	28
Spontaneous vs carcinogen-induced CRC in rodent models.....	29
A/J Min/+ mouse vs Pirr rat.....	29
Flat ACF as a reliable marker for CRC.....	30
USING THE A/J MIN/+ MOUSE MODEL TO TEST THE HEME-HYPOTHESIS	33
Fat in the experimental diet.....	34
Hemin and nitrite.....	35
Effect of hemin on tumor initiation.....	35
FUTURE PERSPECTIVES.....	37
MAIN CONCLUSIONS.....	39
REFERENCE LIST	40
SCIENTIFIC PAPERS I-III.....	52

Acknowledgements

This study was performed at the Department of Food Safety and Infection Biology (MatInf) at the Norwegian University of Life Sciences (NMBU) in the period 2011-2016, and the final year (2015-2016) was part of the project “Identification of the healthiest beef meat”. I would like to thank the former Head of Department, **Per Einar Granum**, as well as the current Head of Department, **Anne Storset**, and the Section for Food Safety for providing excellent working facilities during this PhD period.

I want to thank my main supervisor, **Jan Erik Paulsen**: This has been a long, and at times frustrating, journey, but your door has always been open. You are so passionate about what you do, and your enthusiasm for our research was both motivational and encouraging for me in times when I felt discouraged or overwhelmed. Your guidance has been an invaluable asset to me throughout the PhD project, and I have learned so much from you. Thank you for pushing me, but also for knowing when not to push!

I also want to thank my co-supervisor, **Gjermund Gunnes** for being there for all pathology related issues. Thank you for being available to help me whenever I needed it, your knowledge in this vast field has been of great help.

I want to thank my co-authors, and in particular **Björg Egeland**. Thank you for all you have done for me. I am very grateful for the faith you put in me. I also want to thank **Ellen Margrethe Hovland** for teaching me to become a better pop-science writer, and for ‘holding my hand’ when dealing with press-related things.

Thank you to the Section of Experimental Biomedicine for allowing me to use their facilities, and in particular **Christer** for helping with the mice. Thank you to **Mari** and **Sigbjørn** at the histology lab for making my Swiss rolls a little prettier!

To all my colleagues at MatInf, thank you for the friendly work environment, and for all the laughter and good conversations. Thanks to my ‘roommate’ **Christina**, for all our research and non-research talks. And to **Hildegunn**: thanks (or maybe not?) for teaching me to drink coffee, and, when my newfound addiction was cemented, for always being ready to go to “Kaffekoppen” at a moment’s notice. And thanks for all the silliness (lol); I definitely needed that on more than one occasion!

Thank you, **Mom** and **Dad**, for always being there for me, no matter what! Thank you to my family for all their support over the past years. To my closest friends, who understood that I couldn’t always be there, but who made me smile when I did see them – thank you!

And, last but not least, to **Roger**: thank you, älskling, for being you, for always having my back, for being a shoulder to cry on, and for letting me pick your brain. I love you!

Oslo, April 2016.

Abbreviations

ACF	Aberrant crypt foci
AOM	Azoxymethane
APC	Adenomatous polyposis coli
B6	C57BL/6J
CIMP	CpG island methylator phenotype
CIN	Chromosomal instability
CpG	Cytosine-phosphate-guanine
CRC	Colorectal cancer
CTNNB1	Catenin beta 1
DKK	Dickkopf
DMH	1,2-dimethylhydrazine
DSS	Dextran sulfate sodium
ENU	Ethylnitrosourea
FAP	Familial adenomatous polyposis
GSK3 β	Glycogen synthase kinase 3 β
HID-AB	High iron diamine - Alcian blue
HNPCC	Hereditary non-polyposis colorectal cancer
IARC	International Agency for Research on Cancer
KAD	Kyoto Apc Delta
KRAS	Kirsten rat sarcoma viral oncogene homolog
LOH	Loss of heterozygosity
MB	Methylene blue
MDF	Mucin depleted foci
Min	Multiple intestinal neoplasia
Mom	Modifier of Min
MSI	Microsatellite instability
NOC	N-nitroso compounds
Pirc	Polyposis in the rat colon
Tp53	Tumor protein p53
WCRF	World Cancer Research Fund
Wnt	Wingless integration 1

List of papers

Paper I

Sodring M, Gunnes G, Paulsen JE. Spontaneous initiation, promotion, and progression of colorectal cancer in the novel A/J Min/+ mouse.

International Journal of Cancer. 2016. 138(8):1936-1946.

Paper II

Sodring M, Gunnes G, Paulsen JE. Detection and characterization of the flat aberrant crypt foci (flat ACF) in the novel A/J Min/+ mouse.

Submitted manuscript*

Paper III

Sodring M, Oostindjer M, Egelandstal B, Paulsen JE. Effects of hemin and nitrite on intestinal tumorigenesis in the A/J Min/+ mouse model.

PLOS ONE 2015. 10(4): e0122880.

* Accepted May 4th 2016: Anticancer Research, June 2016. 36(6): 2745-2750

Summary

Colorectal cancer (CRC) is one of the most common cancers worldwide. Most cases of CRC appear to be caused by somatic mutations, but a small number of cases are the result of germline mutations in the tumor-suppressor gene adenomatous polyposis coli (*APC*) which causes an inherited condition called familial adenomatous polyposis (FAP). FAP manifests as hundreds to thousands of adenomas in the colon, and if left untreated, the patient has a 100% risk of developing CRC. The multiple intestinal neoplasia (Min/+) mouse, traditionally bred on a C57BL/6J (B6) genetic background, is one of the most widely used murine models for human FAP, and the mutation in the murine *Apc* gene replicates the fundamental mutational event seen in both FAP and sporadic CRC. The use of animal models to study CRC provides valuable information for diagnosis, treatment, and prevention of the human disease.

In this project we characterized the intestinal tumorigenesis in a novel mouse model where the Min/+ trait has previously been introgressed onto an A/J genetic background, creating an A/J Min/+ mouse. This novel A/J Min/+ mouse spontaneously develops a substantial number of colonic lesions, and although small intestinal tumors also develops, the ratio of colonic to small intestinal lesions in the A/J Min/+ mouse is 1.1:1, which is close to the ratio observed in human FAP (>1:1). The B6 Min/+ mouse, on the other hand, primarily develops adenomas in the small intestine and hardly any lesions in the colon, and has a colonic to small intestinal lesions ratio of <1:40. Small preneoplastic lesions, called flat aberrant crypt foci (flat ACF), are easily identified in the unsectioned, methylene blue stained colon of A/J Min/+ mice. Surface microscopy and histological sectioning of flat ACF show severe dysplasia already from the monocryptal stage, and these early colonic lesions possess genotypic and phenotypic characteristics similar to that of colonic tumors. When flat ACF were compared to mucin depleted foci (MDF), colonic lesions characterized by defective mucin production, a virtually complete overlap was found. This suggests that flat ACF and MDF likely represent the same preneoplastic lesion, which in turn indicates that flat ACF, like MDF, are reliable surface biomarkers of colorectal carcinogenesis. A large number of flat ACF spontaneously develop in the A/J Min/+ mouse, and these early colonic lesions will, with time, progress to carcinomas. In contrast, the fraction of tumors that progress to invasive carcinomas in the B6 Min/+ mouse, is miniscule. This is likely attributable to the short lifespan of the B6 Min/+ mouse. In the A/J Min/+ mouse, age-associated processes

appear to be important for the progression of tumors to malignancy; at 40 weeks old, 21% of colonic tumors recorded in A/J Min/+ mice were categorized as carcinomas. Furthermore, the A/J Min/+ mouse has the potential for, at least, local metastasis. These findings more closely reflect aspects of human colorectal carcinogenesis, suggesting that the novel A/J Min/+ mouse is a reliable model for human CRC.

Red and processed meat has been associated with an increased risk of CRC; however, the underlying mechanism behind this link remains uncertain. One hypothesis that has received ample attention concerns the effect of heme iron in red meat. When testing the effect of diet or dietary components on colorectal cancer development, choosing a model that is as relevant as possible for the human disease, is important. Since the A/J Min/+ mouse model more closely mirrors the human CRC phenotype than, for instance, the B6 Min/+ mouse, the A/J Min/+ mouse model was used to test the heme iron hypothesis. Mice fed diets containing hemin (a model for red meat) and hemin in combination with nitrite (a model for red, processed meat), were examined for intestinal lesions to assess the potential effect of heme on colorectal tumorigenesis. The results showed that, in contrast to what was expected, dietary hemin decreased the number of colonic lesions in the A/J Min/+ mouse, whether in combination with nitrite or not. However, the results also showed that the opposite was true in the small intestine, where dietary hemin seemed to stimulate tumor growth. Additionally, nitrite, which did not have an effect in the colon, appeared to have a suppressive effect on tumor growth in the small intestine.

Sammendrag (Summary in Norwegian)

Tykkttarmskreft er en av de mest vanlige kreftformene på verdensbasis. De fleste tilfeller av tykkttarmskreft er mest sannsynlig forårsaket av somatiske mutasjoner i kroppscellene, men et lite antall oppstår som følge av nedarvede mutasjoner i tumorsuppressorgenet adenomatøs polyposis coli (*APC*). Dette fører til familiær adenomatøs polypose (FAP), en form for arvelig tykkttarmskreft hvor pasienten utvikler et stort antall polypper i tykkttarmen. Om sykdommen ikke behandles øker sjansen for å utvikle tykkttarmskreft til 100%. Den mest brukte musemodellen for FAP er multipel intestinal neoplasia (*Min/+*) musen, som tradisjonelt avles på en C57BL/6J (B6) genetisk bakgrunn. *Min/+* mus har også en nedarvet mutasjon i *Apc* som motsvarer mutasjonen i *APC* genet hos mennesker. Bruken av dyremodeller for å studere tykkttarmskreft gir verdifull informasjon med tanke på diagnose, behandling, og forebygging av denne sykdommen hos mennesker.

I dette prosjektet har vi karakterisert kreftutviklingen i *A/J Min/+* mus, en ny musemodell hvor *Min*-genet har blitt overført til mus med en *A/J* genetisk bakgrunn. Denne nye *A/J Min/+* musen utvikler spontant et betydelig antall tykkttarmslesjoner. Når lesjoner av alle størrelser er medregnet, har *A/J Min/+* musen et gjennomsnittlig antall tykkttarm- til tynntarmslesjoner i forholdet 1,1:1. Selv om *A/J Min/+* musen ikke utvikler svulster utelukkende i tykkttarmen, men også viser en lignende tumorbelastning i tynntarmen, er likefremt forholdet mellom tykk- og tynntarmslesjoner nærmere forholdet observert i humant FAP (større enn 1:1). I motsetning til *A/J Min/+* musen, utvikler B6 *Min/+* musen hovedsakelig svulster i tynntarmen og svært få lesjoner i tykkttarmen, og forholdet mellom tykk- og tynntarmslesjoner er mindre enn 1:40. Små, preneoplastiske tykkttarmslesjoner, som kalles flate aberrant crypt foci (flat ACF), kan lett identifiseres i *A/J Min/+* musens tykkttarmer etter farging med metylenblått. Overflatemikroskopering og histologisk undersøkelse av flate ACF viser grov dysplasi allerede fra første krypt. Disse tidlige lesjonene har både genotypiske og fenotypiske egenskaper som også er karakteristiske for tykkttarmssvulster. Ved sammenligning av flate ACF med mucin depleted foci (MDF), en annen tykkttarmslesjon som kjennetegnes av defekt slimproduksjon, fant vi en praktisk talt fullstendig overlapp mellom lesjonene. Dette tyder på at flate ACF og MDF sannsynligvis representerer samme preneoplastiske lesjon, noe som igjen antyder at flate ACF, slik som MDF, kan anses som pålitelige overflatemarkører for kreftutvikling i tykkttarmen. Et stort antall flate ACF utvikles spontant i tykkttarmen på *A/J Min/+* mus. Disse preneoplastiske

lesjonene vil, med tid, utvikle seg videre til karsinomer. B6 Min/+ mus utvikler sjeldent karsinomer, noe som trolig skyldes den relativt korte levetiden disse musene har. A/J Min/+ mus lever betydelig lenger, noe som sannsynligvis øker sjansen for at adenomene rekker å utvikle seg til karsinomer. Prosesser knyttet til alder syntes å være viktig for at progresjonen av adenomene til karsinomer skal finne sted: ved 40 uker var 21% av alle tykktarmssvulster i A/J Min/+ musen, karsinomer. Det viser seg også at A/J Min/+ musen har potensiale for, i det minste, lokal metastase. Sett i sammenheng gjenspeiler dette human kreftutvikling mer nøyaktig, noe som tyder på at den nye A/J Min/+ musen er en velegnet modell for human tykktarmskreft.

Inntak av rødt og bearbeidet kjøtt har vært forbundet med økt risiko for å utvikle tykktarmskreft; men det er fortsatt uklart hvordan dette henger sammen. En hypotese som har fått mye oppmerksomhet er at hemjernet i rødt kjøtt er årsaken til risikøkningen. Når man tester effekten av kosthold eller kostholdsfaktorer på tykktarmskreftutvikling, er det viktig å velge en modell som i størst mulig grad reflekterer human tykktarmskreft. Siden A/J Min/+ musen mer nøyaktig gjenspeiler kreftutvikling hos mennesker, ble denne modellen brukt for å teste hemjern hypotesen. A/J Min/+ mus ble matet med fôr tilsatt hemin (modell for rødt kjøtt) eller hemin og nitritt (modell for bearbeidet kjøtt), før tarmene ble undersøkt for potensielle effekter av hemjern på tykktarmskreftutvikling. I motsetning til forventet, viste resultatene at hemin, både med og uten nitritt, reduserte antall lesjoner i tykktarmen hos A/J Min/+ mus. Resultatene viste også at det motsatte var tilfelle i tynntarmen, hvor hemin syntes å stimulere svulstvekst. I tillegg fant vi at nitritt, som ikke hadde noen effekt i tykktarmen, så ut til å ha en hemmende effekt på svulstvekst i tynntarmen.

Introduction

Colorectal cancer

Colorectal cancer (CRC) is one of the most common cancers both worldwide and in Norway. Globally, this form of cancer accounted for approximately 1.4 million new cases and close to 700 000 deaths in 2012, while the latest numbers from Norway show that over 4000 new cases and approximately 1500 deaths were attributed to CRC in 2014 [1,2].

Worldwide, CRC is the second most common cancer after breast cancer in women, whereas it is the third most common cancer in males, after prostate and lung cancer. This mirrors the CRC status in Norway. More than half of all CRC cases are registered in developed regions of the world, with the highest rates observed in Australia/New Zealand, Western Europe, and North America. In contrast, this type of cancer appears to be relatively uncommon in less developed regions including South-Central Asia, and most of Africa. Incidence rates are higher in men than in women, and CRC becomes progressively more common with age [1,2].

CRC can be divided into two types; sporadic and hereditary. Sporadic CRC accounts for approximately 80% of all CRC cases, while the remaining 20% of patients have a family history of CRC. Of all CRC cases, only around 5% are due to inherited genetic mutations, with Hereditary Non-Polyposis Colorectal Cancer (HNPCC, or Lynch syndrome) and Familial Adenomatous Polyposis (FAP) being the two most common forms of hereditary CRC. These two disorders differ, as the names suggest, by the absence (HNPCC) or presence (FAP) of colorectal polyposis [3,4]. In FAP, the tumor initiation rate is accelerated while tumor progression is normal. In HNPCC, this is reversed: tumor initiation rates are nearly normal while tumor progression is accelerated. However, both FAP and HNPCC patients develop CRC at a median age of 42 years [5].

Intestinal anatomy

The human and mouse intestines are relatively similar in structure. The small intestine of both species consists of the duodenum, jejunum, and the ileum, the latter of which enters the cecum at the ileocecal valve. Cecum size differs between mice and humans in that mice have a relatively large cecum whereas the human cecum is small. Also, mice lack an appendix which is present in humans. For both species, the luminal surface of the small

intestine contains villi, small finger-like protrusions extending from the mucosa, that increase the surface area of the intestinal mucosa [6]. The colon of mice and humans is also fairly similar (Fig. 1). However, the human large intestine has a segmented appearance that the murine colon lacks. This appearance is due to taenia coli, three long ribbons of smooth muscle on the outside of the colon, that are slightly shorter than the colon itself, causing the colon to be divided into a series of saclike segments called haustra [7].

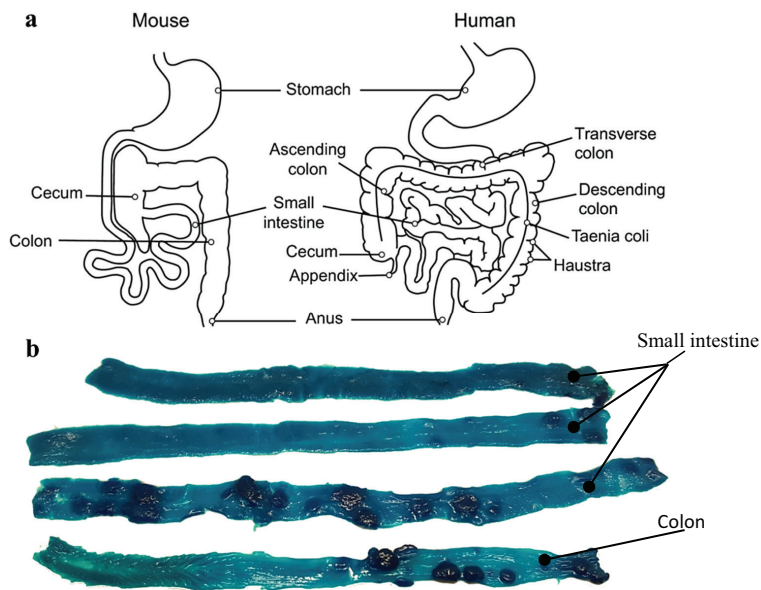


Figure 1. Anatomy of the mouse and human intestine. (a) The human colon is divided into ascending, transverse, and descending sections, and has saclike segments called haustra due to the presence of taenia coli.¹ (b) A representative example of intestinal tumor growth in the A/J Min/+ mouse. The methylene blue stained intestine has been divided into four parts: The top three pieces show the small intestine (the stomach has been removed from the upper right end), while the bottom piece is the colon. Nearly all the dark blue spots are tumors, but a few may be gut associated lymphoid aggregates (GALT). This intestine was harvested from a 43-week old mouse. Photo b: M. Sødning.

The intestinal tract is made up of three tissue layers: an outer layer of smooth muscle which controls peristalsis, a middle layer of stromal tissue called the submucosa, and an inner layer surrounding the lumen which is called the mucosa [8]. The mucosa is divided into three

¹ From “How informative is the mouse for human gut microbiota research?” by T. Nguyen, S. Vieira-Silva, A. Liston, and J. Raes. 2015, *Disease models & mechanisms*, 8 (1), pg 3. Reprinted with permission under the Creative Commons Attribution License

additional layers, where the epithelial layer is the innermost layer closest to the intestinal lumen. Below the epithelial layer lies the lamina propria, a layer of stromal connective tissue, and finally, separating the mucosa from the submucosa, lies a thin layer of smooth muscle called the muscularis mucosa [9].

The mucosa of the small intestine is made up of villi, protrusions into the lumen, and crypts of Lieberkühn, invaginations into the epithelial lining at the base of the villi (Fig. 2a). The colon does not have villi, only crypts (Fig. 2b). Paneth cells, which secrete antimicrobial substances, are only found in the small intestine of mice, and then most often localized to the jejunal section. These cells are not found in the murine colon, while in the human intestinal tract, Paneth cells are found in the small intestine, appendix, and in the caecum [6]. Stem cells are found at the bottom of the colonic crypt, while they are found a little further up the small intestinal crypts, right above the Paneth cells. Stem cells are undifferentiated cells that can continually self-renew as well as produce proliferating progenitor cells which in turn become differentiated cells including endocrine cells, goblet cells, Paneth cells or epithelial cells. In the small intestine, these differentiated cells make up the villi, while in the colon, they reside at the uppermost section of the colonic crypt, as well as on the epithelial surface. Progenitor cells reside between stem cells and differentiated cells, and are slightly more specific than a stem cell, but less so than a differentiated cell. A progenitor cell can differentiate into one or more types of cells, but unlike the stem cell, they only have a limited ability to self-renew [8,10]. The human colonic epithelium renews at least once per week, which is similar in the mouse, where colonic epithelial turnover occurs every 5 to 7 days [11].

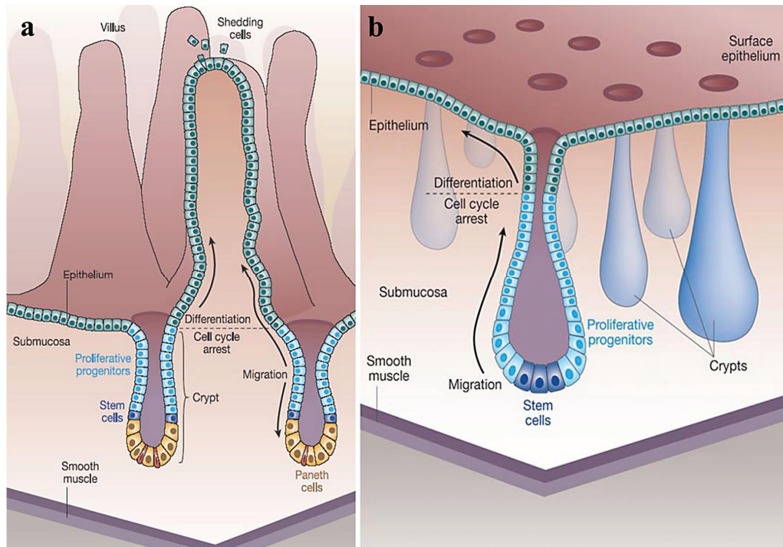


Figure 2. Anatomy of the small intestine (a) and the colon (b). In the small intestine, stem cells (dark blue) are found near the bottom of the crypt, immediately above the Paneth cells (yellow), while in the colon, stem cells reside at the bottom of the crypt. Proliferating progenitor cells (light blue) in the small intestine fill up the remained of the crypt up to the epithelial surface, while in the colon, these cells rise about two thirds up the crypt. The rest of the colonic crypt and the epithelial layer are occupied by differentiated cells (green). In the small intestine, differentiated cells make up the villi.²

Colorectal carcinogenesis

Colorectal cancer develops as a result of several genetic and epigenetic changes that cause a transformation of intestinal epithelium from normal tissue, via benign neoplasms, into colorectal carcinomas. This transformation is the result of activation of oncogenes and inactivation of tumor suppressor genes, in a process known as the adenoma-carcinoma sequence (Fig. 3) [5,12,13]. This is a fundamental concept in CRC, and describes the step-by-step progression from normal epithelium to carcinoma [5]. Mutations in *APC* is considered to be the rate-limiting step in the tumorigenesis of both FAP and most sporadic CRCs, where inactivation of the *APC* tumor suppressor gene initiates neoplasia [14]. Mutations in the oncogene *KRAS* (Kirsten rat sarcoma viral oncogene homolog) promotes growth of early adenomas, while progression to malignant carcinoma is accompanied by loss of all, or part of, the long arm of chromosome 18 (18q), where *DCC* (Deleted in

² From “Wnt signalling in stem cells and cancer” by T. Reya and H. Clevers. 2005. *Nature*. 434 (7035), pgs. 844 and 846. Copyright 2005 Nature Publishing Group. Reprinted with permission.

colorectal cancer), *SMAD2* (Mothers against decapentaplegic homolog 2) and *SMAD4* tumor suppressor genes reside, as well as loss of all, or part of, the short arm of chromosome 17 (17p), where the *TP53* tumor suppressor gene is located [15]. This process from adenoma to carcinoma is a very slow process, and in humans it may take 5-20 years for early lesions to progress to benign adenomas, and yet another 5-15 years before those adenomas become malignant carcinomas [16,17].

There are three distinct pathways by which colorectal carcinogenesis most often is explained; CpG island methylator phenotype (CIMP), chromosomal instability (CIN), and microsatellite instability (MSI or MIN) (Fig. 3). These three pathways are not mutually exclusive, therefore, CRC's may exhibit traits of more than one pathway [18]. The CIMP pathway, also called the serrated pathway due to the serrated appearance of lesions, is considered to be an epigenetic pathway. In this pathway, tumor suppressor genes are silenced by hypermethylation of CpG islands in the promoter region, rather than being caused by mutations. Hypermethylation of *MLH1*, a DNA mismatch repair gene, often occurs in the CIMP pathway, and may lead to microsatellite instability similar to that seen in the MSI pathway [19–21]. The majority of sporadic and FAP colorectal cancers develop through the CIN pathway, a pathway characterized by instability in chromosomal numbers (aneuploidy), or loss of heterozygosity (LOH). The CIN pathway is also called the gatekeeper pathway. Gatekeeper genes, most often tumor suppressor genes, regulate tumor growth directly by either inhibiting growth of the tumor, or by promoting cell death, both of which prevents further tumor development. When a gatekeeper gene is inactivated, for instance due to mutations, tumor growth is no longer controlled, and cancer develops. In CRC, the tumor suppressor gene adenomatous polyposis coli (*APC*) is an example of a gatekeeper gene [5,21]. The MSI pathway accounts for approximately 10-15% of all sporadic CRC cases, as well as most HNPCC cases. This pathway is characterized by nucleotide instability, and is known as the caretaker pathway. Caretaker genes regulate tumorigenesis indirectly by maintaining the integrity of the genome by effectively repairing DNA. When caretaker genes lose their function, the rate of DNA mutations increase, which in turn increases the chance of mutations, and loss of gatekeeper functions [22]. In CRC, mismatch repair (MMR) genes are considered caretakers.

In 1998, Kinzler and Vogelstein [23] added yet another type of genes they called landscaper genes. These genes were associated with the CRC form known as juvenile polyposis syndrome where the first lesions develop in stromal cells rather than in the epithelial cells

that give rise to the tumor. Landscaper genes affect the microenvironment around the lesion, and if they lose their function, abnormal growth or function of the surrounding microenvironment may follow. This, in turn, may lead to neoplasia in neighboring epithelial cells [22,23].

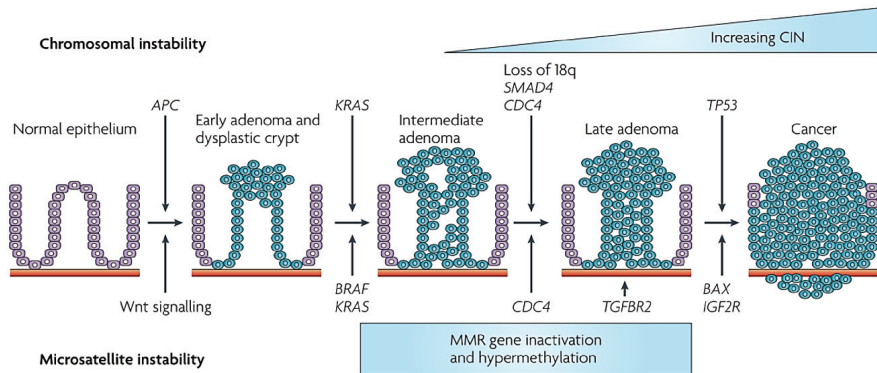


Figure 3. Adenoma-carcinoma sequence for colorectal cancer, and simplified illustration of genetic and epigenetic changes in the three pathways of colorectal carcinogenesis. The Chromosomal instability (CIN) pathway, also known as the gatekeeper pathway, is driven by inactivation of tumor suppressor genes (initiated by loss of APC) and activation of oncogenes, and is characterized by aneuploidy or loss of heterozygosity. The microsatellite instability (MSI) pathway, also known as the caretaker pathway, is driven by instabilities at the nucleotide level due to abnormalities in mismatch repair (MMR) genes. The initial step in the MSI pathway is thought to involve Wnt signaling changes (maybe mutations in the axin gene). The CpG island methylator phenotype (CIMP) pathway is an epigenetic pathway where tumor suppressor genes are silenced by hypermethylation of CpG islands in the promoter region.³

Although most CRC cases appear to be due to somatic mutations (sporadic CRC), some cases are caused by germline mutations (hereditary CRC). There are various hereditary forms of CRC including MYH-associated polyposis (MAP), juvenile polyposis syndrome (JPS), Peutz–Jeghers syndrome (PJS), and Cowden disease. However, the two most common inherited colorectal cancer syndromes are HNPCC, caused by germline mutations in DNA mismatch repair genes, and FAP, caused by germline mutations in the *APC* tumor

³ From “Genetic prognostic and predictive markers in colorectal cancer” by A. Walther, E. Johnstone, C. Swanton, R. Midgley, I. Tomlinson, and D. Kerr. 2009. *Nature reviews Cancer*. 9 (7) pg 491. Copyright 2009 Nature Publishing Group. Reprinted with permission.

suppressor gene. Inactivation of *APC* is the earliest known mutagenic event in the development of colorectal cancer [4,5].

The canonical Wnt pathway and APC

In the classical view of Wnt signaling, three independent pathways are identified: one canonical β -catenin-dependent and two non-canonical β -catenin-independent pathways [24]. In humans and mice, there are 19 Wnt genes which code for cysteine-rich glycoproteins that act as ligands to activate the Wnt signaling pathways [25–27]. Wnt pathways are involved in embryogenesis and the regulation of homeostasis in adult tissue. The intestinal epithelial cells are constantly being renewed, and Wnt signals play an important role in maintaining homeostasis in the intestinal epithelium by balancing cell proliferation, cell migration, cell differentiation, and cell death. An upset of this balance can disrupt normal homeostasis, and in turn lead to tumor development [28].

The tumor suppressor gene *APC* is located at chromosome region 5q21, and a deletion of this section leads to FAP. *APC* encodes a 312 kDa large, 2843-amino acid long, protein that plays an important role in the canonical Wnt signaling pathway (Fig. 4). In this Wnt pathway, the APC protein is a key component of the APC/Axin/CK1/GSK3 β / β -catenin destruction complex, the main function of which is to phosphorylate, and in turn ubiquitinate and degrade, β -catenin [14]. When mutational inactivation of *APC* occurs, this destruction complex cannot be assembled, and consequently, β -catenin will not be degraded. Instead, β -catenin accumulates in the cytoplasm and eventually translocates into the nucleus, where it complexes with lymphoid enhancing factor/ T-cell factor (LEF/TCF) transcription factors to activate the transcription of specific genes associated with dysplasia [26,28,29]. Although very little is known about the location of the Wnt signals in the intestine, during mouse embryogenesis, Wnt gene products are expressed all through the intestines [30]. In human colonic tissue from healthy adults, expression of Wnt ligands are still present, however, their particular location in the colon is still unclear [31]. The Wnt signal is thought to be present at the bottom third of the crypt, where the progenitor cells reside. These cells accumulate β -catenin, which in turn activates target genes. How the Wnt pathway is turned off is not completely clear, but it has been suggested that as the progenitor cells move up the crypt away from the source of the Wnt signals, the signal becomes gradually weaker, β -catenin gene activity is downregulated, and the cells differentiate. The Wnt pathway may also potentially be turned off as a result of interaction with other signaling pathways, such

as the bone morphogenetic (BMP) or the transforming growth factor β (TGF β) signaling pathways [26].

Mutations in the canonical Wnt pathway, for instance in the *APC* gene, causes the cells located in the mid crypt region to act as though the Wnt signal is still present, and as a consequence, these cells will not differentiate. In simpler terms, losing APC function equals constant stimulation of the Wnt signaling pathway, no differentiation of progenitor cells, and subsequent accumulation of aberrant cells which eventually leads to dysplasia [28].

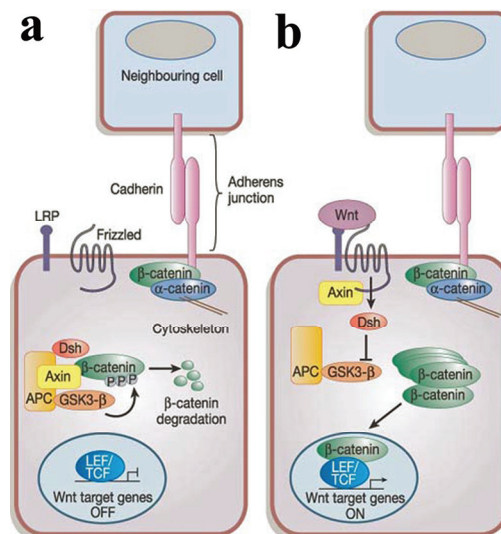


Figure 4. The Wnt signaling pathway. When Wnt ligand is absent (a), β -catenin is phosphorylated and labeled for degradation by the APC/Axin/GSK3- β destruction complex. However, when the Wnt ligand is present (b), the destruction complex does not assemble, β -catenin is not degraded, and accumulates in the cytoplasm before eventually translocating to the nucleus where it complexes with LEF/TCF transcription factors, which in turn activates target genes.⁴

Familial adenomatous polyposis (FAP)

FAP is an autosomal dominant disease characterized by the development of a vast number of adenomas in the colon and rectum. It accounts for less than 1% of all CRC cases [32].

The disease has an early onset with adenomas usually appearing during adolescence. If left untreated, 95% of patients will develop CRC by the age of 50 [32,33]. When a germline

⁴ From “Wnt signalling in stem cells and cancer” by T. Reya and H. Clevers. 2005. *Nature*. 434 (7035) pg 843. Copyright 2005 Nature Publishing Group. Reprinted with permission.

mutation in the adenomatous polyposis coli (*APC*) tumor suppressor gene arises in a parental germ cell, the offspring inherits a constitutional mutation wherein all somatic cells carry the mutation. When an individual that has inherited one mutated *APC* allele experiences LOH, FAP develops. Since FAP patients are born with only one functional *APC* allele, only one mutational event ('one-hit') must occur for CRC to develop. Mutations in the *APC* gene is also evident in roughly 80% of sporadic colorectal cancer cases; however, in sporadic CRC, one allele mutates first, followed by mutation in, or loss of, the second allele, in a 'two-hit' scenario [5,34,35]. In FAP, the two most common mutations sites on the *APC* gene lie at codon 1061 and codon 1309 [36].

Preneoplastic lesions

When a stem cell loses its full length APC protein, it will give rise to a lineage of dysplastic cells, which eventually become dysplastic crypts. The appearance of dysplastic crypts, also called preneoplastic lesions, is the first step in colorectal carcinogenesis [37]. Being able to recognize these initial stages of colorectal cancer is of great importance not only for early detection of CRC, but also for diagnosis and treatment [38]. The first lesions to be considered precursors to CRC were described by Bird in 1987 in the colon of carcinogen-treated mice [39]. These lesions were given the name aberrant crypt foci (ACF), and were described as enlarged crypts with thickened epithelial lining and increased pericryptal space that were elevated from the mucosa [39,40]. These aberrant crypt foci have since been detected in patients with both sporadic CRC and FAP [41–43]. However, in C57BL/6J Min/+ mice [44,45], wild type A/J mice [46], and rats [47], ACF were not directly related to formation of tumors and their histopathology were usually characterized by hyperplasia and only mild signs of dysplasia. In 2000, a similar lesion called ACF_{Min}, later renamed flat ACF, was suggested as a more accurate preneoplastic lesion [44,45,47]. Other lesions have also been suggested as preneoplastic, including the mucin depleted foci (MDF), first described by Caderni et al. in 2003 [48]. This lesion is comparable with the flat ACF. The β -catenin-accumulated crypt (BCAC), first described by Yamada et al. [49], also appears to be similar to the flat ACF, but this lesion is only detectable in histological sections after β -catenin immunostaining [50]. Another lesion, the dark ACF, described in rats, has also been suggested as preneoplastic [51]; however, this lesions was later acknowledge to be the same lesions as the flat ACF [52]. In 2005, Ochiai et al. [53] described yet another preneoplastic lesion in the colon of rats fed a diet containing heterocyclic amines. These lesions were given the name dysplastic ACF, and were only detected after methanol decolorization of

methylene blue stained colons, where dysplastic ACF retained the blue color, while ‘classic’ ACF did not.

Flat ACF and MDF

In a study examining the colons of untreated Min/+ mice, not a single ACF was detected. Instead, a similar lesion that did not protrude into the lumen was discovered. This new lesion was given the name ACF_{Min} [44]. When Min/+ mice were given azoxymethane (AOM), a colon carcinogen, both ACF and ACF_{Min} were observed; however, only ACF_{Min} appeared to be directly related to tumors [45]. When the ACF_{Min} was observed in the colon of carcinogen-treated rats, it was renamed flat ACF [47]. The flat ACF can be detected from the monocryptal stage, and is identified based on a set of criteria. To find the flat ACF, the intestine must be stained with methylene blue (MB) and examined by transillumination. In a methylene blue-stained colon, the flat ACF differs from normal, healthy crypts in that it adopts a bright blue-green color (Fig. 5a). Furthermore, the flat ACF must have enlarged crypts with compressed luminal openings, and show elongated pit patterns giving the lesion a gyrus-like look.

The mucin depleted foci (MDF) was first observed in the colon of AOM-treated rats [48], and has since been detected in both murine and human colon [54–56]. The MDF exhibits dysplastic features similar to those observed in colorectal tumors, which suggests that this lesion is a precursor to colorectal cancer. The MDF is also identified based on a set of criteria. To find the MDF, the intestine must be stained with high-iron diamine alcian blue (HID-AB), a mucin stain. With this staining method, the MDF acquires a pink coloration due to the lack of- or very limited amounts of mucins present in the lesion, while normal, healthy crypts stain dark brown or blue, colors attributable to sulfomucin or sialomucin secretion, respectively (Fig. 5b) [48,57]. The characteristic lack of mucins of the MDF is a recognized sign of dysplasia [58]. The MDF has distorted luminal openings, is elevated from the colonic surface, and each focus consists of at least 3 crypts. To be considered an MDF, the lesion must fulfill the mucin depletion criteria, and at least two of the remaining criteria mentioned above [48].

In 2008, flat ACF and MDF were compared using both staining methods, and of all the flat ACF observed in the MB-stained colon of AOM-treated Min/+ mice, 57% were identified as MDF with HID-AB staining. In rats exposed to 1,2-dimethylhydrazine (DMH), this

correspondence was 42%. These findings suggested a considerable, but not complete, overlap between the two dysplastic lesions [54].

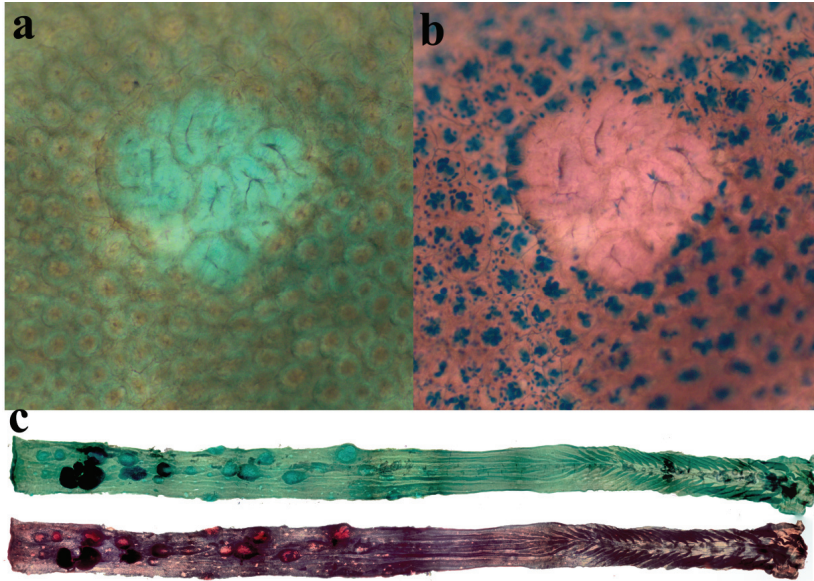


Figure 5. Surface morphology of (a) flat ACF and (b) MDF, stained with methylene blue (MB) and high-iron diamine alcian blue (HID-AB), respectively. (c) Surface images of a mouse colon initially stained with MB (top), and subsequently stained with HID-AB (bottom), as observed in an inverted microscope. Photos: M. Sødning.

Animal models for colorectal cancer

Animal models in cancer research are useful for studying disease development, molecular mechanisms, genetic anomalies, pathology, importance of microbiota and their metabolites etc. Such models are also used when drugs and strategies of preventive medicine are studied. To increase the translational potential of an animal model, it is important that the chosen model reflects both mechanisms and pathologies seen in the human disease counterpart. Models that well reflect human CRC can help in several ways by for example increasing our understanding of colorectal cancer etiology, via development of reliable biomarkers for early detection, or by finding chemopreventive strategies. However, there are challenges when using animal models to study CRC; many of these animal models develop cancers outside of the colon, to a greater extent than humans, and many models do not experience all stages of human CRC [59–61].

Murine models for *Apc*-driven tumorigenesis

Apc-driven tumorigenesis appears to be dependent on somatic genetic events that lead to loss of function of the wild-type *Apc* allele, by mutations, LOH, or epigenetic silencing [62]. There are both rat and mouse models that specifically address *Apc* mutations so as to resemble human FAP. Currently, two rat models for CRC carrying mutations in *Apc*, the rodent homolog to the human *APC* gene, exist: the Kyoto *Apc* Delta (KAD) rat and the polyposis in the rat colon (Pirc). The KAD rat model does not spontaneously develop intestinal tumors even though this rat is homozygous for the *Apc* mutation. Furthermore, AOM treatment does not induce colonic tumors in this model; however, AOM in combinations with the ulcerogenic and inflammatory agent dextran sulfate sodium (DSS) results in an increase in colonic tumors when compared to wild-type rats on the same F344 genetic background. The KAD rat has a nonsense mutation at codon 2523 that results in a truncated APC protein, not much smaller than the wild-type protein which contains 2843 amino acids [63]. The Pirc rat was created by exposing F344/NTac males to the carcinogen ethylnitrosourea (ENU), and was found to spontaneously develop tumors in the colon. The Pirc rat has a nonsense mutation at codon 1137 resulting in a truncated APC protein. This rat is heterozygous for the *Apc* mutation, and the recessive phenotype is lethal [64].

The APC Min/+ mouse

The multiple intestinal neoplasia (*Min/+*) mouse is one of the most widely used murine models for human FAP. The conventional *Min/+* mouse is on a C57BL/6 genetic background, which is perhaps one of the best known and most widely used inbred mouse strains. The C57BL/6J substrain was established at the Jackson Laboratory in 1948 [65]. The *Min/+* mouse was generated after exposure to ENU, which caused a random germline mutation. Moser et al. [66] mated ENU-treated C57BL/6J (B6) males with untreated AKR/J females, and one of the pups exhibited circling behavior. This female offspring was mated with a B6 male to see if the circling behavior was hereditary. Some of the resulting progeny of that cross exhibited the circling behavior, but, in addition, a new trait was noted: progressive, adult-onset anemia. The circling trait was later found to be genetically unlinked to the anemia trait, and has since been lost from the lineage. They also found that only anemic mice developed multiple adenomas in the intestines. The mutant gene responsible was named multiple intestinal neoplasia (*Min*) [66]. The *Min/+* mouse has a heterozygous truncation mutation at codon 850 of the tumor suppressor gene *Apc*. This mutation is located

on chromosome 18 (in contrast to the human *APC* which is on chromosome 5), and is an autosomal dominant trait that is fully penetrant, meaning that clinical signs will develop in all individuals that have this mutation [66]. The *Min* mutation is analogous to the mutation seen in the human *APC* gene, and results in the spontaneous formation of several neoplastic lesions in the mouse intestines [67,68]. Although the B6 *Min*⁺ mouse is one of the most commonly used rodent models for FAP, it does not mirror the disease phenotype of FAP well; in contrast to FAP patients that develop hundreds to thousands of adenomas in the colon, B6 *Min*⁺ mice primarily develop small intestinal tumors, and very few lesions in the colon, which rarely progress to cancer [32,66,69].

Numerous *Apc* mouse models have been described since the original B6 *Min*⁺ mouse was identified by Moser et al. in 1990 [66,70]. Some of these alternate models have mutations that generate a shorter (*Apc*^{Δ716}, *Apc*¹⁴) or longer (*Apc*^{1638N}, *Apc*¹³⁰⁹) APC protein, and consequently, altered phenotypes (Fig. 6): *Apc*^{Δ716}, with a truncation mutation at codon 716, develops approximately 300 tumors mostly in the small intestine [71]; *Apc*¹⁴, where exon 14 has been deleted, essentially develops the same number of lesions as the *Min*⁺ mouse, but, in contrast, most of these are located in the distal colon [72]; *Apc*^{1638N} has a truncation at codon 1638, and presents with about 3 intestinal polyps [73,74]; *Apc*¹³⁰⁹, with a truncation mutation at codon 1309, also resembles the *Min*⁺ mouse in number of lesions, but with more polyps in the colon, and a more severe phenotype [75]. Two hypomorphic *Apc* mice have also been created; *Apc*^{NeoF} and *Apc*^{NeoR}, where *Apc* is expressed at much lower levels than in the wild-type. These hypomorphic mutants lived long, but developed on average less than 1 tumor in the small intestine [76].

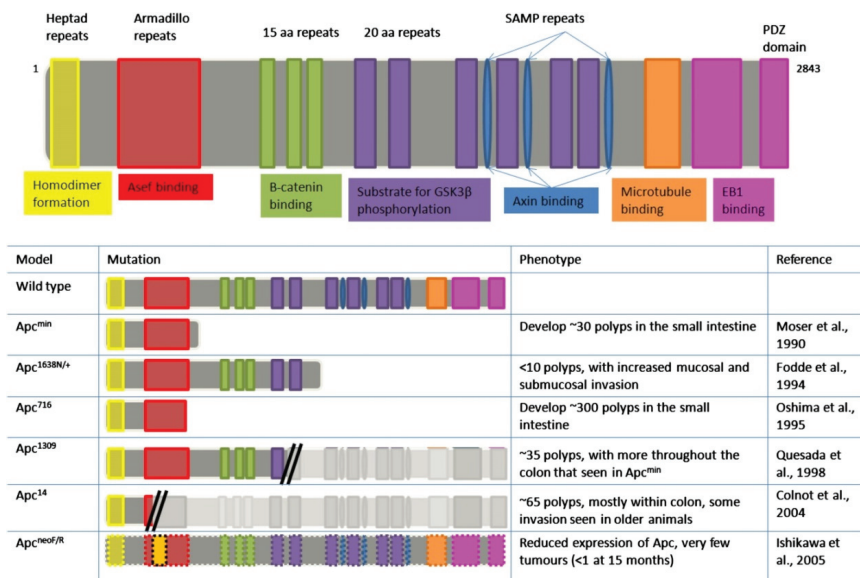


Figure 6. The Apc protein and some Apc-mutation mouse models⁵

Modifiers of Min

Although FAP patients have the same *APC* mutation, the disease phenotype may be very different. This is thought to be due to environmental and genetic modifiers. Genetic modifiers are loci present in the background strain genome that directly or indirectly affect the expression of the disease phenotype [77]. Genetic modifiers are probably the reason for variations observed in disease phenotype in the *Min*^{+/+} mouse, even under controlled laboratory conditions. The *Min*^{+/+} trait has been introgressed on various inbred backgrounds. These variants showed a broad spectrum of intestinal tumour multiplicity: BTBR was the most enhancing background and AKR was the most resistant background [36]. By quantitative trait locus analyses and strain crossing, several genes that modify intestinal tumorigenesis in the *Min*^{+/+} mouse have been identified [36]. The first of these modifiers to be discovered was the Modifier of Min 1 (*Mom1*) [78]. The gene *Pla2g2a* (a secretory phospholipase) was found to be responsible for the effect of *Mom1* [79,80]. When B6 *Min*^{+/+} mice crossed with eight other strains resulted in offspring with different number of intestinal lesions, it was suggested that the different strains carried modifiers capable of reducing tumor burden, and that the genetic background was of great importance to tumorigenesis

⁵ From “What are the best routes to effectively model human colorectal cancer?” by M. Young, L. Ordonez, and A.R. Clarke. 2013. *Mol Oncol*. 7(2) pg 182. Copyright 2013 Elsevier. Reprinted with permission.

[78,81,82]. *Mom1* has two alleles, one sensitive and one resistant. Mice carrying the *Min/+* mutations can be either sensitive or resistant to the modifying *Mom1* allele; mice carrying the sensitive *Mom1* allele showed an increased tumor burden when compared to those with the resistant *Mom1* allele [81,82]. Subsequently, several other modifiers of the *Min* phenotype have been described including *Mom2*, *Mom3*, *Mom5*, *Mom7*, *Mom12*, and *Mom13* [83–87].

The A/J *Min/+* mouse

The B6 substrain is quite resistant to colon carcinogens such as AOM and DSS, which may explain the lack of colonic tumors in the *Min/+* mouse on this particular genetic background. The A/J strain, however, has been found to be highly sensitive to such colon carcinogens [46,69,88,89]. A double backcross between A/J (susceptible) and B6 (resistant) parents produced recombinant congenic mouse strains that helped identify three colon cancer susceptibility loci (*Ccs3*, *Ccs4* and *Ccs5*) responsible for the susceptibility variation of these two strains to AOM-induced CRC [90–92]. Since A/J mice are highly susceptible to AOM-induced colon carcinogenesis, it could be inferred that this genetic background could potentially modify *Min/+* related intestinal tumorigenesis.

The *Min/+* trait has now been introgressed onto an A/J genetic background, creating an A/J *Min/+* mouse (Fig. 7). Preliminary studies on this novel *Min/+* mouse showed that also the A/J *Min/+* mouse was more susceptible to AOM-induced colon carcinogenesis than its B6 *Min/+* counterpart [93].

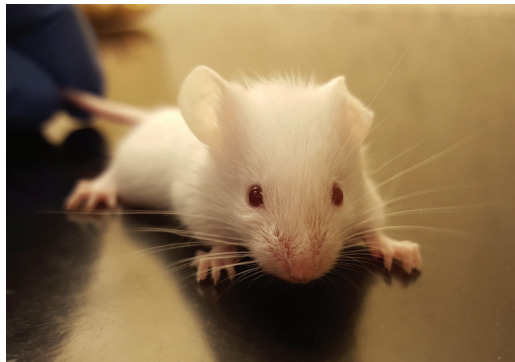


Figure 7. The A/J *Min/+* mouse. Photo M. Södring

Diet and Colorectal cancer

Although the cause of sporadic CRC is still unclear, food and nutrition appears to be associated with both causation and prevention of this type of cancer [94]. Intake of processed meat, red meat, and alcohol, as well as higher body/abdominal fatness has been

associated with an increased risk of developing colon cancer. Cheese and foods containing iron, sugar, or animal fats may also cause colon cancer; however, the evidence supporting this is limited. In contrast, physical activity, dietary fiber, garlic, milk, and calcium likely decreases the risk of this form of cancer, and, although supporting evidence is limited, fruits, fish, non-starchy vegetables, and foods containing vitamin D, selenium, or folate may potentially protect against colon cancer [94].

Red and processed meat

“Red meat and processed meat are among the foods suggested to be associated with an increased risk of developing certain cancers [95]. The definition of red meat varies considerably, and ranges from categorization based on meat color prior to cooking, to the animal origin of the meat, or meat flavor. Often, the term red meat refers to meats that are red in color prior to cooking, such as beef, lamb, veal, and (frequently) pork, while the term white meat incorporates meats that are pale pre-cooking, such as chicken, fish, and (occasionally) pork [96]. However, in some cases, meats that are relatively pale before cooking, such as meat from ducks and geese, may nevertheless be categorized as red meats. Another meat categorization is based on the flavor of the meat, where red meats are considered to have a stronger, more intense flavor as compared to the blander flavor of white meats. Additionally, red and white meats can also be defined by animal origin, where red meats are from mammals, and white meats are from other animals [96]. Clearly, there does not appear to be one universal definition of what is to be considered red meat, and thus, the challenge in comparing meats with regards to cancer risk becomes greater. No collectively agreed-upon definition exists for processed meats either, but processed meat typically refers to meats (usually red meats, but may include white meats) that have been preserved by for example curing (nitrite treatment), smoking, drying, or by the addition of chemical preservatives [94,97].

The strength of the association between intake of red and processed meat and cancer varies. For some cancers, including esophageal, lung, pancreatic, prostate, endometrial, and stomach cancers, only limited evidence has been provided to support a potential link to intake of red and processed meat. However, the association between CRC . . . and red and processed meat consumption has been deemed convincing by both the World Cancer Research Fund (WCRF), and the International Agency for Research on Cancer (IARC) [94,95]. More than half of all CRC cases are seen in developed regions . . . In contrast,

CRC is quite uncommon in less developed regions . . . and is also remarkably uncommon in certain meat-consuming regions such as the Middle east, China and Mongolia [98,99].”⁶

Animal studies on the link between meat and colorectal cancer

“Several experimental studies published prior to 2004 failed to show the promoting effect of red meat on carcinogen-induced rat colorectal carcinogenesis [100–102]. Many of these studies showed that tumor incidence was not significantly different in animals fed red meat compared to soy or casein-fed animals, and some studies even showed a protective effect of beef meat [103] or beef protein [104]. More recently, experimental studies have emerged suggesting a positive connection between CRC and red meat intake. Interestingly, these experimental studies were not successful until the basal diets were modified to reflect a “Western style diet”: high fat, low calcium, low antioxidant etc. [105,106]. Several studies have shown that an intake of red and processed meat leads to an increase in fecal water cytotoxicity, lipid peroxidation products including thiobarbituric acid reactive substances (TBARS), and apparent total nitroso-compounds (ATNCs), supporting the potential adverse effects that red and processed meat intake may have on CRC development [107–111].”⁶

Potential mechanisms linking red meat and CRC

Several pathways have been proposed to explain the association between intake of red meat and CRC (Fig. 8), and are reviewed in detail elsewhere [96,112,113]. Two hypotheses in particular are considered to be the frontrunners when trying to explain this link: i) the catalytic effect of heme iron on the formation of lipid peroxidation end-products and carcinogenic N-nitroso Compounds (NOCs), and ii) heat-induced carcinogens formed in any grilled or fried meat.

⁶ From “Chapter 20: Meat and Cancer Evidence For and Against” by M. Sødring, M. Oostindjer, L.O. Dragsted, A. Haug, J. E. Paulsen, and B. Egeland. In: *Meat Quality Aspects: From Genes to Ethics*. Eds. P. Purslow (in press). Amsterdam: Elsevier Inc. Copyright 2016. Elsevier Ltd. Reprinted with permission.

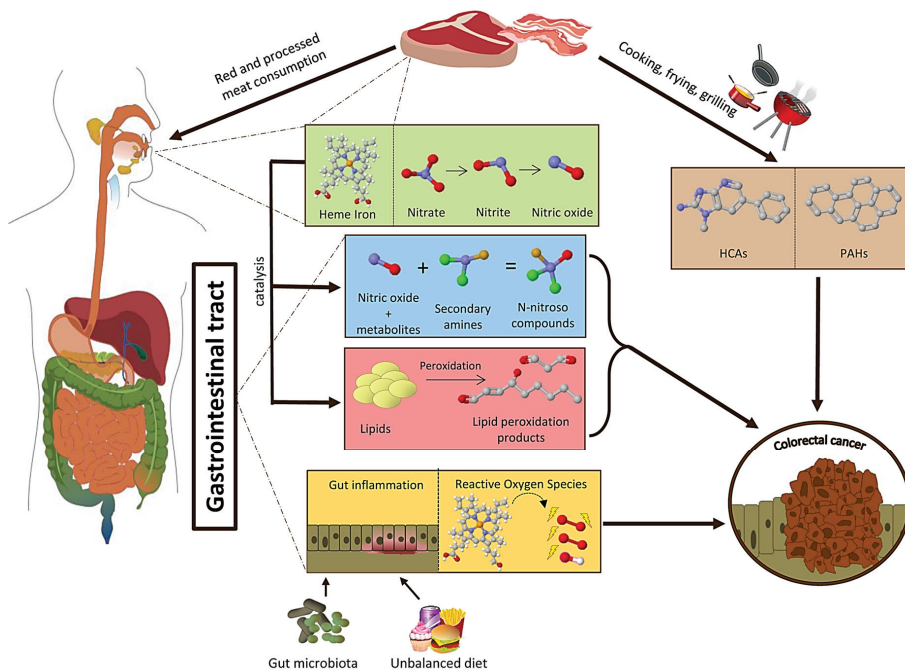


Figure 8. Potential mechanisms behind the association between red and processed meat intake and CRC. Heme iron in red meat catalyzes the formation of N-nitroso compounds (NOCs) and the formation of genotoxic lipid peroxidation products, which may increase CRC development. Grilling or frying red and processed meat can induce the formation of heterocyclic amines (HCA) and polycyclic aromatic hydrocarbons (PAH) which represent potential colorectal carcinogens. Increased gut inflammation as a result of eating an unbalanced diet, or due to abnormal gut microflora may also increase the risk of CRC.⁷

Heme iron and the N-nitroso pathway

Heme iron is an iron-porphyrin pigment found in both red and white meat; however, heme iron quantities are much lower in white meat. This may explain why the link between CRC and red meat is stronger than the link between CRC and white meat [97,114]. Two pathways by which CRC and heme iron may be linked have been suggested; fat peroxidation and N-nitrosation. The first pathway, where fat peroxidation results in the production of aldehydes capable of forming mutagenic DNA-adducts, may explain CRC promotion by fresh, red meat. The second pathway, where N-nitrosation may result in the formation of N-nitroso-specific DNA adducts, may clarify CRC promotion by processed

⁷ From "Chapter 20: Meat and Cancer Evidence For and Against" by M. Sødring, M. Oostindjer, L.O. Dragsted, A. Haug, J. E. Paulsen, and B. Egeland. In: *Meat Quality Aspects: From Genes to Ethics*. Eds. P. Purslow (in press). Amsterdam: Elsevier Inc. Copyright 2016. Elsevier Ltd. Reprinted with permission.

meat [105]. Heme iron in red meat may catalyze endogenous formation of NOCs in the colon, although it has recently been suggested that stimulation of NOC formation may be due to free iron, rather than heme iron [115,116]. In processed meat, nitrite is added to both cure and preserve the meat, as well as to prevent growth of *Clostridium botulinum*, pathogenic bacteria responsible for the potentially fatal disease botulism [117]. Using nitrite to cure meat may contribute to exogenous NOC formation in the meat itself, while also potentially increasing the endogenous formation of NOCs in the gastrointestinal tract. This potential for both exogenous and endogenous NOC formation may explain the hypothesis that processed meat is more closely related to CRC promotion than fresh meat [94,107]. Moreover, recent research suggests that specific sulfide-producing bacteria in the colon may be involved in heme-induced colonic hyperproliferation by reducing the protective mucus layer, and thereby allowing heme to damage the epithelial cells [118].

Aims of the study

The main objective of this PhD-project was to characterize the spontaneous intestinal tumorigenesis in the likely more susceptible A/J Min/+ mouse model, and to better define the flat ACF and its method of detection in this mouse. A sub goal was to employ this mouse model to explore potential carcinogenic effects of factors in red meat. The following specific aims were chosen:

- Describe the spontaneous tumorigenesis in the A/J Min/+ mouse, and evaluate the A/J Min/+ mouse as a complete model for FAP and spontaneous *APC*-driven CRC (paper I).
- Characterize flat aberrant crypt foci (flat ACF) in the colon of the A/J Min/+ mouse, assess its potential as a biomarker for colorectal cancer, and follow the flat ACF from monocryptal stage via benign adenoma to malignant carcinoma (paper I and II).
- Further develop the method of detection of the flat ACF, and compare this lesions to the mucin-depleted foci (MDF) in the colon of the A/J Min/+ mouse to clarify the relationship between these lesions (paper II).
- Use the A/J Min/+ mouse model to test the heme-hypothesis in a spontaneous model for CRC to provide information on the potential effect of heme in red and processed meat on colorectal carcinogenesis (paper III).

Summary of papers

Paper I

Spontaneous initiation, promotion, and progression of colorectal cancer in the novel A/J Min/+ mouse. *Marianne Sødning*, Gjermund Gunnes, and Jan Erik Paulsen. **International Journal of Cancer (2016)**

The C57BL/6J multiple intestinal neoplasia (Min/+) mouse is a widely used murine model for familial adenomatous polyposis, a hereditary form of human colorectal cancer. However, it is a questionable model partly because the vast majority of tumors arise in the small intestine, and partly because the fraction of tumors that progress to invasive carcinomas is minuscule. A/J mice are typically more susceptible to carcinogen-induced colorectal cancer than C57BL/6J mice. To investigate whether the novel Min/+ mouse on the A/J genetic background could be a better model for colorectal cancer we examined the spontaneous intestinal tumorigenesis in 81 A/J Min/+ mice ranging in age from 4 to 60 weeks. The A/J Min/+ mouse exhibited a dramatic increase in number of colonic lesions when compared to what has been reported for the conventional Min/+ mouse, however, an increase in small intestinal lesions did not occur. In addition, this novel mouse model displayed a continual development of colonic lesions highlighted by the transition from early lesions (flat ACF) to tumors over time. In mice older than 40 weeks, 13 colonic (95% CI [8.7-16.3]), and 21 small intestinal (95% CI [18.6-24.3]) tumors were recorded. Notably, a considerable proportion of those lesions progressed to carcinomas in both the colon (21%) and small intestine (51%). These findings more closely reflect aspects of human colorectal carcinogenesis. In conclusion, the novel A/J Min/+ mouse may be a relevant model for initiation, promotion, and progression of colorectal cancer.

Paper II

Detection and characterization of the flat aberrant crypt foci (flat ACF) in the novel A/J Min/+ mouse. *Marianne Sødning*, Gjermund Gunnes, and Jan Erik Paulsen. **Submitted manuscript***

Background: Flat aberrant crypt foci (flat ACF) and mucin depleted foci (MDF) have previously been described as preneoplastic colonic lesions. We used the novel A/J Min/+ mouse model, which demonstrates extensive spontaneous colon carcinogenesis, to refine the method of detection of flat ACF, and to further characterize and define them as early lesions by histological examination and comparison with MDF. **Materials and Methods:** Colons

* Accepted May 4th 2016: *Anticancer Research*, June 2016. 36(6): 2745-2750

were stained with methylene blue (MB) for flat ACF detection and restained with HID-AB for MDF detection. Results: Optimal flat ACF recognition required at least 24 hours of storage post MB staining and adherence to a set of characteristics. The fraction of flat ACF corresponding with MDF was 93%. Flat ACF/MDF displayed the same picture of severe dysplasia, lack of mucus and goblet cells and accumulation of cytoplasmic β -catenin. Conclusion: The easily detectable flat ACF are reliable surface biomarkers of APC-driven colon carcinogenesis.

Paper III

Effects of hemin and nitrite on intestinal tumorigenesis in the A/J Min/+ mouse model.

Marianne Sødning, Marije Oostindjer, Bjørg Egelanddal, and Jan Erik Paulsen.

PLOS ONE (2015)

Red and processed meats are considered risk factors for colorectal cancer (CRC); however, the underlying mechanisms are still unclear. One cause for the potential link between CRC and meat is the heme iron in red meat. Two pathways by which heme and CRC promotion may be linked have been suggested: fat peroxidation and N-nitrosation. In the present work we have used the novel A/J Min/+ mouse model to test the effects of dietary hemin (a model of red meat), and hemin in combination with nitrite (a model of processed meat) on intestinal tumorigenesis. Mice were fed a low Ca^{2+} and vitamin D semi-synthetic diet with added hemin and/or nitrite for 8 weeks post weaning, before termination followed by excision and examination of the intestinal tract. Our results indicate that dietary hemin decreased the number of colonic lesions in the A/J Min/+ mouse. However, our results also showed that the opposite occurred in the small intestine, where dietary hemin appeared to stimulate tumor growth. Furthermore, we find that nitrite, which did not have an effect in the colon, appeared to have a suppressive effect on tumor growth in the small intestine.

Discussion

The A/J *Min*⁺ mouse as a model for CRC

Colorectal cancer (CRC) is one of the most common cancers worldwide [2]. The use of animal models to study CRC provides valuable information and insight to better understand the human disease. Moreover, animal models allow for assessment of the efficacy of potential chemopreventive agents and other strategies for preventive medicine [119]. Examining the literature, it is evident that rodents (usually rats or mice) are the most commonly used animals in CRC experimental studies. Using mice for research has its advantages. For instance, the small size and short generation time of the mouse allows for large-scale, cost-effective studies [120], and the similarity between the mouse and human genome, where about 99% of mouse genes have a homolog in the human genome [121], allows for targeted genome manipulation to provide mouse models that more closely mirror the human disease of interest. But there are also limitations when modeling human diseases in mice including great differences in body size, lifespan, and cellular processes in mice and men [122].

A number of mouse models for spontaneous intestinal cancer exist today; however, the disadvantage with these models is that tumors mainly develop in the small intestine, which is unusual in human CRC. A high tumor load in the small intestine results in a shorter lifespan, and as a consequence, the mice do not acquire sufficient mutations to undergo the last, crucial phase of the cancer process, where cancer cells invade surrounding tissue and eventually metastasize.

The perfect murine model for CRC would completely, and precisely, mirror the human disease, both genotypically and phenotypically, spontaneously develop in immunocompetent animals without the use of chemical carcinogens, and go through all stages of human CRC during the animal's lifetime, from early colonic lesion to distant metastasis [123]. As of yet, no such model exists; however, selecting a model that fulfills as many of these criteria as possible may increase the translatability to human CRC diagnosis, treatment, and prevention.

Although not an ideal model for human CRC, the A/J *Min*⁺ mouse does check at least a few boxes: the *Min* mutation is analogous to the mutation seen in the human *APC* gene; intestinal tumorigenesis occurs spontaneously; colonic to small intestinal tumor ratio is

1.1:1; flat ACF progress to carcinomas, and a potential for (at least) local metastasis is likely (**paper I**). Collectively, this makes the A/J Min/+ mouse a good model for CRC.

The importance of genetic background

In **paper I**, spontaneous tumorigenesis in the novel A/J Min/+ mouse was examined. Since the A/J genetic background has been found to be highly susceptible to colon-specific carcinogens, while the B6 background is relatively resistant [69,88,89,124], it could follow that introgressing the Min/+ trait onto the A/J background would produce a Min/+ mouse more prone to developing colon tumors than the conventional B6 Min/+ mouse.

It has become increasingly clear that the genetic background, i.e. all genetic information other than the gene of interest, can have a profound effect on the phenotypic expression of a specific model animal carrying a mutation in a particular gene. This is thought to be due to the presence of unique ‘background’ loci that can modify the phenotype expressed as a result of the mutation. In experimental genetics, these modifying loci are considered to have no phenotypic consequence if the mutation of interest is not present [36]. In the Min/+ mouse the genetic background has an effect on tumor formation, and thereby indirectly on lifespan. The Min/+ trait has been introgressed onto various inbred genetic backgrounds with different effects on tumor multiplicity [36,78,81,82]. The first generation (F1) Min/+ mice resulting from crosses of AKR, 129, CAST, MA, SWR, DBA, and BALB mice with B6 Min/+ mice exhibited a clear decrease in the number of intestinal tumors when compared to the B6 Min/+ parent. In contrast, the resulting F1 Min/+ mice from a BTBR and B6 Min/+ cross did not show a reduction in tumor numbers. However, backcross analysis (crossing the F1 Min/+ mice to B6 mice) revealed that Min/+ mice on a B6, 129, or BTBR genetic background carries a sensitive *Mom1* allele, while mice on an AKR, MA, CAST, SWR, DBA, or BALB genetic background carries a resistant *Mom1* allele [81,82]. Another modifier was later found when AKR, BTBR, and A/J (represented by a B6-Chr 18^{A/J} chromosome substitution (consomic) strain, where chromosome 18 from an A/J mouse had replaced the homologous B6 chromosome) mice crossed with B6 Min/+ mice revealed a vast difference in small intestinal tumor numbers in the progeny. This modifier was identified as *Mom7*, and could potentially affect tumor initiation [86]. *Mom7* was a dominant suppressor in B6, but a strong recessive enhancer in AKR, BTBR and A/J strains. It could be speculated that, if homozygous for the enhancing *Mom7* alleles, the A/J Min/+ mouse may also show an increase in colonic tumors, as observed in **paper I**. Genetic

background also greatly affects the lifespan of the Min/+ mouse; the conventional B6 Min/+ mouse seldom lives past 120 days and develops an average of 30 small intestinal tumors, and less than 1 colonic tumor [45,66,125,126]. The Min/+ trait on a BTBR background resulted in over 600 small intestinal lesions and 12 colonic lesions, and a short lifespan of no more than 84 days, likely due to the heavy small intestinal tumor load. Furthermore, transferring the Min/+ trait onto an AKR background barely produced any tumors in the intestinal tract, and the lifespan of mice with the Min/+ trait was extended to up to 336 days [36,86]. The novel A/J Min/+ mouse develops a greater number of colonic tumors, without suffering the extreme increase in small intestinal tumors seen in the BTBR Min/+ mouse. This likely accounts for the long lifespan of the A/J Min/+ mouse of up to 420 days (**paper I**).

Tumor progression and the importance of age

Colorectal carcinogenesis is a lengthy process in humans, and it may take decades for normal epithelium to progress to cancer [17]. The B6 Min/+ mouse is a great model for studying early stages of CRC development; however, most tumors observed in the B6 Min/+ mouse are benign adenomas that rarely progress to cancer, which limits its usefulness in regards to the human disease [66,78]. Aging is considered one of the leading risk factors for cancer, including CRC [127], thus, the lack of tumor progression in the B6 Min/+ mouse may be due to its limited 120-day lifespan [66]. Many alternate Min/+ mouse models, where the lifespan of the mouse carrying the Min/+ trait has been extended, have been made. Crossing B6 Min/+ males with B6 wild-type females from an independent colony at the Fox Chase Cancer Center generated the $Apc^{+}/Min-FCCC$ mouse [128]. This Min/+ mouse had a maximum lifespan of 241 days, and developed adenocarcinomas, but only in the small intestine. Even with the extended life span, colonic adenomas did not progress to cancer without the addition of a colitis inducing chemical, DSS [128,129]. Crossing B6 Min/+ mice with SWR and BR females produced F1 Min/+ hybrids with a mean lifespan of 232 and 370 days, respectively [130]. Both SWR and BR Min/+ hybrids developed a low number of intestinal lesions with an average of 15 and 19 tumors along the entire length of the intestines, respectively. Of these tumors, less than 10% were located in the colon. In SWR Min/+ mice, the reduction in tumor number was attributed to the presence of the resistant *Mom1* allele in this strain, while the tumor reduction observed in the BR Min/+ mouse suggested that this strain also carries a modifier allele that suppresses tumorigenesis. However, both the BR and SWR F1 Min/+ hybrids developed adenocarcinomas in the

intestinal tract; 56% in BR, and 87% in SWR. The progression to carcinoma observed was likely due to the increased lifespan. In the SWR Min/+ mouse, 3% of tumors observed had metastasized to local lymph nodes by direct extension [130]. In **paper I**, we found that the novel A/J Min/+ mouse, which has a much longer lifespan than the B6 Min/+ mouse, developed both small intestinal and colonic carcinomas, and that the incidence of intestinal carcinomas in mice older than 30 weeks was 100%. The first colon carcinoma observed in the A/J Min/+ mouse was found in a 41 week old mouse. The human age equivalent to this is approximately 38 years [131], and FAP patients develop cancer at a median age of 42 years [5]. Furthermore, in one 37-week old A/J Min/+ mouse, invasive growth into a local lymphatic vessel was observed, which indicates a high risk for metastases in this individual, and signifies that the potential for metastasis is present in this mouse model. The importance of age in tumor progression is evident, and, it is likely that a short lifespan (for instance that of the B6 Min/+ mouse) limits the accumulation of additional genetic mutations that are required for benign adenomas to progress to carcinomas.

To progress, chromosomal instability CRCs acquire an accumulation of sequential mutations: *APC*, *KRAS*, loss of 18q, *TP53* [12]. Mutational inactivation of *APC* occurs early and results in the formation of early dysplastic lesions such as flat ACF. When studying genetic changes in 172 colorectal tumors from both FAP and non-FAP patients, mutations in the oncogene *KRAS* was observed in 58% of colorectal adenomas larger than 1 cm, and in 47% of carcinomas, but was only present in 9% of adenomas smaller than 1 cm [132]. This indicates a role for *KRAS* in promotion rather than initiation of colorectal tumorigenesis. Approximately 50% of large adenomas (> 1 cm) and 73% of carcinomas had lost a specific region of 18q, and 75% of carcinomas had lost parts of chromosome 17, where the tumor suppressor gene *TP53* resides [132].

Since *Apc* mutations alone will not result in invasive tumors, mutations in subsequent genes of the adenoma-carcinoma sequence have been added to mouse models in order to make them more relevant for human CRC. Congenic 129/B6 Min/+ mice homozygous or heterozygous for a *Tp53* null allele exhibited an increase in intestinal adenomas when compared to mice homozygous for the wild-type allele, suggesting that *Tp53* suppresses adenoma formation in the Min/+ mouse. Furthermore, in mice homozygous for the *Tp53* null allele, approximately 22% of colonic tumors had features characteristic of carcinoma in situ [133]. When the *Apc*^{1638N} mouse was crossed with *KRAS*^{V12G}, a transgenic mouse expressing the activated form of the human *KRAS* oncogene, it was evident that *Apc* and

Kras mutations together increased the number of intestinal lesions, but also caused a progression from adenoma to carcinoma not observed in mice carrying only one of the two mutations. The KRAS^{V12G}/ *Apc*^{1638N} mouse exhibited an adenoma to carcinoma ratio of 1:10.3 [134]. *Apc* mutant mice with mutations in known CRC genes located on chromosome 18 (*Dcc*, *Smad2*, or *Smad4*), have also been created. *Apc*^{Δ716} mice with mutations in either *Smad2* or *Smad4* exhibited accelerated tumor growth, although growth was more prominent in the *Apc/Smad4* mutant. Furthermore, invasive growth was more frequent in the *Apc/Smad4* mutant than in *Apc/Smad2* mutant [135,136]. *Apc*^{1638N} mice with two mutated *Dcc* alleles did not develop many tumors, but all mice did develop adenocarcinomas [137]. The progression to large adenoma, and subsequently to carcinoma, observed in the A/J *Min*⁺ mouse in **paper I**, may potentially be due to additional mutations in genes such as *Tp53*, *Kras*, or genes on chromosome 18.

It has been suggested that there are two distinct stages of tumorigenesis in the *Min*⁺ mouse colon: microadenomas (equivalent to flat ACF described in **paper II**), and macroscopic tumors [138]. Previous research found that a majority of microadenomas in the colon of untreated *Min*⁺ mice exhibited loss of the wild-type *Apc* allele, which indicated that loss of heterozygosity (LOH), and consequently loss of APC function, lead to development of these microadenomas. However, *Apc*-LOH was not sufficient to allow for progression from microadenoma to tumor; the addition of a chemical stimulus was essential [139,140]. In the A/J *Min*⁺ mouse we observed that, as the mice aged, flat ACF spontaneously progressed to adenoma and eventually to carcinomas (**paper I**). This progression occurred without the addition of chemical carcinogens. From this, it appears that for microadenomas/ flat ACF to progress to tumors, an additional stimulus or event, either in the form of a chemical substance, or something else that spontaneously occurs as time passes, is required. This time-related event may potentially be an increase in inflammation, which naturally occurs during aging [141]. Both aging and increased inflammation is thought to be associated with an increase in methylation drift, which is a gradual increase or decrease of DNA methylation at specific loci [142,143]. Dickkopf (*DKK/Dkk*) genes code for Wnt pathway antagonistic proteins that play an important role in vertebrate development [144]. The expression of one of these genes, *Dkk-1*, appears to decrease in colonic tumors, but not in healthy tissue, thereby indicating that this gene may have tumor suppressive effects in CRC [145,146]. Furthermore, expression of *DKK-1* is also inversely correlated with tumor stage and metastasis [147]. In *Min*⁺ mice, expression of *Dkk-1* was only reduced in colonic tumors,

not in healthy epithelium. However, microadenomas still had increased expression of *Dkk-1*, which in turn suggests that *Dkk-1* expression decreases somewhere during the progression from small lesions to larger tumor [140]. In the A/J Min/+ mouse, a spontaneous surge of transition from flat ACF to tumor was observed around 30 weeks (**paper I**), and although we do not know what causes this shift, it may potentially be due to epigenetic silencing of *Dkk-1* by CpG island promoter hypermethylation, which was shown to be specific for advanced stages of colorectal cancer [145,148].

Colonic turnover

Approximately 90% of human cancers arise in epithelial tissues, and epithelial tissues that are constantly renewing, such as skin and colon epithelium, may have an increased risk of developing cancer [149]. Most renewing tissues originate from a small number of stem cells, and mutations in these stem cells pose a central risk for cancer. Cancer incidence in tissues that are constantly renewing also greatly increases with age [150].

Tomasetti & Vogelstein [151] showed that the cumulative number of lifetime stem cell division correlated with the lifetime risk of developing cancer in the corresponding tissue. They found that, of the 31 cancer types they studied, cancer types with the highest lifetime risks coincidentally also had the highest stem cell division number, while those with a low lifetime risk showed low number of stem cell divisions. For instance, FAP patients primarily develop tumors in the colon, but tumors also arise in the small intestine; however, FAP patients have a much greater lifetime risk of developing colorectal cancer (100%) than of duodenal cancer (3.5%). These risk numbers coincided with the total number of stem cell divisions in the colon and duodenum, which was calculated to be 1.2×10^{12} and 7.8×10^9 , respectively [151]. That B6 Min/+ mice develop small intestinal tumors rather than colonic tumors may be due to the fact that the small intestine of mice has more stem cell divisions than the colon does [152].

When B6 and A/J mice were administered the colon carcinogen DMH, proliferative characteristics of the colonic crypt cells of the A/J mouse were higher than in the B6 mouse, indicating that the A/J strain has a higher colonic cell turnover compared to the B6 mouse [89]. Similar results were seen when cell proliferation in A/J and AKR mice treated with AOM were compared: AOM-treated A/J mice exhibited enhanced cell proliferation when compared to saline-treated control A/J mice, while no such increase was seen in AOM-treated AKR mice [153]. Elevated cell turnover in the colon of the A/J strain may explain

the increased susceptibility of this strain for developing colonic neoplasia, which in turn may be the reason why the A/J Min/+ mouse developed more colonic tumors (**Paper I**) than what has been reported for the B6 Min/+ mouse.

Spontaneous vs carcinogen-induced CRC in rodent models

Since most spontaneous rodent models for CRC, such as the Min/+ mouse, rarely develop colorectal cancer, chemicals have been used to induce CRC in rodents [69]. The Min/+ mouse model has the advantage of being a pure adenoma model where the genetic event that initiates tumorigenesis, inactivation of the *Apc* tumor suppressor gene, closely mimics that of human FAP and most sporadic CRC, a trait often lacking in rodent models where CRC is chemically induced [154,155]. Although chemically induced colonic tumors may possess mutations in *Apc* [156,157], other mutations, not necessarily typical in human CRC, have also been detected in carcinogen-induced adenomas [154,157–159]. When treating B6 wild-type mice and B6 Min/+ mice with AOM, Suzui et al. [160] found that mutations in the β -catenin gene (*Ctnnb1*) was only present in wild-type B6 mice, not in Min/+ mice, suggesting that there can be different genetic pathways for chemically induced versus spontaneous colon tumorigenesis. Elevated levels of β -catenin have also been observed in colonic tumors of AOM-treated B6 Min/+ mice, however, the increase in β -catenin observed was likely due to loss of the wild-type *Apc* allele rather than *Ctnnb1* mutations [45]. The absence of *Ctnnb1* mutations in the Min/+ mouse coincides with the lack of germline mutations in *CTNNB1* in FAP patients [161]. Thus, combining the *Min* trait with the sensitive A/J genetic background makes a good model for spontaneous *Apc*-driven tumorigenesis.

A/J Min/+ mouse vs Pirc rat

Although some of the aforementioned mouse models, where mutations in genes involved in CRC have been added to *Apc* mice, may develop a high number of colon tumors and show cancer progression, such models represent genotypes that are more complex than the human FAP genotype. The Min/+ mouse and the Pirc rat are two rodent CRC models for *Apc*-driven tumorigenesis that mirror the fundamental mutational event in FAP. The Min/+ mouse was discovered after exposure to ENU resulted in an offspring phenotype that differed from the parental phenotype [66]. The Pirc rat was also the result of ENU mutagenesis; however, in contrast to the Min/+ mouse, it was intentionally made by genetically screening the offspring of ENU-treated rats for truncation mutations in the *Apc*

gene [64]. The A/J Min/+ mouse model resembles the Pirc rat model, in that both models develop a greater number of colonic lesions than other spontaneous models [64]. In the A/J Min/+ mouse, the average colonic to small intestinal lesion count ratio, when lesions of all sizes were scored, was found to be 1.1:1 (**paper I**), which is closer to the ratio observed in human FAP (>1:1) than that of the B6 Min/+ mouse (<1:40) [64]. Nuclear accumulation of β -catenin is considered a hallmark of *APC*-driven tumorigenesis, and is present throughout the adenoma–carcinoma sequence [162]. When scoring the intestinal tract of the A/J Min/+ mouse, all lesions, from monocryptal flat ACF to adenoma, were included in the count because β -catenin accumulation was evident in lesions of all sizes. The colonic to small intestinal tumor ratio in the Pirc rat averages 1:1; however, microadenomas (lesions smaller than 0.5 mm in size, which would include all flat ACF) were not included since β -catenin accumulation was not observed in microadenomas [64]. As was observed in the A/J Min/+ mouse in **paper I**, Femia et al. [163] also found that the number of mucin-depleted foci, which are comparable to the flat ACF (**Paper II**), and macroscopic tumors in the Pirc rat colon increased with age.

Male Pirc rats become moribund at 11 months due to rectal bleeding, anemia, and weight loss, while female Pirc rats have survived more than 17 months [64]. The long lifespan of the Pirc rat allows for progression to carcinomas; however, metastases have yet to be seen in this model [164]. The A/J Min/+ mouse lives at least 13 months, and invasion into a local lymph vessel was present in an 8.5 month old female A/J Min/+ mouse, which signifies that this model can reach this stage of carcinogenesis. Albeit non-significant, A/J Min/+ males developed more colonic lesions than females. This pattern has previously been observed in both B6 Min/+ mice and in Pirc rats [64,163,165], and has been suggested to be due to tumor-promoting effects of testosterone [165].

Flat ACF as a reliable marker for CRC

The appearance of dysplastic crypts is the first step in colorectal carcinogenesis, and being able to identify these preneoplastic lesions is important for early CRC detection, diagnosis, and treatment [38]. Although tumors are considered to be good endpoints for CRC studies in rodent models, using tumors is not ideal since they require a long time to develop and lengthy studies are more costly. Therefore, finding alternate CRC endpoints that can be identified earlier than the macroscopic tumor is of relevance. The first putative precursor lesion, the classic ACF, was described in the colon of carcinogen-treated mice in 1987

[166], and since then, a wide variety of potential preneoplastic lesions have been introduced. However, it has proved to be challenging to separate true precursor lesions from lesions of minor significance to colorectal carcinogenesis. For instance, classic ACF were not directly related to tumor formation in B6 Min/+ mice [44,45], wild type A/J mice [46], or rats [47], and the classic ACF observed had normal levels of β -catenin expression [45–47]. Moreover, histological examination of classic ACF collected from colorectal cancer patients revealed that only 8.3% of classic ACF showed signs of dysplasia, while the remaining lesions were either hyperplastic crypts or merely enlarged crypts [167]. Although Bird's classic ACF was suggested as an early precancerous lesion, Paulsen et al. [47] observed a greater number of initial classic ACF as opposed to terminal tumors, signifying that only a small fraction of classic ACF had the potential to progress to tumors. Furthermore, they found that the number of flat ACF decreased while the number of tumors reciprocally increased, which mirrors what was observed in **paper I**.

Although flat ACF have been recognized as suitable preneoplastic colonic lesions [69,168,169], they are rarely chosen as surface markers by other groups, likely due to a notion that flat ACF identification is problematic in an unsectioned colon [170,171]. In **paper II**, the method of detection for flat ACF was refined, and critical elements of both preparation and detection were illuminated. To be able to identify the flat ACF, the intestine must be stained with MB for 8-10 seconds, followed by at least 24 hours of storage in 10% formalin or 70% ethanol before surface examination by transillumination. Dysplastic lesions retain the MB color better than normal tissue, thus, a color variance is produced. Without the 24 hour storage period there is barely any difference between flat ACF and normal mucosa, making flat ACF detection virtually impossible. Why the flat ACF retains more color compared to healthy crypts is uncertain, but it may be on account of dysplastic tissue potentially being more resilient to decolorization after treatment with ethanol or formalin than normal tissue is. This has previously been observed in lesions decolorized with methanol [53]. After 24 hours of storage, flat ACF adopt a bright blue-green color, which allows for distinction from the more subdued, brownish-green coloration of normal crypts. There are certain criteria that must be met for a lesion to be categorized as a flat ACF. Besides the blue-green coloration, the lesion must have enlarged crypts with compressed luminal openings, and show elongated pit patterns which gives it a gyrus-like look. Although the name suggests that this lesion lays flat against the mucosa, a small

number of flat ACF may actually be slightly elevated from the surrounding epithelium, giving them a polypoid appearance (**paper II**).

The flat ACF shows severe dysplasia and β -catenin accumulation already at the monocryptal stage (**paper I and II**), making it a more suitable preneoplastic colonic lesion than the classic ACF. The flat ACF and the MDF, a preneoplastic colonic lesion with scarce or absent mucous production, appear to be quite similar, differing mostly in the method of detection (MB for flat ACF, HID-AB for MDF), rather than in morphology. In 2008, the labs of Caderni and Paulsen collaborated on comparing MDF and flat ACF using both staining methods [54]. Of all the flat ACF observed in the MB-stained colon of AOM-treated Min/+ mice, 57% were identified as MDF with HID-AB staining. In rats exposed to 1,2-dimethylhydrazine (DMH), this correspondence was 42%. These findings suggested a substantial, but not complete, overlap between the two dysplastic lesions [54]. However, when comparing flat ACF with MDF in the A/J Min/+ mouse model, we found a clear overlap between the two types of lesions: of the flat ACF scored in MB stained colons, 93% corresponded with MDF scored in HID-AB stained colons (**paper II**). The flat ACF/MDF exhibited severe dysplasia, lack of mucus and goblet cells, and β -catenin accumulation, which strongly suggested that these two surface markers represent the same dysplastic lesions formed in APC-driven colon carcinogenesis.

The observed difference in the percent of corresponding lesions in Femia et al. [54] (57%) and **paper II** (93%), may be a result of using AOM-treated B6 Min/+ mice in one study, and the spontaneous A/J Min/+ mouse model in the other. Classic ACF are common in AOM-induced mice and rats [46,47], while in the A/J Min/+ mouse, classic ACF are rarely observed (**paper I**). In **paper II**, it was evident that flat ACF may in fact have a polypoid appearance, which in turn may potentially lead to flat ACF mistakenly being counted as classic ACF. Some of the MDF scored in the AOM-treated B6 Min/+ mice were counted as classic ACF in the MB stained colon [54]. It may be that some of these classic ACF were actually polypoid flat ACF incorrectly scored, mostly based on the thought that flat ACF must lay flat against the surrounding mucosa. In **paper II** we found that, when restaining polypoid flat ACF with HID-AB, mucin depletion was unmistakable. As a consequence, the 'flat' criteria of a flat ACF needs not be fulfilled for a lesion to be considered a flat ACF.

The results observed in **paper I and II** further supports the flat ACF as a reliable surrogate endpoint for tumors in the A/J Min/+ mouse model. Flat ACF can easily be detected with

MB-staining and transillumination in unsectioned colons, and, using the spontaneous A/J Min/+ mouse model, rather than a carcinogen-induced model, for identifying flat ACF provides an additional advantage since classic ACF are nearly absent in this model, thereby virtually eliminating the challenge of separating true precursor lesions, such as flat ACF and MDF, from lesions that may not progress to cancer, such as classic ACF.

Using the A/J Min/+ mouse model to test the heme-hypothesis

Intake of red and processed meat has been associated with an increased risk of CRC [94]. A large number of epidemiological studies have focused on this relationship with varying conclusions: some studies were unable to find a link, while others report that there is a consistent relationship, although relatively small in magnitude, between red and processed meat and CRC which may present a serious public health impact [105,112,113]. Recently, the evidence for this association was considered convincing enough to categorize red meat as a Group 2A agent (probably carcinogenic to humans) and processed meat as a Group 1 agent (carcinogenic to humans) by the International Agency for Research on Cancer (IARC) [95]. However, it is still unclear exactly how red meat intake and CRC are connected. Several hypotheses have been put forth to attempt to explain this link. One hypothesis that has received ample attention concerns the effect of heme iron in red meat. Two pathways by which CRC and heme iron may be linked have been suggested; fat peroxidation and N-nitrosation [105].

Numerous experimental rodent studies on the association between red and processed meat intake and CRC have been conducted.; however, it was not until the rodent base-diets were modified to reflect a “Western style diet”(high fat, low calcium, low antioxidant etc.), that a positive connection between CRC and red and processed meat intake began to emerge [105,106]. Various rodent studies have reported on potential adverse effects, such as increased fecal water cytotoxicity, TBARS, or ATNCs, of red and processed meat intake [107–111].

When testing the effect of diet or dietary components on colorectal cancer development, choosing a model that is as relevant as possible for the human disease, is important. **Paper I** showed that the A/J Min/+ mouse spontaneously develops a substantial number of colonic lesions that eventually progress to cancer, which makes this model better than for instance the conventional Min/+ mouse in regards to mirroring the human CRC phenotype. Furthermore, **paper II** showed that the flat ACF shares multiple features with the MDF, a

preneoplastic lesion more commonly used in experimental studies, which in turn support the flat ACF as an endpoint for colorectal carcinogenesis. Identifying flat ACF, rather than tumors, in the A/J Min/+ mouse allows for short-term carcinogenesis experiments. Therefore, in **paper III**, the A/J Min/+ mouse model was used to observe the effects of hemin (a model for red meat) and hemin in combination with nitrite (a model for red, processed meat) on colorectal tumorigenesis.

Of the rodent studies examining colonic tumor development following red and processed meat intake, either provided as separate components (hemoglobin, myoglobin, hemin) or in its entirety (cured meat, freeze-dried meat), most support the opinion that red and processed meat leads to an increase in colonic lesions [108,109,111,172–174]. Although the number of rodent studies that show an increase in colonic tumors after red meat intake far outweighs the number of studies that have failed to see this connection, the studies finding a link between red meat and tumor development administered chemical carcinogens, such as AOM or DMH, to the animals to induce cancer. In contrast, in **paper III**, as well as in Winter et al. [175], where an increase in colonic neoplasms could not be linked to red meat intake, no carcinogens were administered.

Fat in the experimental diet

While most studies that investigate the effect of dietary heme on CRC often add 40% fat to the experimental diet to simulate a typical westernized diet [176–180], no additional fat source was added to the experimental diets in **paper III**. The experimental studies with additional dietary fat also usually observed an increased risk of CRC; thus, the low fat content in the diet in **paper III** may be a potential reason for the observed decrease in tumorigenic effect of dietary hemin in the A/J Min/+ mouse colon. Intake of heme iron in combination with fat may result in elevated levels of lipid peroxidation end-products, some of which are known risk factors for various diseases including cancer [105,181,182]. Lipid peroxides can also covalently bind to the protoporphyrin ring of heme to form a cytotoxic heme factor (CHF), and when enough CHF accumulates, cytotoxicity of the colonic luminal contents may increase, thereby damaging the colonic mucosa and lead to hyperproliferation and hyperplasia [180,183]. This may explain the adverse effects observed in studies where experimental heme-diets contain higher amounts of fat. It could be speculated that, without additional fat added to the heme-diet in **paper III**, heme-induced formation of lipid peroxidation end-products or CHF, may have been insufficient to cause damage.

Hemin and nitrite

Heme iron in red meat may catalyze endogenous formation of NOCs in the gastrointestinal tract, while nitrite-cured meat may cause both exogenous NOC formation in the meat itself, and also potentially increase the endogenous formation of NOCs [94,107,115,116].

Therefore, combining hemin with nitrite (**paper III**) was hypothesized to increase tumorigenesis in the A/J Min/+ mouse. However, this combination did not result in an increase in colonic lesions, and, when examining the effects of nitrite and hemin separately, the protective effect observed in the colon of the A/J Min/+ mouse was attributed to hemin, while nitrite did not have an effect at all. Interestingly, the pattern was reversed in the small intestine where hemin appeared to stimulate tumor growth, while nitrite had a suppressive effect on small intestinal tumor promotion in the A/J Min/+ mouse.

Effect of hemin on tumor initiation

While initiating agents are mutagenic, tumor promoters are generally non-mutagenic nor carcinogenic on their own [184,185]. In the A/J Min/+ mouse, tumor initiation occurs after loss of the second functional *Apc* allele in a dividing cell, which in turn gives rise to a line of dysplastic cells. The number of lesions per colon is a marker for initiation [186], therefore, if heme was an initiator capable of causing a mutation in the *Apc* tumor suppressor gene, one would expect an increase in flat ACF in hemin-fed animals. In **paper III**, a significant decrease in both number and load (the sum of the area of all lesions) of flat ACF was evident in A/J Min/+ mice fed hemin or hemin in combination with nitrite. Also, mice fed the modified, synthetic control diet (**paper III**) had less flat ACF and tumors at termination than what was observed in mice of the same age that had been fed a natural, standard rodent maintenance diet (**paper I, paper III**), suggesting that the base-diet used in **paper III** had a lower tumor inducing potential than the standard rodent diet. Adding heme to the synthetic base diet further decreased the number of colonic lesions. From this, it appears that hemin suppressed flat ACF initiation in the A/J Min/+ mouse model. This suppressive effect may in some way, be the result of a potential indirect anti-inflammatory effect of hemin: hemin administered intraperitoneally to DSS-induced BALB/c mice, reduced colitis by decreasing colonic inflammation and maintaining the integrity of the colonic epithelium [187]. It has previously been shown that anti-inflammatory drugs decrease the number of tumors in B6 Min/+ mice [155,188].

The amount of heme added to the feed in **paper III** is higher than what would be considered a relevant dosage from a human consumption perspective [189], nonetheless, since an increase in tumorigenesis was not observed in mice fed heme, it may suggest that the amount of heme present in a typical westernized diet may not be sufficient for CRC initiation. However, in multiple experimental studies where administration of a chemical carcinogen, such as AOM, provides the initiating event, heme has been suggested to be a promoter of colon carcinogenesis [109,111,172–174]. The number of crypts per lesion (lesions size) is a marker for tumor promotion [186]. In **paper III**, when mice fed heme and heme in combination with nitrite were pooled together, the size of flat ACF in heme-fed mice was smaller than those seen in mice not fed heme, which could suggest that in the A/J Min/+ mouse, heme did not promote growth of spontaneously initiated lesions. But, since **Paper I** showed that the growth of flat ACF is slow in younger mice, and only begins to accelerate at a later stage, with a surge of transition and tumor formation around 30 weeks, keeping A/J Min/+ mice on a ‘red meat’ diet for a longer time period could allow for detection of potential promoting effects of heme on spontaneous colon tumorigenesis in the A/J Min/+ mouse.

However, the aforementioned does not dismiss heme as the culprit behind the link to CRC, but it does suggest that heme alone, at least, is not a strong initiator, and that heme may need to be modulated by other dietary factors, such as fat, or interact with other components of red and processed meat, such as NOCs, in order to cause CRC.

Future perspectives

- ✓ In this PhD-project we characterized long-term tumorigenesis in the novel A/J Min/+ mouse. Inactivation of the functional *Apc* allele, with subsequent Wnt pathway activation, is the initial mutational event in the Min/+ mouse; however, the subsequent genetic events of tumorigenesis and progression from flat ACF to carcinomas in the A/J Min/+ mouse have not yet been characterized. Analyzing tumors for genetic or epigenetic alterations would be important for a further understanding of this novel mouse model for *Apc*-driven tumorigenesis. It would be of interest to do mutational analysis on tumor DNA from lesions at different stages of progression to look for mutations in typical CRC genes such as *Tp53* and *Kras*. This would allow for determining whether progression towards malignancy in the A/J Min/+ mouse is associated with mutations of these particular genes that are frequently mutated in human colorectal tumors.
- ✓ During the long-term tumorigenesis study, we observed invasive growth into a regional lymph vessel in a 37-week old A/J Min/+ mouse, which indicates that the A/J Min/+ mouse has the potential for, at least, local metastasis. Therefore, it would be interesting to conduct metastasis studies, to determine whether the potential for distant metastasis exists in this mouse.
- ✓ In this project we also studied the effects of heme and nitrite on intestinal tumorigenesis in the A/J Min/+ mouse. Besides the fat included in the base diet, no additional fat source was supplemented to the experimental diets, which may explain the effects observed. Future experiments where the heme-diet is supplemented with various levels of dietary fat to represent both low and high fat red meat diets would be of interest in order to shed light on whether fat is an important component of the suggested colorectal cancer causing potential of heme iron in red meat.
- ✓ It would be interesting to conduct chemopreventive studies in the A/J Min/+ mouse. The B6 Min/+ mouse is often used to test the efficacy of potential chemopreventive agents. However, the B6 Min/+ mouse develops small intestinal tumors and barely any colorectal tumors, and, since the colonic and small intestinal environment (including the contents of the lumen) differs in the two intestinal segments, the B6 Min/+ mouse may not be able to accurately forecast whether a potential chemopreventive agent will be

effective in humans. By using a model animal that more closely mimics the human disease phenotype, such as the A/J Min/+ mouse, more useful information regarding chemopreventive effects of an agent on colorectal cancer would be gathered. We have shown that the flat ACF is easily detected in an unsectioned, methylene blue stained colon, and also that flat ACF possess phenotypic and genotypic characteristics similar to that of colonic tumors. The flat ACF is therefore a precursor for colorectal tumors, simply detected at an earlier stage of crypt multiplication. This makes the flat ACF a valid surrogate endpoint for tumors that can be used when testing potential chemopreventive agents in short-term chemoprevention studies. Furthermore, the A/J Min/+ mouse lives at least a year, which makes them more suitable than the B6 Min/+ mouse for, for instance, testing chemopreventive agents that require long-term administration.

Main Conclusions

The main conclusions drawn from this PhD project were as follows:

- ✓ Studying the long-term spontaneous intestinal tumorigenesis in the novel A/J Min/+ mouse revealed that this mouse develops a substantial number of colonic lesions that will, with time, progress to carcinomas, with the potential for metastasis. The A/J Min/+ mouse has a colonic to small intestinal lesions ration of 1.1:1, which is more representative of the human FAP phenotype than what is observed in the conventional B6 Min/+ mouse. These findings suggest that the novel A/J Min/+ mouse model is a relevant model for initiation, promotion, and progression of colorectal cancer.

- ✓ Flat ACF are easily detected in the methylene blue stained colon of A/J Min/+ mice. The flat ACF shows severe dysplasia from the monocryptal stage, and possess phenotypic and genotypic characteristics similar to that of colonic tumors. Furthermore, flat ACF show a nearly complete overlap with MDF, a preneoplastic lesions marked by scarce or absent mucous production, which is a recognized hallmark of dysplasia. This suggests that the flat ACF is a reliable surface biomarker of, and an appropriate surrogate endpoint for, APC-driven colon carcinogenesis.

- ✓ In the A/J Min/+ mouse, the hypothesis that heme is behind the link between intake of red and processed meat and an increased risk of colorectal cancer could not be confirmed. Dietary heme decreased the number of colonic lesions in the A/J Min/+ mouse, suggesting instead a suppressive effect of heme. Heme may not be sufficient for tumor initiation, and, in order to lead to colorectal cancer, an interaction with other components of red and processed meat, or modulation by other dietary factors, may be required. Furthermore, dietary nitrite appeared to have no effect on colonic tumorigenesis in the A/J Min/+ mice, however, a suppressive effect on CRC promotion in the small intestine was noticed.

Reference list

1. Cancer Registry of Norway. Cancer in Norway 2014 - Cancer incidence, mortality, survival and prevalence in Norway. 2015.
2. Ferlay J, Soerjomataram I, Dikshit R, Eser S, Mathers C, Rebelo M, et al. Cancer incidence and mortality worldwide: Sources, methods and major patterns in GLOBOCAN 2012. *Int J Cancer*. 2015;136: E359–E386.
3. Jasperson KW, Tuohy TM, Neklason DW, Burt RW. Hereditary and familial colon cancer. *Gastroenterology*. 2010;138: 2044–58.
4. Gryfe R. Inherited colorectal cancer syndromes. *Clin Colon Rectal Surg*. 2009;22: 198–208.
5. Kinzler KW, Vogelstein B. Lessons from hereditary colorectal cancer. *Cell*. 1996;87: 159–70.
6. Treuting PM, Valasek MA, Dintzis SM. Upper Gastrointestinal Tract. In: Treuting PM, Dintzis SM, editors. *Comparative Anatomy and Histology: A Mouse and Human Atlas*. 1st ed. Waltham, MA: Academic Press; 2012. pp. 155–175.
7. Treuting PM, Dintzis SM. Lower Gastrointestinal Tract. In: Treuting PM, Dintzis SM, editors. *Comparative Anatomy and Histology: A Mouse and Human Atlas*. 1st ed. Waltham, MA: Academic Press; 2012. pp. 177–192.
8. Sancho E, Batlle E, Clevers H. Signaling Pathways in Intestinal Development and Cancer. *Annu Rev Cell Dev Biol*. 2004;20: 695–723.
9. Ponz de Leon M, Di Gregorio C. Pathology of colorectal cancer. *Dig Liver Dis*. 2001;33: 372–88.
10. Radtke F, Clevers H. Self-Renewal and Cancer of the Gut† Two Sides of a Coin. *Science (80-)*. 2005;307: 1904–1909.
11. Barker N. Adult intestinal stem cells: critical drivers of epithelial homeostasis and regeneration. *Nat Rev Mol Cell Biol*. Nature Publishing Group; 2014;15: 19–33.
12. Leslie A, Carey FA, Pratt NR, Steele RJC. The colorectal adenoma-carcinoma sequence. *Br J Surg*. 2002;89: 845–60.
13. Fearon ER, Vogelstein B. A genetic model for colorectal tumorigenesis. *Cell*. 1990. pp. 759–767.
14. Fodde R. The APC gene in colorectal cancer. *Eur J Cancer*. 2002;38: 867–871.
15. Markowitz S, Bertagnolli M. Molecular Basis of Colorectal Cancer. *N Engl J Med*. 2009;361: 2449–2460.
16. Ilyas M, Straub J, Tomlinson IPM, Bodmer WF. Genetic pathways in colorectal and other cancers. *Eur J Cancer*. 1999;35: 335–351.
17. Kelloff GJ, Schilsky RL, Alberts DS, Day RW, Guyton KZ, Pearce HL, et al. Colorectal adenomas: a prototype for the use of surrogate end points in the development of cancer prevention drugs. *Clin Cancer Res*. 2004;10: 3908–18.
18. Pino MS, Chung DC. The chromosomal instability pathway in colon cancer. *Gastroenterology*. 2010;138: 2059–72.
19. Migliore L, Migheli F, Spisni R, Coppedè F. Genetics, cytogenetics, and epigenetics of colorectal cancer. *J Biomed Biotechnol*. 2011;2011: 792362.

20. Toyota M, Ahuja N, Ohe-Toyota M, Herman JG, Baylin SB, Issa JP. CpG island methylator phenotype in colorectal cancer. *Proc Natl Acad Sci U S A*. 1999;96: 8681–6.
21. Kinzler KW, Vogelstein B. Cancer-susceptibility genes. Gatekeepers and caretakers. *Nature*. 1997;386: 761, 763.
22. Macleod K. Tumor suppressor genes. *Curr Opin Genet Dev*. 2000;10: 81–93.
23. Kinzler KW, Vogelstein B. Landscaping the Cancer Terrain. *Science (80-)*. American Association for the Advancement of Science; 1998;280: 1036–1037.
24. Widelitz R. Wnt signaling through canonical and non-canonical pathways: recent progress. *Growth Factors*. 2005;23: 111–6.
25. Clevers H, Nusse R. Wnt/catenin signaling and disease. *Cell*. 2012;149: 1192–1205.
26. Gregorieff A, Clevers H. Wnt signaling in the intestinal epithelium: from endoderm to cancer. *Genes Dev*. 2005;19: 877–90.
27. Nusse R. Wnt signaling in disease and in development. *Cell Res*. 2005;15: 28–32.
28. Giles RH, van Es JH, Clevers H. Caught up in a Wnt storm: Wnt signaling in cancer. *Biochim Biophys Acta - Rev Cancer*. 2003;1653: 1–24.
29. Reya T, Clevers H. Wnt signalling in stem cells and cancer. *Nature*. Macmillan Magazines Ltd.; 2005;434: 843–50.
30. Lickert H, Kispert A, Kutsch S, Kemler R. Expression patterns of Wnt genes in mouse gut development. *Mech Dev*. 2001;105: 181–184.
31. Holcombe RF, Marsh JL, Waterman ML, Lin F, Milovanovic T, Truong T. Expression of Wnt ligands and Frizzled receptors in colonic mucosa and in colon carcinoma. *Mol Pathol*. 2002;55: 220–226.
32. Half E, Bercovich D, Rozen P. Familial adenomatous polyposis. *Orphanet J Rare Dis*. 2009;4: 22.
33. Samadder NJ, Jasperson K, Burt RW. Hereditary and Common Familial Colorectal Cancer: Evidence for Colorectal Screening. *Dig Dis Sci*. 2014; 734–747.
34. Fearhead NS, Britton MP, Bodmer WF, Hospital JR, Ox O. The ABC of APC. *Hum Mol Genet*. 2001;10.
35. Knudson AG. Mutation and Cancer: Statistical Study of Retinoblastoma. *Proc Natl Acad Sci*. 1971;68: 820–823.
36. Kwong LN, Dove WF. APC and its modifiers in colon cancer. *Adv Exp Med Biol*. 2009;656: 85–106.
37. Paulsen JE. Modulation by dietary factors in murine FAP models. *Toxicol Lett*. 2000;112-113: 403–409.
38. Srivastava S, Verma M, Henson DE. Biomarkers for Early Detection of Colon Cancer. *Clin Cancer Res*. 2001;7: 1118–1126.
39. Bird RP. Observation and quantification of aberrant crypts in the murine colon treated with a colon carcinogen: preliminary findings. *Cancer Lett*. 1987;37: 147–51.
40. Bird RP, Good CK. The significance of aberrant crypt foci in understanding the pathogenesis of colon cancer. *Toxicol Lett*. 2000;112-113: 395–402.

41. Roncucci L, Modica S, Pedroni M, Tamassia MG, Ghidoni M, Losi L, et al. Aberrant crypt foci in patients with colorectal cancer. *Br J Cancer*. 1998;77: 2343–8.
42. Nucci MR, Robinson CR, Longo P, Campbell P, Hamilton SR. Phenotypic and genotypic characteristics of aberrant crypt foci in human colorectal mucosa. *Hum Pathol*. 1997;28: 1396–407.
43. Bird RP. Role of aberrant crypt foci in understanding the pathogenesis of colon cancer. *Cancer Lett*. 1995;93: 55–71.
44. Paulsen JE, Namork E, Steffensen IL, Eide TJ, Alexander J. Identification and quantification of aberrant crypt foci in the colon of Min mice—a murine model of familial adenomatous polyposis. *Scand J Gastroenterol*. 2000;35: 534–539.
45. Paulsen JE, Steffensen IL, Løberg EM, Husøy T, Namork E, Alexander J. Qualitative and quantitative relationship between dysplastic aberrant crypt foci and tumorigenesis in the Min/+ mouse colon. *Cancer Res*. 2001;61: 5010–5015.
46. Paulsen JE, Knutsen H, Ølstørn HB, Løberg EM, Alexander J. Identification of flat dysplastic aberrant crypt foci in the colon of azoxymethane-treated A/J mice. *Int J Cancer*. 2006;118: 540–546.
47. Paulsen JE, Løberg EM, Ølstørn HB, Knutsen H, Steffensen I, Alexander J. Flat Dysplastic Aberrant Crypt Foci Are Related to Tumorigenesis in the Colon of Azoxymethane-Treated Rat. *Cancer Res*. 2005;65: 121–129.
48. Caderni G, Femia A Pietro, Giannini A, Favuzza A, Luceri C, Salvadori M, et al. Identification of Mucin-depleted Foci in the Unsectioned Colon of Azoxymethane-treated Rats: Correlation with Carcinogenesis. *Cancer Res*. 2003;63: 2388–2392.
49. Yamada Y, Yoshimi N, Hirose Y, Kawabata K, Matsunaga K, Shimizu M, et al. Frequent beta-catenin gene mutations and accumulations of the protein in the putative preneoplastic lesions lacking macroscopic aberrant crypt foci appearance, in rat colon carcinogenesis. *Cancer Res*. 2000;60: 3323–7.
50. Yamada Y, Mori H. Pre-cancerous lesions for colorectal cancers in rodents: a new concept. *Carcinogenesis*. 2003;24: 1015–9.
51. Lu Q, Jiang B, Lin C, Shan T. Dark Aberrant Crypt Foci with activated Wnt pathway are related to tumorigenesis in the colon of AOM-treated rat. *J Exp Clin Cancer Res*. 2008;27.
52. Lu Q, Jiang B, Lin C, Shan T. Dark Aberrant Crypt Foci with activated Wnt pathway are related to tumorigenesis in the colon of AOM-treated rat - retraction. *J Exp Clin Cancer Res*. BioMed Central; 2008;27.
53. Ochiai M, Watanabe M, Nakanishi M, Taguchi A, Sugimura T, Nakagama H. Differential staining of dysplastic aberrant crypt foci in the colon facilitates prediction of carcinogenic potentials of chemicals in rats. *Cancer Lett*. 2005;220: 67–74.
54. Femia A Pietro, Paulsen JE, Dolara P, Alexander J, Caderni G. Correspondence between flat aberrant crypt foci and mucin-depleted foci in rodent colon carcinogenesis. *Anticancer Res*. 2008;28: 3771–5.
55. Femia A Pietro, Dolara P, Luceri C, Salvadori M, Caderni G. Mucin-depleted foci show strong activation of inflammatory markers in 1,2-dimethylhydrazine-induced carcinogenesis and are promoted by the inflammatory agent sodium dextran sulfate. *Int J Cancer*. 2009;125: 541–7.
56. Femia A Pietro, Giannini A, Fazi M, Tarquini E, Salvadori M, Roncucci L, et al. Identification of

mucin depleted foci in the human colon. *Cancer Prev Res (Phila)*. 2008;1: 562–7.

57. Caderni G, Giannini A, Lancioni L, Luceri C, Biggeri A, Dolara P. Characterisation of aberrant crypt foci in carcinogen-treated rats: association with intestinal carcinogenesis. *Br J Cancer*. 1995;71: 763–9.
58. Filipe MI. Mucous secretion in rat colonic mucosa during carcinogenesis induced by dimethylhydrazine. A morphological and histochemical study. *Br J Cancer*. 1975;32: 60–77.
59. Johnson RL, Fleet JC. Animal models of colorectal cancer. *Cancer Metastasis Rev*. 2013;32: 39–61.
60. Mak IW, Evaniew N, Ghert M. Lost in translation: animal models and clinical trials in cancer treatment. *Am J Transl Res*. 2014;6: 114–8.
61. Irving AA, Yoshimi K, Hart ML, Parker T, Clipson L, Ford MR, et al. The utility of Apc-mutant rats in modeling human colon cancer. *Dis Model Mech*. 2014;7: 1215–1225.
62. Amos-Landgraf JM, Irving AA, Hartman C, Hunter A, Laube B, Chen X, et al. Monoallelic silencing and haploinsufficiency in early murine intestinal neoplasms. *Proc Natl Acad Sci U S A*. 2012;109: 2060–5.
63. Yoshimi K, Tanaka T, Takizawa A, Kato M, Hirabayashi M, Mashimo T, et al. Enhanced colitis-associated colon carcinogenesis in a novel Apc mutant rat. *Cancer Sci*. 2009;100: 2022–2027.
64. Amos-Landgraf JM, Kwong LN, Kendzierski CM, Reichelderfer M, Torrealba J, Weichert J, et al. A target-selected Apc-mutant rat kindred enhances the modeling of familial human colon cancer. *Proc Natl Acad Sci U S A*. 2007;104: 4036–41.
65. Mekada K, Abe K, Murakami A, Nakamura S, Nakata H, Moriwaki K, et al. Genetic differences among C57BL/6 substrains. *Exp Anim*. 2009;58: 141–9.
66. Moser AR, Pitot HC, Dove WF. A dominant mutation that predisposes to multiple intestinal neoplasia in the mouse. *Science (80-)*. 1990;247: 322–324.
67. van Es JH, Giles RH, Clevers HC. The many faces of the tumor suppressor gene APC. *Exp Cell Res*. 2001;264: 126–34.
68. Su LK, Kinzler KW, Vogelstein B, Preisinger AC, Moser AR, Luongo C, et al. Multiple intestinal neoplasia caused by a mutation in the murine homolog of the APC gene. *Science (80-)*. 1992;256: 668–670.
69. Rosenberg DW, Giardina C, Tanaka T. Mouse models for the study of colon carcinogenesis. *Carcinogenesis*. 2009;30: 183–96.
70. Zeineldin M, Neufeld KL. More than two decades of Apc modeling in rodents. *Biochim Biophys Acta - Rev Cancer*. Elsevier B.V.; 2013;1836: 80–89.
71. Oshima M, Oshima H, Kitagawa K, Kobayashi M, Itakura C, Taketo M. Loss of Apc heterozygosity and abnormal tissue building in nascent intestinal polyps in mice carrying a truncated Apc gene. *Proc Natl Acad Sci U S A*. 1995;92: 4482–6.
72. Colnot S, Niwa-Kawakita M, Hamard G, Godard C, Le Plénier S, Houbron C, et al. Colorectal cancers in a new mouse model of familial adenomatous polyposis: influence of genetic and environmental modifiers. *Lab Invest*. 2004;84: 1619–30.
73. Smits R, van der Hoven van Oordt W, Luz A, Zurcher C, Jagmohan-Changur S, Breukel C, et al. Apc1638N: A mouse model for familial adenomatous polyposis-associated desmoid tumors and cutaneous cysts. *Gastroenterology*. 1998;114: 275–283.

74. Fodde R, Edelmann W, Yang K, van Leeuwen C, Carlson C, Renault B, et al. A targeted chain-termination mutation in the mouse *Apc* gene results in multiple intestinal tumors. *Proc Natl Acad Sci U S A*. 1994;91: 8969–73.
75. Niho N, Takahashi M, Kitamura T, Shoji Y, Itoh M, Noda T, et al. Concomitant suppression of hyperlipidemia and intestinal polyp formation in *Apc*-deficient mice by peroxisome proliferator-activated receptor ligands. *J Control Release*. 2003;63: 6090–6095.
76. Li Q, Ishikawa T-OO, Oshima M, Taketo MM. The threshold level of adenomatous polyposis coli protein for mouse intestinal tumorigenesis. *Cancer Res*. 2005;65: 8622–8627.
77. Young M, Ordonez L, Clarke AR. What are the best routes to effectively model human colorectal cancer? *Mol Oncol*. Elsevier B.V; 2013;7: 178–89.
78. Moser AR, Dove WRF, Roth KA, Gordon JI. The *Min* (multiple intestinal neoplasia) mutation: its effect on gut epithelial cell differentiation and interaction with a modifier system. *J Cell Biol*. 1992;116: 1517–26.
79. Cormier RT, Hong KH, Halberg RB, Hawkins TL, Richardson P, Mulherkar R, et al. Secretory phospholipase *Pla2g2a* confers resistance to intestinal tumorigenesis. *Nat Genet*. 1997;17: 88–91.
80. MacPhee M, Chepenik KP, Liddell R a, Nelson KK, Siracusa LD, Buchberg a M. The secretory phospholipase *A2* gene is a candidate for the *Mom1* locus, a major modifier of *ApcMin*-induced intestinal neoplasia. *Cell*. 1995;81: 957–966.
81. Dietrich WF, Lander ES, Smith JS, Moser a R, Gould K a, Luongo C, et al. Genetic identification of *Mom-1*, a major modifier locus affecting *Min*-induced intestinal neoplasia in the mouse. *Cell*. 1993;75: 631–9.
82. Gould KA, Luongo C, Moser AR, McNeley MK, Borenstein N, Shedlovsky A, et al. Genetic evaluation of candidate genes for the *Mom1* modifier of intestinal neoplasia in mice. *Genetics*. 1996;144: 1777–1785.
83. Silverman KA, Koratkar R, Siracusa LD, Buchberg AM. Identification of the modifier of *Min 2* (*Mom2*) locus, a new mutation that influences *Apc*-induced intestinal neoplasia. *Genome Res*. 2002;12: 88–97.
84. Haines J, Johnson V, Pack K, Suraweera N, Slijepcevic P, Cabuy E, et al. Genetic basis of variation in adenoma multiplicity in *ApcMin/+ Mom1S* mice. *Proc Natl Acad Sci U S A*. 2005;102: 2868–2873.
85. Oikarinen SI, Cleveland AG, Cork KM, Bynot?? KK, Rafter JJ, Gustafsson J ??ke, et al. Genetic mapping of *Mom5*, a novel modifier of *ApcMin*-induced intestinal tumorigenesis. *Carcinogenesis*. 2009;30: 1591–1596.
86. Kwong LN, Shedlovsky A, Biehl BS, Clipson L, Pasch C a, Dove WF. Identification of *Mom7*, a novel modifier of *Apc(Min/+)* on mouse chromosome 18. *Genetics*. 2007;176: 1237–44.
87. Crist RC, Roth JJ, Lisanti MP, Siracusa LD, Buchberg AM. Identification of *Mom12* and *Mom13*, two novel modifier loci of *Apc Min*-mediated intestinal tumorigenesis. *Cell Cycle*. 2011;10: 1092–1099.
88. Papanikolaou A. Sequential and morphological analyses of aberrant crypt foci formation in mice of differing susceptibility to azoxymethane-induced colon carcinogenesis. *Carcinogenesis*. 2000;21: 1567–1572.
89. Glickman LT, Suissa S, Fleischer DM. Proliferative characteristics of chronic crypt cells in

- C57BL/6J and A/J mice as predictors of subsequent tumor formation. *Cancer Res.* 1987;47: 4766–70.
90. Meunier C, Cai J, Fortin A, Kwan T, Marquis J-F, Turbide C, et al. Characterization of a major colon cancer susceptibility locus (Ccs3) on mouse chromosome 3. *Oncogene.* Nature Publishing Group; 2010;29: 647–61.
 91. Meunier C, Kwan T, Turbide C, Beauchemin N, Gros P. Genetic control of susceptibility to carcinogen-induced colorectal cancer in mice: The Ccs3 and Ccs5 loci regulate different aspects of tumorigenesis. *Cell Cycle.* 2011;10: 1739–1749.
 92. Van Der Kraak L, Meunier C, Turbide C, Jothy S, Gaboury L, Marcus V, et al. A two-locus system controls susceptibility to colitis-associated colon cancer in mice. *Oncotarget.* 2010;1: 436–446.
 93. Ølstørn HB. The effect of acrylamide and glycidamide on intestinal carcinogenesis in mice. PhD Dissertation. Faculty of Mathematics and Natural Sciences, University of Oslo. 2009.
 94. World Cancer Research Fund, American Institute for Cancer Research. Food, Nutrition, Physical Activity, and the Prevention of Cancer: a Global Perspective. Washington DC; 2007.
 95. Bouvard V, Loomis D, Guyton KZ, Grosse Y, Ghissassi F El, Benbrahim-Tallaa L, et al. Carcinogenicity of consumption of red and processed meat. *Lancet Oncol.* Elsevier; 2015;
 96. Oostindjer M, Alexander J, Amdam GV, Andersen G, Bryan NS, Chen D, et al. The role of red and processed meat in colorectal cancer development: A review, based on findings from a workshop. *Meat Sci.* Elsevier B.V.; 2014;97: 583–596.
 97. Santarelli RL, Pierre F, Corpet DE. Processed meat and colorectal cancer: a review of epidemiologic and experimental evidence. *Nutr Cancer.* 2008;60: 131–44.
 98. zur Hausen H. Red meat consumption and cancer: reasons to suspect involvement of bovine infectious factors in colorectal cancer. *Int J Cancer.* 2012;130: 2475–83.
 99. Ferlay J, Soerjomataram I, Ervik M, Dikshit R, Eser S, Mathers C, et al. GLOBOCAN 2012 v1.0, Cancer Incidence and Mortality Worldwide: IARC CancerBase No. 11 [Internet]. 2013 [cited 21 May 2015].
 100. Lai C, Dunn DM, Miller MF, Pence BC. Non-promoting effects of iron from beef in the rat colon carcinogenesis model. *Cancer Lett.* 1997;112: 87–91.
 101. McIntosh GH, Regester GO, Le Leu RK, Royle PJ, Smithers GW. Dairy proteins protect against dimethylhydrazine-induced intestinal cancers in rats. *J Nutr.* 1995;125: 809–16.
 102. Pence BC, Landers M, Dunn DM, Shen CL, Miller MF. Feeding of a well-cooked beef diet containing a high heterocyclic amine content enhances colon and stomach carcinogenesis in 1,2-dimethylhydrazine-treated rats. *Nutr Cancer.* 1998;30: 220–6.
 103. Pence BC, Butler MJ, Dunn DM, Miller MF, Zhao C, Landers M. Non-promoting effects of lean beef in the rat colon carcinogenesis model. *Carcinogenesis.* 1995;16: 1157–60.
 104. Nutter RL, Gridley DS, Kettering JD, Goude AG, Slater JM. BALB/c mice fed milk or beef protein: differences in response to 1,2-dimethylhydrazine carcinogenesis. *J Natl Cancer Inst.* 1983;71: 867–74.
 105. Corpet DE. Red meat and colon cancer: should we become vegetarians, or can we make meat safer? *Meat Sci.* 2011;89: 310–6.
 106. Pierre FHF, Martin OCB, Santarelli RL, Taché S, Naud N, Guéraud F, et al. Calcium and α -

- tocopherol suppress cured-meat promotion of chemically induced colon carcinogenesis in rats and reduce associated biomarkers in human volunteers. *Am J Clin Nutr.* 2013;98: 1255–62.
107. Chenni FZ, Taché S, Naud N, Guéraud F, Hobbs DA, Kunhle GGC, et al. Heme-induced biomarkers associated with red meat promotion of colon cancer are not modulated by the intake of nitrite. *Nutr Cancer.* 2013;65: 227–33.
 108. Bastide NM, Chenni F, Audebert M, Santarelli RL, Taché S, Naud N, et al. A central role for heme iron in colon carcinogenesis associated with red meat intake. *Cancer Res.* 2015;75: 870–879.
 109. Pierre F, Freeman A, Tache S, Van der Meer R, Corpet DE. Beef Meat and Blood Sausage Promote the Formation of Azoxymethane-Induced Mucin-Depleted Foci and Aberrant Crypt Foci in Rat Colons. *J Nutr.* 2004;134: 2711–2716.
 110. Pierre F, Tache S, Guéraud F, Rerole AL, Jourdan M-L, Petit C. Apc mutation induces resistance of colonic cells to lipoperoxide-triggered apoptosis induced by faecal water from haem-fed rats. *Carcinogenesis.* 2007;28: 321–7.
 111. Pierre F, Santarelli RL, Allam O, Tache S, Naud N, Gueraud F, et al. Freeze-dried ham promotes azoxymethane-induced mucin-depleted foci and aberrant crypt foci in rat colon. *Nutr Cancer.* 2010;62: 567–73.
 112. Demeyer D, Mertens B, De Smet S, Ulens M. Mechanisms Linking Colorectal Cancer to the Consumption of (Processed) Red Meat: A Review. *Crit Rev Food Sci Nutr.* 2015;15.
 113. Hammerling U, Laurila JB, Grafström R, Ilbäck N-G. Consumption of Red/processed Meat and Colorectal Carcinoma: Possible Mechanisms underlying the Significant Association. *Crit Rev Food Sci Nutr.* 2015;
 114. Bastide NM, Pierre FHF, Corpet DE. Heme iron from meat and risk of colorectal cancer: a meta-analysis and a review of the mechanisms involved. *Cancer Prev Res.* 2011;4: 177–84.
 115. Cross AJ, Pollock JRA, Bingham SA. Haem, not protein or inorganic iron, is responsible for endogenous intestinal N-nitrosation arising from red meat. *Cancer Res.* 2003;63: 2358–60.
 116. Herrmann SS. N-nitrosamines in processed meat products – analysis, occurrence, formation, mitigation and exposure. Technical University of Denmark. 2014.
 117. Cross AJ, Sinha R. Meat-related mutagens/carcinogens in the etiology of colorectal cancer. *Environ Mol Mutagen.* 2004;44: 44–55.
 118. Ijssennagger N, Belzer C, Hooiveld GJ, Dekker J, van Mil SWC, Müller M, et al. Gut microbiota facilitates dietary heme-induced epithelial hyperproliferation by opening the mucus barrier in colon. *Proc Natl Acad Sci.* 2015;112: 201507645.
 119. Corpet DE, Pierre F. Point : From Animal Models to Prevention of Colon Cancer. Systematic Review of Chemoprevention in Min Mice and Choice of the Model System. *Cancer Epidemiol Biomarkers Prev.* 2003;12: 391–400.
 120. Maddison K, Clarke AR. New approaches for modelling cancer mechanisms in the mouse. *J Pathol.* 2005;205: 181–193.
 121. Waterston RH, Lindblad-Toh K, Birney E, Rogers J, Abril JF, Agarwal P, et al. Initial sequencing and comparative analysis of the mouse genome. *Nature.* 2002;420: 520–562.
 122. Rangarajan A, Weinberg RA. Opinion: Comparative biology of mouse versus human cells: modelling human cancer in mice. *Nat Rev Cancer.* 2003;3: 952–959.

123. Evans JP, Sutton PA, Winiarski BK, Fenwick SW, Malik HZ, Vimalachandran D, et al. From mice to men; murine models of colorectal cancer for use in translational research. *Crit Rev Oncol Hematol*. Elsevier Ireland Ltd; 2015;98: 94–105.
124. Papanikolaou a, Wang QS, Delker D a, Rosenberg DW. Azoxymethane-induced colon tumors and aberrant crypt foci in mice of different genetic susceptibility. *Cancer Lett*. 1998;130: 29–34.
125. Paulsen JE, Steffensen IL, Andreassen a, Vikse R, Alexander J. Neonatal exposure to the food mutagen 2-amino-1-methyl-6-phenylimidazo[4,5-b]pyridine via breast milk or directly induces intestinal tumors in multiple intestinal neoplasia mice. *Carcinogenesis*. 1999;20: 1277–1282.
126. Paulsen JE, Elvsaaas IK, Steffensen IL, Alexander J. A fish oil derived concentrate enriched in eicosapentaenoic and docosahexaenoic acid as ethyl ester suppresses the formation and growth of intestinal polyps in the Min mouse. *Carcinogenesis*. 1997;18: 1905–1910.
127. Ershler WB, Longo DL. Aging and cancer: issues of basic and clinical science. *J Natl Cancer Inst*. 1997;89: 1489–97.
128. Cooper HS, Chang W-CL, Coudry R, Gary MA, Everley L, Spittle CS, et al. Generation of a unique strain of multiple intestinal neoplasia (Apc(+)/Min-FCCC) mice with significantly increased numbers of colorectal adenomas. *Mol Carcinog*. 2005;44: 31–41.
129. Cooper HS, Everley L, Chang WC, Pfeiffer G, Lee B, Murthy S, et al. The role of mutant Apc in the development of dysplasia and cancer in the mouse model of dextran sulfate sodium–induced colitis. *Gastroenterology*. 2001;121: 1407–1416.
130. Halberg RB, Waggoner J, Rasmussen K, White A, Clipson L, Prunuske AJ, et al. Long-lived Min mice develop advanced intestinal cancers through a genetically conservative pathway. *Cancer Res*. 2009;69: 5768–75.
131. Flurkey K, Currer JM, Harrison DE. Mouse models in ageing research. In: Fox JG, Barthold S, Davisson M, Newcomer CE, Quimby FW, Smith A, editors. *The Mouse in Biomedical Research: Normative Biology, Husbandry, and Models*. 2nd ed. Academic Press; 2006. pp. 637–672.
132. Vogelstein B, Fearon ER, Hamilton SR, Kern SE, Preisinger AC, Leppert M, et al. Genetic alterations during colorectal-tumor development. *N Engl J Med*. 1988;319: 525–32.
133. Halberg RB, Katzung DS, Hoff PD, Moser a R, Cole CE, Lubet R a, et al. Tumorigenesis in the multiple intestinal neoplasia mouse: redundancy of negative regulators and specificity of modifiers. *Proc Natl Acad Sci U S A*. 2000;97: 3461–3466.
134. Janssen K-P, Alberici P, Fsihi H, Gaspar C, Breukel C, Franken P, et al. APC and oncogenic KRAS are synergistic in enhancing Wnt signaling in intestinal tumor formation and progression. *Gastroenterology*. 2006;131: 1096–1099.
135. Taketo MM, Takaku K. Gastrointestinal tumorigenesis in Smad4 (Dpc4) mutant mice. *Hum Cell*. 2000;13: 85–95.
136. Hamamoto T, Beppu H, Okada H, Kawabata M, Kitamura T, Miyazono K, et al. Compound disruption of Smad2 accelerates malignant progression of intestinal tumors in Apc knock-out mice. *Cancer Res*. 2002;62: 5955–5961.
137. Castets M, Broutier L, Molin Y, Brevet M, Chazot G, Gadot N, et al. DCC constrains tumour progression via its dependence receptor activity. *Nature*. 2011;482: 534–537.
138. Yamada Y, Mori H. Multistep carcinogenesis of the colon in Apc(Min/+) mouse. *Cancer Sci*.

2007;98: 6–10.

139. Yamada Y, Hata K, Hirose Y, Hara A, Sugie S, Kuno T, et al. Microadenomatous lesions involving loss of Apc heterozygosity in the colon of adult Apc(Min/+) mice. *Cancer Res.* 2002;62: 6367–6370.
140. Oyama T, Yamada Y, Hata K, Tomita H, Hirata A, Sheng H, et al. Further upregulation of beta-catenin/Tcf transcription is involved in the development of macroscopic tumors in the colon of ApcMin/+ mice. *Carcinogenesis.* 2008;29: 666–72.
141. Chung HY, Cesari M, Anton S, Marzetti E, Giovannini S, Seo AY, et al. Molecular inflammation: underpinnings of aging and age-related diseases. *Ageing Res Rev.* 2009;8: 18–30.
142. Issa J. Aging and epigenetic drift: a vicious cycle. *J Clin Invest.* 2014;124.
143. Jung M, Pfeifer GP. Aging and DNA methylation. *BMC Biol.* 2015;13: 7.
144. Niehrs C. Function and biological roles of the Dickkopf family of Wnt modulators. *Oncogene.* 2006;25: 7469–7481.
145. Aguilera O, Fraga MF, Ballestar E, Paz MF, Herranz M, Espada J, et al. Epigenetic inactivation of the Wnt antagonist DICKKOPF-1 (DKK-1) gene in human colorectal cancer. *Oncogene.* 2006;25: 4116–21.
146. González-Sancho JM, Aguilera O, García JM, Pendás-Franco N, Peña C, Cal S, et al. The Wnt antagonist DICKKOPF-1 gene is a downstream target of beta-catenin/TCF and is downregulated in human colon cancer. *Oncogene.* 2005;24: 1098–1103.
147. Qi L, Sun B, Liu Z, Li H, Gao J, Leng X. Dickkopf-1 inhibits epithelial-mesenchymal transition of colon cancer cells and contributes to colon cancer suppression. *Cancer Sci.* 2012;103: 828–835.
148. Maehata T, Taniguchi H, Yamamoto H, Noshio K, Adachi Y, Miyamoto N, et al. Transcriptional silencing of Dickkopf gene family by CpG island hypermethylation in human gastrointestinal cancer. *World J Gastroenterol.* 2008;14: 2702–2714.
149. Frank S a. History of Theories. Dynamics of Cancer Incidence, Inheritance, and Evolution. Princeton, New Jersey: Princeton University Press; 2007. pp. 59–81.
150. Frank S. Stem Cells: Tissue Renewal. Dynamics of Cancer Incidence, Inheritance, and Evolution. Princeton, New Jersey: Princeton University Press; 2007. pp. 251–270.
151. Tomasetti C, Vogelstein B. Variation in cancer risk among tissues can be explained by the number of stem cell divisions. *Science (80-).* 2015;347: 78–81.
152. Potten CS, Booth C, Hargreaves D. The small intestine as a model for evaluating adult tissue stem cell drug targets. *Cell Prolif.* 2003;36: 115–129.
153. Guda K, Marino JN, Jung Y, Cray KEN, Dong M, Rosenberg DW. Strain-specific homeostatic responses during early stages of Azoxymethane-induced colon tumorigenesis in mice. *Int J Oncol.* 2007;31: 837–842.
154. Corpet DE, Pierre F. How good are rodent models of carcinogenesis in predicting efficacy in humans? A systematic review and meta-analysis of colon chemoprevention in rats, mice and men. *Eur J Cancer.* 2005;41: 1911–22.
155. Jacoby RF, Marshall DJ, Newton MA, Novakovic K, Tutsch K, Cole CE, et al. Chemoprevention of Spontaneous Intestinal Adenomas in the Apc Min Mouse Model by the

Nonsteroidal Anti-inflammatory Drug Piroxicam. *Cancer Res.* 1996;56: 710–714.

156. Maltzman T, Whittington J, Driggers L, Stephens J, Ahnen D. AOM-induced mouse colon tumors do not express full-length APC protein. *Carcinogenesis.* 1997;18: 2435–2439.
157. Møllersen L, Paulsen JE, Alexander J. Loss of heterozygosity and nonsense mutation in Apc in azoxymethane-induced colonic tumours in min mice. *Anticancer Res.* 2004;24: 2595–9.
158. Takahashi M, Wakabayashi K. Gene mutations and altered gene expression in azoxymethane-induced colon carcinogenesis in. 2004;95: 475–480.
159. Kohno H, Suzuki R, Sugie S, Tanaka T. B-Catenin mutations in a mouse model of inflammation-related colon carcinogenesis induced by 1,2-dimethylhydrazine and dextran sodium sulfate. *Cancer Sci.* 2005;96: 69–76.
160. Suzui M, Okuno M, Tanaka T, Nakagama H, Moriwaki H. Enhanced colon carcinogenesis induced by azoxymethane in min mice occurs via a mechanism independent of beta-catenin mutation. *Cancer Lett.* 2002;183: 31–41.
161. Cao X, Eu KW, Seow-Choen F, Cheah PY. Germline mutations are frequent in the APC gene but absent in the beta-catenin gene in familial adenomatous polyposis patients. *Genes Chromosomes Cancer.* 1999;25: 396–8.
162. Iwamoto M. Expression of beta-catenin and full-length APC protein in normal and neoplastic colonic tissues. *Carcinogenesis.* 2000;21: 1935–1940.
163. Femia A Pietro, Luceri C, Soares PV, Lodovici M, Caderni G. Multiple mucin depleted foci, high proliferation and low apoptotic response in the onset of colon carcinogenesis of the PIRC rat, mutated in Apc. *Int J Cancer.* 2015;136: E488–95.
164. Washington MK, Powell AE, Sullivan R, Sundberg JP, Wright N, Coffey RJ, et al. Pathology of rodent models of intestinal cancer: Progress report and recommendations. *Gastroenterology.* Elsevier Inc.; 2013;144: 705–717.
165. Amos-Landgraf JM, Heijmans J, Wielenga MCB, Dunkin E, Krentz KJ, Clipson L, et al. Sex disparity in colonic adenomagenesis involves promotion by male hormones, not protection by female hormones. *Proc Natl Acad Sci U S A.* National Academy of Sciences; 2014;111: 16514–9.
166. Bird RP, McLellan EA, Bruce WR. Aberrant crypts, putative precancerous lesions, in the study of the role of diet in the aetiology of colon cancer. *Cancer Surv.* 1989;8: 189–200.
167. Di Gregorio C, Losi L, Fante R, Modica S, Ghidoni M, Pedroni M, et al. Histology of aberrant crypt foci in the human colon. *Histopathology.* 1997;30: 328–334.
168. Suzui M, Morioka T, Yoshimi N. Colon Preneoplastic Lesions in Animal Models. *J Toxicol Pathol.* 2013;26: 335–341.
169. Wargovich MJ, Brown VR, Morris J. Aberrant crypt foci: the case for inclusion as a biomarker for colon cancer. *Cancers (Basel).* 2010;2: 1705–16.
170. Corpet DE. ACF, MDF, BCAC: Pre-Cancerous Lesions? [Internet]. [cited 23 Feb 2016].
171. Femia A Pietro, Caderni G. Rodent models of colon carcinogenesis for the study of chemopreventive activity of natural products. *Planta Med.* 2008;74: 1602–1607.
172. Pierre F, Taché S, Petit CR, Van der Meer R, Corpet DE. Meat and cancer: haemoglobin and haemin in a low-calcium diet promote colorectal carcinogenesis at the aberrant crypt stage in rats. *Carcinogenesis.* 2003;24: 1683–90.

173. Pierre F, Santarelli R, Taché S, Guéraud F, Corpet DE. Beef meat promotion of dimethylhydrazine-induced colorectal carcinogenesis biomarkers is suppressed by dietary calcium. *Br J Nutr*. 2008;99: 1000–6.
174. Santarelli RL, Naud N, Taché S, Guéraud F, Vendevre JL, Zhou L, et al. Calcium inhibits promotion by hot dog of 1,2-dimethylhydrazine-induced mucin-depleted foci in rat colon. *Int J Cancer*. 2013;133: 2533–2541.
175. Winter J, Young GP, Hu Y, Gratz SW, Conlon MA, Le Leu RK. Accumulation of promutagenic DNA adducts in the mouse distal colon after consumption of heme does not induce colonic neoplasms in the western diet model of spontaneous colorectal cancer. *Mol Nutr Food Res*. 2014;58: 550–8.
176. IJssennagger N, Derrien M, van Doorn GM, Rijnierse A, van den Bogert B, Müller M, et al. Dietary heme alters microbiota and mucosa of mouse colon without functional changes in host-microbe cross-talk. *PLoS One*. 2012;7: e49868.
177. IJssennagger N, Rijnierse A, de Wit N, Jonker-Termont D, Dekker J, Müller M, et al. Dietary haem stimulates epithelial cell turnover by downregulating feedback inhibitors of proliferation in murine colon. *Gut*. 2012;61: 1041–9.
178. IJssennagger N, de Wit N, Müller M, van der Meer R. Dietary heme-mediated PPAR α activation does not affect the heme-induced epithelial hyperproliferation and hyperplasia in mouse colon. Veitia RA, editor. *PLoS One*. Public Library of Science; 2012;7: e43260.
179. de Vogel J, Van-Eck WB, Sesink ALA, Jonker-Termont DSML, Kleibeuker J, van der Meer R. Dietary heme injures surface epithelium resulting in hyperproliferation, inhibition of apoptosis and crypt hyperplasia in rat colon. *Carcinogenesis*. 2008;29: 398–403.
180. IJssennagger N, Rijnierse A, de Wit NJW, Boekschoten M V, Dekker J, Schonewille A, et al. Dietary heme induces acute oxidative stress, but delayed cytotoxicity and compensatory hyperproliferation in mouse colon. *Carcinogenesis*. 2013;34: 1628–35.
181. Sawa T, Akaike T, Kida K, Fukushima Y, Takagi K, Maeda H. Lipid peroxy radicals from oxidized oils and heme-iron: implication of a high-fat diet in colon carcinogenesis. *Cancer Epidemiol biomarkers Prev*. 1998;7: 1007–1012.
182. Negre-Salvayre A, Coatrieux C, Ingueneau C, Salvayre R. Advanced lipid peroxidation end products in oxidative damage to proteins. Potential role in diseases and therapeutic prospects for the inhibitors. *Br J Pharmacol*. 2008;153: 6–20.
183. Sesink ALA, Termont DSML, Kleibeuker JH, Van der Meer R. Red Meat and Colon Cancer: The Cytotoxic and Hyperproliferative Effects of Dietary Heme. *Cancer Res*. 1999;59: 5704–5709.
184. Weston A, Harris CC. Multistage Carcinogenesis. In: Kufe DW, Pollock RE, Weichselbaum RR, Bast RC, Gansler TS, Holland JM, et al., editors. *Holland-Frei Cancer Medicine*. 6th ed. Hamilton, ON: BC Decker; 2003.
185. Irigaray P, Belpomme D. Basic properties and molecular mechanisms of exogenous chemical carcinogens. *Carcinogenesis*. 2010;31: 135–148.
186. Parnaud G, Peiffer G, Taché S, Corpet DE. Effect of meat (beef, chicken, and bacon) on rat colon carcinogenesis. *Nutr Cancer*. 1998;32: 165–173.
187. Zhong W, Xia Z, Hinrichs D, Rosenbaum JT, Wegmann KW, Meyrowitz J, et al. Hemin exerts multiple protective mechanisms and attenuates dextran sulfate sodium-induced colitis. *J*

Pediatr Gastroenterol Nutr. 2010;50: 132–9.

188. Barnes CJ, Lee M. Chemoprevention of spontaneous intestinal adenomas in the adenomatous polyposis coli Min mouse model with aspirin. *Gastroenterology.* 1998;114: 873–877.
189. Lombardi-Boccia G, Martinez-Dominguez B, Aguzzi A. Total Heme and Non-heme Iron in Raw and Cooked Meats. *J Food Sci.* 2002;67: 1738–1741.

Scientific papers I-III



Spontaneous initiation, promotion and progression of colorectal cancer in the novel A/J Min/+ mouse

Marianne Sørdring¹, Gjermund Gunnes² and Jan Erik Paulsen¹

¹Department of Food Safety and Infection Biology, Norwegian University of Life Sciences, Oslo, Norway

²Department of Basic Sciences and Aquatic Medicine, Norwegian University of Life Sciences, Oslo, Norway

The C57BL/6J multiple intestinal neoplasia (Min/+) mouse is a widely used murine model for familial adenomatous polyposis, a hereditary form of human colorectal cancer. However, it is a questionable model partly because the vast majority of tumors arise in the small intestine, and partly because the fraction of tumors that progress to invasive carcinomas is minuscule. A/J mice are typically more susceptible to carcinogen-induced colorectal cancer than C57BL/6J mice. To investigate whether the novel Min/+ mouse on the A/J genetic background could be a better model for colorectal cancer, we examined the spontaneous intestinal tumorigenesis in 81 A/J Min/+ mice ranging in age from 4 to 60 weeks. The A/J Min/+ mouse exhibited a dramatic increase in number of colonic lesions when compared to what has been reported for the conventional Min/+ mouse; however, an increase in small intestinal lesions did not occur. In addition, this novel mouse model displayed a continual development of colonic lesions highlighted by the transition from early lesions (flat ACF) to tumors over time. In mice older than 40 weeks, 13 colonic (95% CI: 8.7–16.3) and 21 small intestinal (95% CI: 18.6–24.3) tumors were recorded. Notably, a considerable proportion of those lesions progressed to carcinomas in both the colon (21%) and small intestine (51%). These findings more closely reflect aspects of human colorectal carcinogenesis. In conclusion, the novel A/J Min/+ mouse may be a relevant model for initiation, promotion and progression of colorectal cancer.

Colorectal cancer is the third most common cancer worldwide and accounted for approximately 1.4 million new cases and close to 700,000 deaths in 2012. Incidence rates are slightly higher in men than in women, and this cancer becomes increasingly more common with age.¹ One of the most common inherited colorectal cancer syndromes is familial adenomatous polyposis (FAP), which is caused by germline mutations in the tumor-suppressor gene adenomatous polyposis coli (*APC*).^{2,3} FAP patients inherit a mutated *APC* allele and when the second allele is inactivated by mutation, a large number of adenomas develop in the colon.⁴ Inactivation of the second *APC* allele leads to reduced degradation of β -catenin and activation of the canonical Wnt signaling pathway, which in turn leads to dysplasia.^{5,6} Mutation in one *APC* allele followed by mutation in, or loss of, the second allele is also apparent in ~80% of sporadic colorectal cancer cases.⁷ In humans, most colorectal cancers progress slowly, taking anywhere from 5 to 20 years for early colonic lesions to develop into benign adenomas, and an additional 5 to 15

years for those adenomas to develop into malignant carcinomas.^{8,9}

One of the most frequently used murine models for colorectal cancer is the multiple intestinal neoplasia (Min/+) mouse (*Mus musculus*). This particular mouse model was discovered after a random mutation by the mutagen ethylnitrosourea caused spontaneous formation of adenomas throughout the intestinal tract.¹⁰ Similar to the mutation seen in the human *APC* gene, the Min/+ mouse has a heterozygous truncation mutation at codon 850 of its *Apc* gene, which results in the spontaneous formation of numerous neoplastic lesions in the mouse intestine.^{4,11–13}

The appearance of preneoplastic lesions is the first step in colon carcinogenesis, and the ability to recognize these early stages of colorectal cancer is an important factor in the development of reliable biomarkers for colorectal cancer early detection, diagnosis and treatment.¹⁴ Putative preneoplastic lesions known as aberrant crypt foci (ACF) were originally described in the colon of carcinogen-treated mice.¹⁵ These lesions were identified by a characteristic morphology of enlarged crypts, thickened epithelial lining, irregular lumens, increased pericryptal space and elevation from the mucosa.^{15,16} In 2000, Paulsen *et al.*¹⁷ did not detect any ACF in the colon of C57BL/6 Min/+ mice, but instead discovered enlarged, flat dysplastic crypts with compressed luminal openings that were given the name ACF_{Min}, later renamed flat ACF when identical lesions were identified in rats.^{17,18} These flat ACF differed from the “classic” ACF first described by Bird¹⁵ in that they were not elevated from the mucosa,

Key words: colorectal cancer, A/J Min/+ mouse, intestinal tumorigenesis, carcinoma

DOI: 10.1002/ijc.29928

History: Received 20 July 2015; Accepted 2 Nov 2015; Online 13 Nov 2015

Correspondence to: Marianne Sørdring, Department of Food Safety and Infection Biology, Norwegian University of Life Sciences, PO Box 8146 Dep., 0033 Oslo, Norway, Fax: +47-6496-5001, E-mail: marianne.sordring@nmbu.no

What's new?

Human colorectal cancer (CRC) manifests itself as benign tumors in the colon that progress to carcinomas. In contrast, most rodent CRC models for Apc-driven tumorigenesis primarily develop benign tumors in the small intestine instead of the colon, which rarely progress to carcinomas. Here, the novel A/J Min/+ mouse was observed to spontaneously develop numerous colonic lesions, and a progression from benign tumor to carcinoma was found in both the colon and small intestine.

and they were not visible without methylene blue staining and transillumination. Later studies revealed that only the flat ACF, not the classic ACF, exhibited a continuous development from the monocryptal stage to tumors, suggesting that these flat ACF are in fact early stages of colon carcinogenesis.^{17,19}

The conventional Min/+ mouse is bred on a C57BL/6J (B6) genetic background, a substrain of the C57BL/6 which is likely one of the best known and most widely used inbred mouse strains.²⁰ It has been shown that the B6 substrain is relatively resistant to colonic carcinogens, and the B6 Min/+ mouse primarily develops adenomas in the small intestine and only a few lesions in the colon that rarely progress to cancer.^{10,21–23} On the other hand, an A/J genetic background strain has been found to be highly susceptible to colon-specific carcinogens.^{23–25} A new Min/+ mouse model has been established at the Norwegian Institute of Public Health, where the Min/+ trait has been transferred from the B6 Min/+ mouse to mice with an A/J genetic background by backcrossing for >12 generations, producing an A/J Min/+ mouse.²⁶ After establishing the A/J Min/+ mouse, it was discovered that this mouse was more susceptible to both spontaneous and azoxymethane (AOM)-induced colon carcinogenesis than the B6 Min/+ mouse.²⁶

The objective of this work was to study the long-term spontaneous intestinal tumorigenesis in the novel A/J Min/+ mouse with focus on determining its potential use as a model for colorectal cancer.

Material and Methods**Animals, housing and diet**

This study was conducted in strict accordance with The Norwegian Regulation on Animal Experimentation, and approved by the Institutional Animal Care and Use Committee at the Norwegian University of Life Sciences, Campus Adamstuen. The A/J Min/+ mouse was created at the Norwegian Institute of Public Health after backcrossing of the Min/+ trait onto an A/J genetic background for >12 generations, securing their status as inbred.²⁶ This mouse strain was transferred to the Department of Experimental Biomedicine at the Norwegian University of Life Sciences, Campus Adamstuen, where it has been maintained as an inbred colony for several additional generations. A/J Min/+ males were mated with A/J +/+ females, and the resulting A/J Min/+ pups ($n = 81$, 48 females and 33 males) were used for the study. All animals were housed in Makrolon Type III open top plastic

cages in a room with a 12-hr light/dark cycle, 55–65% humidity and 20–22°C. Water and feed were given *ad libitum*. All animals were fed the standard rodent diet RM1 (SDS Special Diet Services, Witham, UK) for the duration of the study. Mice were euthanized at various time points in order to get an overview of tumorigenesis in the A/J Min/+ mouse model. All mice were sacrificed by cervical dislocation.

For this study, a total of six age groups were represented: early juvenile, juvenile, mature adult, early middle-aged adult, middle-aged adult and late middle-aged adult (Table 1). The age groups were chosen based on Flurkey *et al.*²⁷ As only one Min/+ mouse lived to the age of 60 weeks, the late middle-aged adult age group was excluded from all data analyses, except correlation analysis. To describe the distribution of flat ACF and tumors in relation to age, all recorded lesions were grouped into lesion size classes. As the colonic lesions considered to be the smallest ranged in size from 0.002 to 0.008 mm², this was chosen as the first size class. The remaining lesions were grouped into four other size classes based on a suitable logarithmic scale with a base of 8: 0.009–0.064 mm², 0.065–0.512 mm², 0.513–4.096 mm² and lesions greater than 4.097 mm².

Identification of intestinal lesions

The colon and small intestines were prepared as previously described.²⁸ Once prepared, surface microscopy and transillumination using an inverted light microscope (CKX41, Olympus Inc., Hamburg, Germany) equipped with a digital color camera (DP25, Olympus) was used to examine the intestines for small intestinal and colonic tumors, as well as flat ACF. The flat ACF can be recognized by the color difference when

Table 1. Number and age span of A/J Min/+ mice separated into five age groups

Group	Age (weeks)	Number of mice (females/males)
Early juvenile	4–6	15 (15/0)
Juvenile	7–12	11 (6/5)
Mature adult	13–24	12 (10/2)
Early middle-aged adult	25–39	20 (9/11)
Middle-aged adult	40–56	22 (8/14)
Late middle-aged adult ¹	57–71	1 (0/1)

¹The late middle-aged adult age group was excluded from data analysis owing to the low number of mice in this age range.

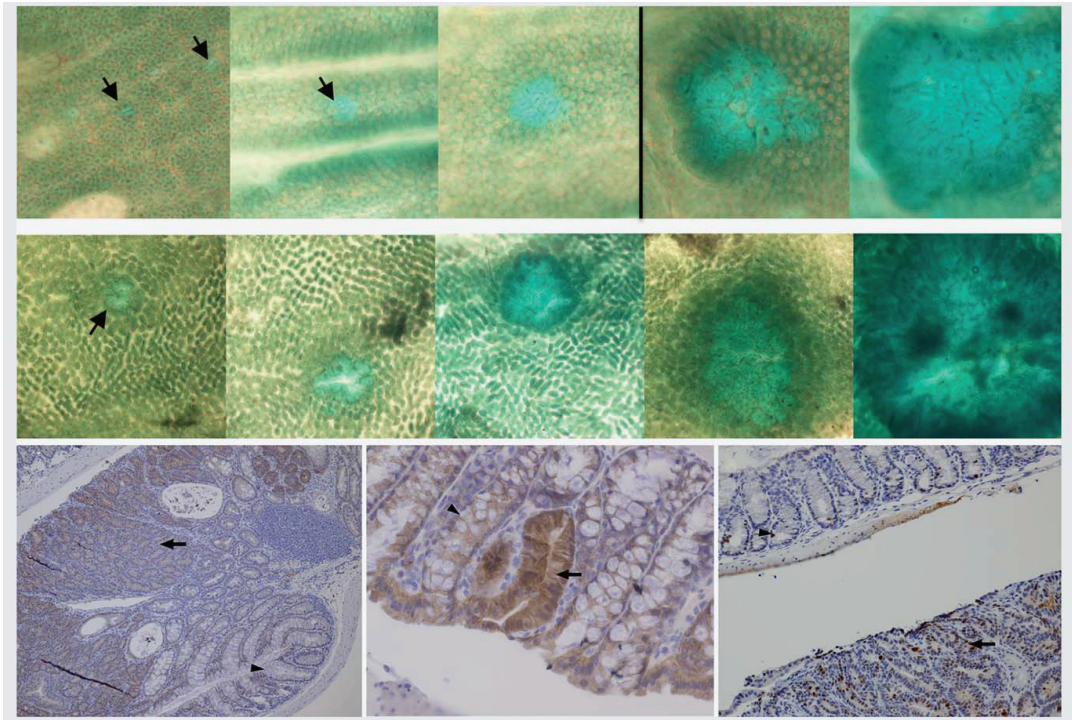


Figure 1. Representative examples of morphological features of intestinal lesions. Identification of methylene blue-stained (a) flat ACF and tumors in the colon (magnification $\times 100$) and (b) tumors in the small intestine (magnification $\times 40$). Both panel (a) and (b) are made up of different original images grouped together for clarity. Arrows point to small lesions. Images to the left of the vertical bar in panel (a) show flat ACF, while colonic tumors are shown to the right of the bar. Immunohistochemical analysis of β -catenin expression in the colon (c, d) shows that β -catenin in normal crypts (arrowheads) is present almost entirely at the cell border, while in the flat ACF/tumor, β -catenin accumulates in the cytoplasm (arrows). Panel (c) shows β -catenin accumulation in a tumor (magnification $\times 100$), while panel (d) shows β -catenin accumulation in a single-crypt flat ACF (magnification $\times 400$). Immunohistochemical analysis of the proliferation marker Ki67 in the colon (e) shows numerous Ki67-positive nuclei throughout the tissue of tumors (bottom right, arrow) but only in scattered cells at the bottom of the crypts in normal tissue (top left, arrowhead) (magnification $\times 200$).

compared to normal epithelia; flat ACF stain a brighter blue/green while normal crypts a more subdued brownish-green (Fig. 1a). Furthermore, flat ACF have enlarged crypts, lay flat against the surrounding epithelium and have compressed luminal opening which give the lesions a gyrus-like appearance. The tumor resembles the flat ACF, but contains 30 or more aberrant crypts, and is usually elevated from the mucosa. Tumors in the small intestine resemble tumors in the colon, but they appear as discrete depressions with multiple aberrant crypts surrounded by adjacent villi (Fig. 1b).

To study lesion development in the intestine, three variables were measured: (i) lesion size (mm^2), calculated from the diameter measured by surface microscopy using an eyepiece graticule, (ii) number of lesions and (iii) tumor load (mm^2), defined as the sum of the area of all lesions observed in an intestine. Two types of lesions were examined in the colon: flat ACF and tumor. As flat ACF are not present in

the small intestines, only tumors were recorded in this segment of the intestinal tract.

Histology

Intestines from 16 mice aged 15–60 weeks were used to examine whether carcinomas were formed in the A/J Min/+ mouse. These intestines were prepared as described above, followed by a modification of the Swiss roll technique.²⁹ Briefly, the longitudinally cut, flat-fixed, methylene blue-stained intestines were carefully rolled lengthwise, from proximal to distal end with the mucosa facing inward, using a pair of tweezers. The prepared Swiss rolls were embedded in paraffin, and each prepared paraffin block contained the small intestine (three segments: proximal, middle and distal) and the colon from one mouse. Histological sections (2–3 μm) were made at three different depths in the paraffin block in order to detect a larger number of intestinal lesions.

As the intestines were slit open longitudinally before Swiss roll preparation, the three depths were chosen to detect lesions on the right, center and left areas of the flattened intestine. Each section was then stained with periodic acid-Schiff (PAS) and scored by a pathologist. Lesions with clear infiltrative growth through the muscularis mucosae and into the submucosa were classified as carcinomas, while those without infiltrative growth were classified as adenomas. Regional lymph nodes and livers from a few older animals were embedded in paraffin, sliced and stained with hematoxylin and eosin (HE). Histological sections were examined for metastases.

Immunohistochemistry

The tissue was stained for β -catenin and Ki67 to assess Wnt signaling activation and increased proliferation, respectively. Paraffin sections were deparaffinized and rehydrated, before quenching endogenous peroxidases with 3.0% H_2O_2 . Antigen retrieval was performed in Tris/EDTA (pH 9.1) for β -catenin and in citrate buffer (pH 6.0) for Ki67. For β -catenin, sections were blocked using the Mouse on Mouse (M.O.M) kit (Vector Laboratories, Burlingame, CA), before incubation with a primary monoclonal antibody against β -catenin (Purified mouse anti- β -catenin, C19220; Transduction Laboratories, Lexington, KY) at a 1:2,500 dilution. Sections were incubated in M.O.M. biotinylated anti-mouse IgG reagent followed by addition of the avidin-biotinylated peroxidase complex. For Ki67, DAKO Envision kit was used (K401111-2, DAKO, Glostrup, Denmark). Sections were blocked using N-serum from goat in 5% BSA/TBS (1:50 dilution), before incubation with a primary polyclonal antibody against Ki67 (rabbit anti-Ki67, AB15580, Abcam PLC, Cambridge, UK) at a 1:1,000 dilution. Next, sections were incubated in anti-rabbit HRP-labeled polymer reagent (K401111-2, DAKO). For both β -catenin and Ki67, antibody binding was detected with DAB substrate according to the manufacturer's protocol (34065, Thermo Scientific Pierce, Waltham, MA for β -catenin, and K401111-2, DAKO for Ki67). Sections were counterstained with hematoxylin.

Statistics

Results are expressed as mean values with 95% confidence intervals. All comparisons were performed two-tailed with a significance level of 5%. A Spearman rank correlation coefficient (r_s) was computed to assess the relationship between intestinal lesions and age. Tumor distribution along the small intestine was tested with a one-way ANOVA followed by Tukey *post hoc* test. All statistical tests were completed using SigmaPlot statistical software (Systat Software, San Jose, CA).

Results

Gender differences

Because of the uneven gender distribution over time (Table 1), it was not possible to test for gender differences. However, both genders showed similar developmental trends with age;

males and females showed an increase in number of lesions and lesion load in both colon and small intestine, and both genders developed carcinomas. Therefore, data for males and females were pooled for further analysis. Males appeared to have a slightly higher incidence of lesions and lesion load, which has previously been seen in B6 Min/+ mice^{30,31}; however, in the 16 intestines examined for carcinomas, no significant difference between males and females was detected (two-tailed *t*-test: $p = 0.250$).

Colon

Scoring the total number of flat ACF and tumors in A/J Min/+ mice at different ages revealed large interindividual variation in colonic tumorigenesis, as illustrated by the scatter plot in Figure 2a. The highest number of colonic lesions (flat ACF and tumors) observed in a single colon was 82 lesions, while the highest number of colonic tumors in one colon was 41. An average of eight (95% CI: 5.82–9.83) colonic tumors developed in A/J Min/+ mice from 11 to 60 weeks, with the majority of tumors occurring in animals over the age of 25 weeks (mean 11; 95% CI: 7.98–13.13). In mice over the age of 40 weeks, an average of 13 (95% CI: 8.74–16.30) colonic tumors was observed. Colonic tumors were not evident before the age of 11 weeks, after which they continued to increase in number ($r_s = 0.805$, $n = 81$, $p < 0.001$). In contrast, flat ACF were observed in all animals. However, their numbers varied with age (Fig. 2a): from 0 to 24 weeks (from early juvenile to mature adult), the number of flat ACF increased ($r_s = 0.857$, $n = 38$, $p < 0.001$) while after 24 weeks, the number of flat ACF decreased ($r_s = -0.607$, $n = 43$, $p < 0.001$). This pattern of fluctuating number of flat ACF and increasing number of tumors is consistent with a possible transition of lesions from flat ACF to tumor as mice age, as previously suggested.^{18,19} This potential developmental relationship between flat ACF and tumors is further illustrated when the animals were separated into five age groups: early juvenile, juvenile, mature adult, early middle-aged adult and middle-aged adult (Fig. 2b; Table 1). During the last three periods, the number of flat ACF declined and the number of tumors increased. Grouping the animals also made it possible to calculate the fraction of newly formed flat ACF (influx) at the different ages (Fig. 2b), given that the total number of lesions solely comprises new flat ACF, previously formed flat ACF and tumors, and that flat ACF develop into tumors. The formation of flat ACF peaked at the juvenile age group and declined to a minimum in middle-aged adult. The total number of lesions was somewhat reduced in middle-aged adult, possibly due to some regression of small lesions or merging of larger lesions. The tumor load (total area of tumors per animal) increased dramatically with age (Fig. 2c).

All flat ACF and tumors recorded in each colon in each age group were grouped together according to size, and the average number of lesions per size group per animal was calculated (Fig. 2d). These size distributions of pooled flat ACF

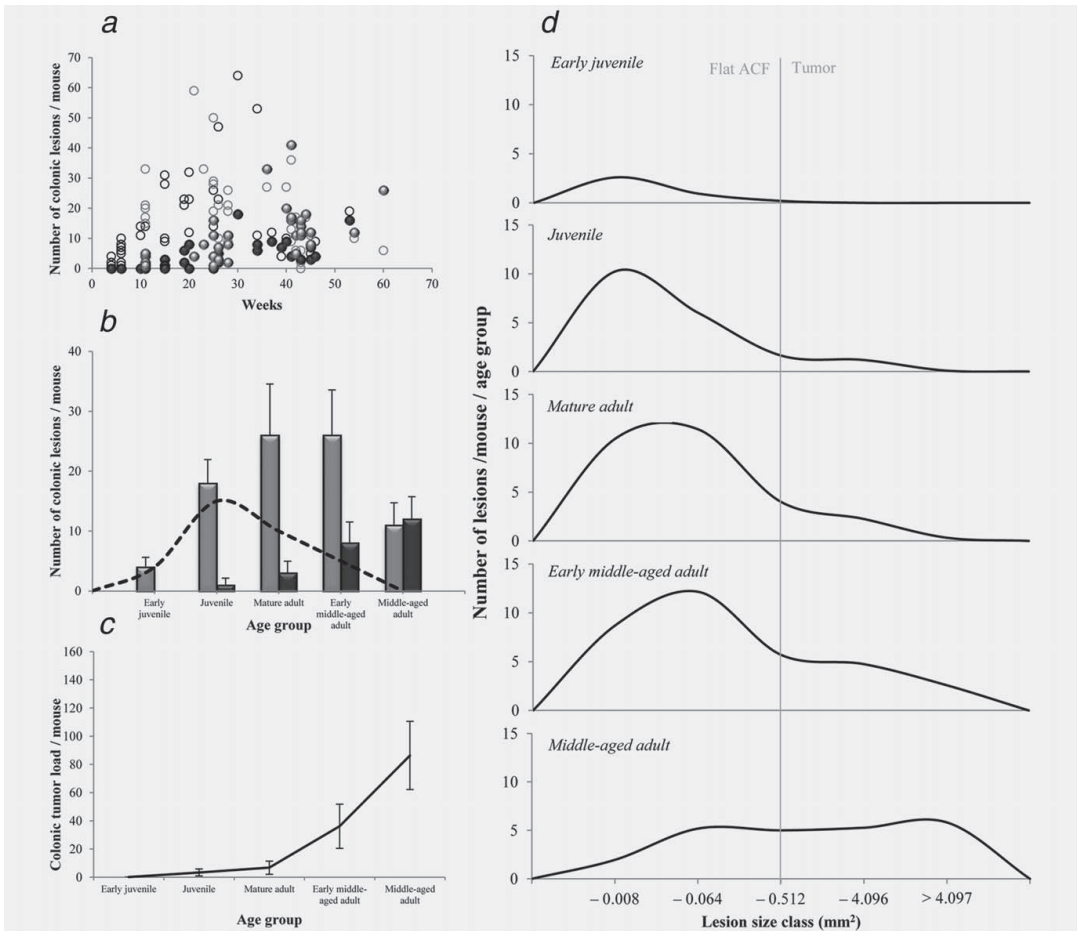


Figure 2. Number, size and load of lesions spontaneously formed in the colon of A/J Min/+ mice. (a) Distribution of flat ACF and tumors in mice ranging from 4 to 60 weeks. Solid gray and solid black circles represent tumors in males and females, respectively; open gray circles and open black circles represent flat ACF in males and female, respectively. Each data point in each category represents one mouse. (b) The average number of flat ACF (gray) and tumors (black) in mice ranging from 4 to 54 weeks, separated into five age groups. Error bars represent a 95% confidence interval. The dashed line represents the influx of new lesions over time. (c) Tumor load in mice separated into five age groups. Tumor load represents the sum of the area of all lesions observed. All values show group mean with the 95% confidence interval. (d) Size distribution of flat ACF and tumors. Graphs represent size distribution in the age groups early juvenile, juvenile, mature adult, early middle-aged adult and middle-aged adult. The smallest size class contains lesions with 1–4 crypts. In the colon, lesions are considered tumors if they contain >30 crypts/lesion (~0.4 mm²).

and tumors displayed a gradual shift toward larger size classes with age (Fig. 2d). As indicated in the figure, only flat ACF were recorded in early juvenile. In mature adult more flat ACF were observed (area under the curve) and more lesions reached the size of a tumor. In middle-aged adult the size distribution of flat ACF and tumors was continuous and overlapping. Altogether these size distributions demonstrated age-dependent growth of flat ACF and transition from flat ACF to tumor (Fig. 2d).

Classic ACF made up only 0.4% of the lesions scored, thus suggesting that spontaneous formation of these lesions is uncommon in the A/J Min/+ mouse, which coincides with previous findings.¹⁷

Observed tumors displayed an increased cytoplasmic β -catenin accumulation (Figs. 1c and 1d), indicating Wnt signaling activation. An increased frequency of Ki67-positive nuclei was also detected in tumors, indicating enhanced proliferation in tumor tissue (Fig. 1e).

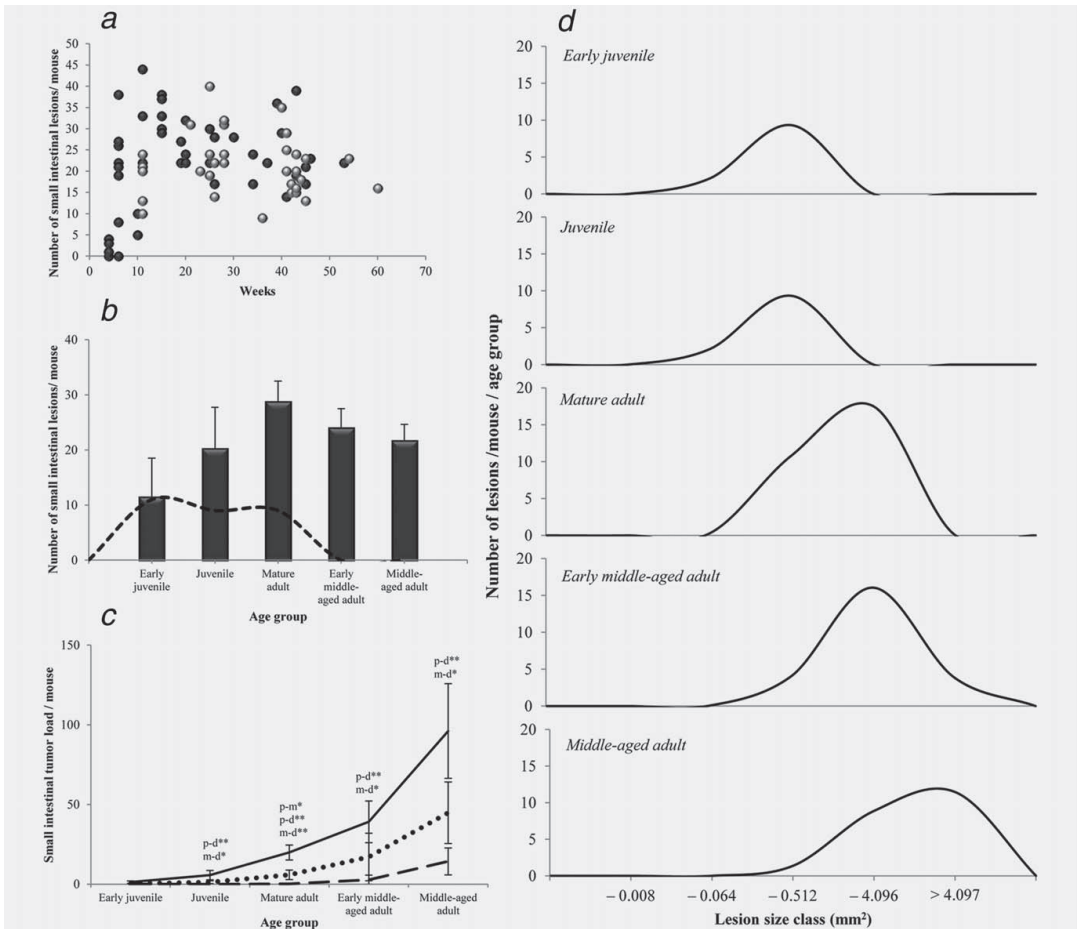


Figure 3. Number, size and load of lesions spontaneously formed in the small intestine of A/J Min/+ mice. (a) Distribution of small intestinal tumors in mice ranging from 4 to 60 weeks. Solid gray and solid black circles represent tumors in males and females, respectively. Each data point represents one mouse. (b) The average number of small intestinal tumors in mice ranging from 4 to 54 weeks, separated into five age groups. Error bars represent a 95% confidence interval. The dashed line represents the influx of new lesions over time. (c) Tumor load in three small intestinal segments: proximal (dashed line), middle (dotted line) and distal (solid line). All values show group mean with a 95% confidence interval. Labels show significant difference between the three segments: proximal (p), middle (m) and distal (d). * $p < 0.05$, ** $p < 0.001$. (d) Size distribution of small intestinal tumors. Graphs represent size distribution in the age groups early juvenile, juvenile, mature adult, early middle-aged adult and middle-aged adult. The smallest size class contains lesions with 1–4 crypts.

Small intestine

Scoring the total number of tumors at different ages revealed large interindividual variation also in small intestinal tumorigenesis, as illustrated by the scatter plot in Figure 3a. An average of 21 tumors (95% CI: 18.91–23.38) developed in the small intestine of mice from 4 to 60 weeks, with 44 tumors being the highest number of lesions observed in a single mouse. When examining mice older than 40 weeks, the average number of tumors was still 21 (95% CI: 18.57–24.30), suggesting that the number of lesions was relatively uniform over the lifespan of the mouse (Fig. 3a). Small intestinal

tumors were represented in all ages, and a weak, nonsignificant correlation was found between the number of lesions and age ($r_s = 0.167$, $n = 81$, $p = 0.137$). When mice were grouped into the five age groups, a decrease in number of lesions from mature adult to early middle-aged adult was evident (Fig. 3b). An increase in number of lesions was correlated with age in mice from 4 to 24 weeks ($r_s = 0.642$, $n = 38$, $p < 0.001$), while a nonsignificant, negative correlation of number of tumors and age was observed after 24 weeks ($r_s = -0.265$, $n = 43$, $p = 0.085$). The number of calculated newly formed tumors was steady from age group early

juvenile up to age group mature adult, after which formation of new lesions appeared to slow down or cease (Fig. 3b).

To determine tumor distribution along the small intestine, the intestine was cut into three equally long segments when prepared: proximal, middle and distal. Microscopy revealed that these three segments had very different number of tumors, with the distal end being the most densely populated. Figure 3c shows the difference in tumor load in these three segments as observed in the five age groups. A significant difference in tumor load in the three segments was found in all age groups: juvenile, mature adult, early middle-aged adult and middle-aged adult (all $p < 0.001$); early juvenile ($p = 0.001$). However, *post hoc* tests revealed that there was no significant difference between tumor load in the proximal and middle segments in any of the age groups, except for in the mature adult age group ($p = 0.025$). Furthermore, for all groups, tumor load in both the proximal and middle segments was significantly smaller than that in the distal segment.

The small intestinal tumors recorded in each animal in each age group were grouped together according to size, and the average number of lesions per size group per animal was calculated (Fig. 3d). The same five lesion size classes as in Figure 2d were used to describe the distribution of small intestinal tumors in relation to age. As the mice aged (Fig. 3d), both the number (area under the curve) and the size of the tumors increased, which is represented by the shift to the right seen in the graphs. Interestingly, the smallest tumors observed in the small intestine (Fig. 3d, early juvenile—mature adult) exhibited sizes that were comparable to the largest flat ACF in the colon (Fig. 2d).

Carcinoma formation

A set of 16 intestines were prepared as Swiss rolls to examine the spontaneous formation of carcinomas in the A/J Min/+ mouse. As carcinomas are likely linked to aging, the majority of intestines chosen were from older animals. Upon examination of the Swiss rolls, numerous distinct proliferative lesions were detected. The lesions were well demarcated from normal mucosal tissue, and were slightly raised above the normal level of the mucosa, often with a narrow base and wider top. The lesions displayed loss of villus formation (small intestine) and aberrant, irregular, branching crypts with marked loss of mucus-secreting cells (dedifferentiation). Cells showed pronounced atypia with considerable variation in size of both cells and nuclei, with multiple, distinct, magenta nucleoli up to 2 μm , and a mitotic index of 1–2 per high-power field. The lesions were expansile and compressed the surrounding tissue. Lesions clearly invading the muscularis mucosae into the submucosa were classified as carcinomas, while those without infiltrative growth were classified as adenomas (Figs. 4a and 4d).

Of the 16 intestines, three were from mice under the age of 30 weeks. In those three animals, no carcinomas were detected. The first small intestinal lesion scored as a carci-

noma appeared in the middle segment of the small intestine at week 30. Small intestinal carcinomas were identified in at least one small intestinal segment in all mice above this age (Fig. 5a). The distal end of the small intestine was the most densely populated, which mimics what was observed with surface microscopy for tumor distribution (see Fig. 3c). Carcinomas were not identified in the colon until week 41 (Fig. 5b), and of the examined mice from 41 weeks and up, 78% had colon carcinomas. When carcinomas in the small intestine and carcinomas in the colon were combined, all mice above the age of 30 had intestinal carcinomas. Furthermore, in mice older than 40 weeks, 21% of colonic tumors and 56% of small intestinal tumors were identified as carcinomas. Grouping the examined mice into age groups (including the late middle-aged adult group) revealed that the frequency of animals with intestinal carcinomas within a group increased with age: 0% in the juvenile and mature adult age groups, 75% in the early middle-aged adult age group, 100% in the middle-aged adult and late middle-aged adult age groups (Fig. 5c). Histological sections of regional lymph nodes and liver from older mice were examined for metastases, but none were detected. However, in one mouse, invasive growth into a local lymphatic vessel was observed, indicating high risk for metastases in this individual (Fig. 4e).

Discussion

In this work, spontaneous tumorigenesis in the novel A/J Min/+ mouse was studied. After examining the intestines of mice ranging from 4 to 60 weeks, it was evident that the colon and the small intestine developed a comparable tumor load represented by a large number of adenomas and carcinomas. In addition, the proportion of carcinomas increased progressively with age. There were two types of colonic lesions: flat ACF and tumors. Previous studies have demonstrated that these lesions share multiple characteristics such as compressed crypt openings, severe dysplasia and stimulated Wnt signaling.^{17,19} Using AOM-stimulated B6 Min/+ mice¹⁹ or AOM-stimulated rats¹⁸ with rapidly growing flat ACF, it was hypothesized that flat ACF and tumors in fact could represent the same type of dysplastic lesions at different stages of crypt multiplication and colonic tumorigenesis. This potential developmental relationship between flat ACF and tumors could be further studied in the A/J Min/+ mouse as they spontaneously form a large number of colonic lesions. Several observations in this study supported this hypothesis: as the A/J Min/+ mice aged the number of flat ACF was reduced while the number of tumors increased; the size distribution of pooled flat ACF and tumors shifted toward larger size classes with age; in older animals the size distribution of flat ACF and tumors overlapped, indicating a continuous growth of flat ACF to the size of a tumor; no tumors evolved without the presence of flat ACF as they were scored in all mice, regardless of age. Initiation of new lesions may potentially be limited to certain susceptible periods of life. In BL6 Min/+ mice, initiation of both

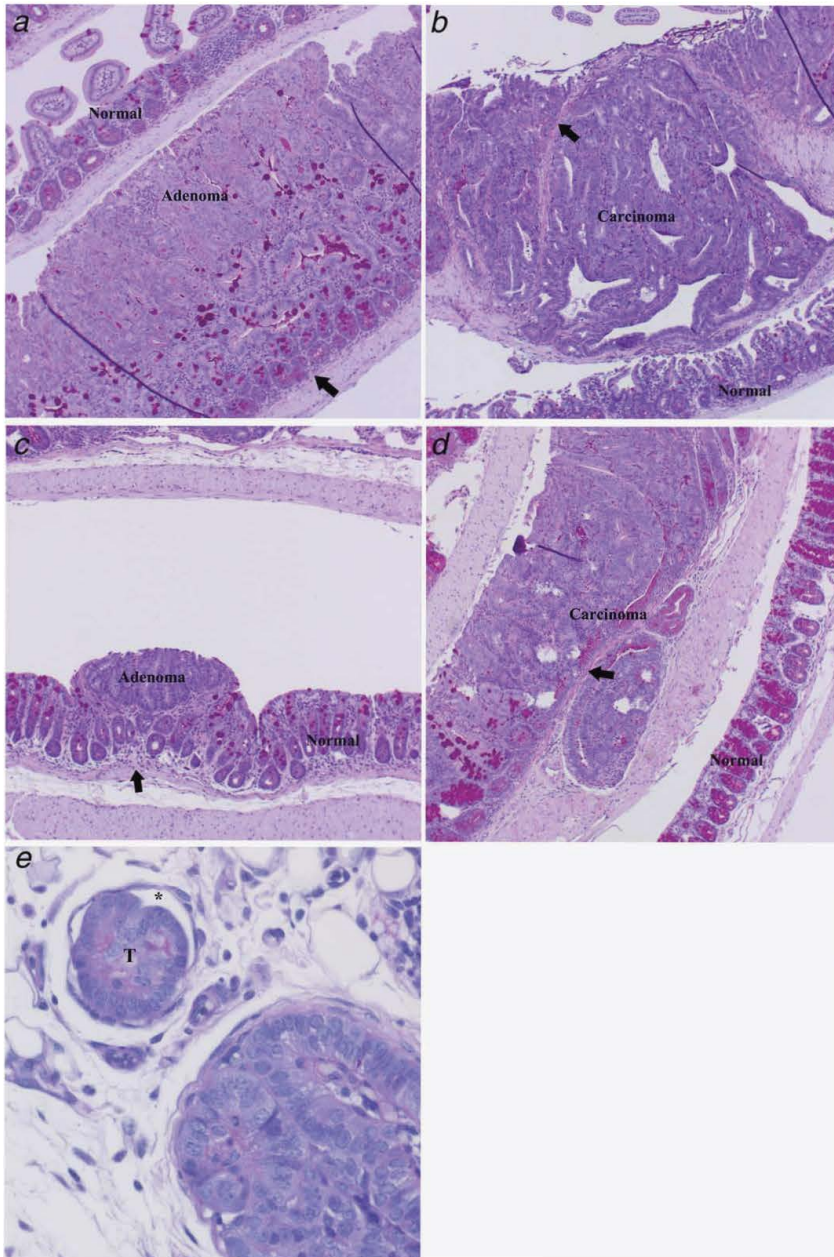


Figure 4. PAS-stained Swiss roll sections showing (a) small intestinal adenoma, (b) small intestinal carcinoma, (c) colonic adenoma, (d) colonic carcinoma and (e) invasive growth into a local lymph vessel. In (a–d), arrows point to the muscularis mucosae. Carcinomas show infiltration through the muscularis mucosae, while adenomas do not. For comparison, examples of normal intestinal tissue are labeled. All magnifications are $\times 100$. Panel (e) shows growth of tumor tissue (T) into the lumen of a lymphatic vessel (*) (magnification $\times 400$).

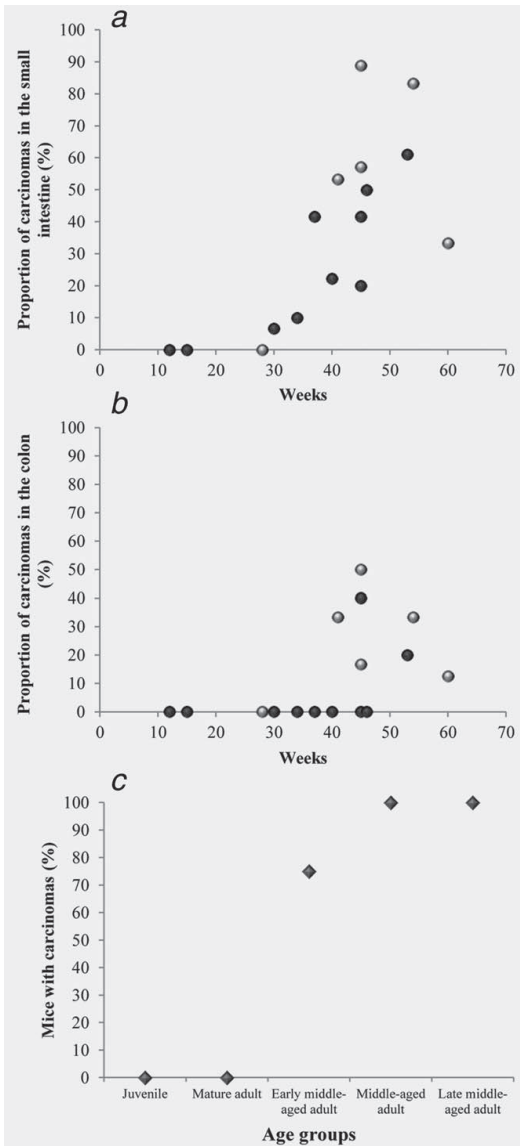


Figure 5. Formation of carcinomas in the small intestine and colon of the A/J Min/+ mouse. (a) Small intestinal carcinomas. (b) Colonic carcinomas. Solid gray and solid black circles represent tumors in males and females, respectively. Each data point in each category represents one mouse. (c) Frequency of mice in each age group with carcinomas.

carcinogen-induced and spontaneous lesions appeared to occur before the age of 2–3 weeks, and the period of spontaneous initiation coincided with when the mice were most susceptible to carcinogens.^{32,33} The influx of lesions observed

in the A/J Min/+ mouse may indicate that the window of time when new lesions are formed is considerably longer in this mouse. Already in the juvenile group, formation of flat ACF appeared to have reached a maximum. It also appeared that the growth of flat ACF was slow in younger mice, and that these lesions only began to accelerate at a later stage in the animals' life, with a surge of transition and tumor formation around 30 weeks.

Traditionally, lesions that develop in the small intestine of Min/+ mice have been termed microadenomas, adenomas or tumors, while in the colon, small lesions have been assigned an additional name, for instance flat ACF.¹⁸ Based on the structure of the small intestinal tumors, their origin may be similar to the flat ACF in the colon. Previous research has shown that both flat ACF and emerging small intestinal tumors initially arise as a single dysplastic crypt,³² which may suggest that even small intestinal tumors start out as lesions similar to flat ACF. In the small intestine of the A/J Min/+ mouse, a decrease in the number of tumors in mice older than 24 weeks was detected. However, the observed tumor load highlights that, even if the number of small intestinal tumors appeared to decrease, tumors in older mice were much larger than those observed in younger animals. Thus, the decrease in tumor numbers may simply be due to difficulty distinguishing larger lesions *via* surface microscopy, resulting in lesions potentially made up of more than one tumor being scored as a single, large tumor. Also, in all age groups, the majority of tumors were found in the distal segment of small intestine, which is consistent with previous findings in the intestine of B6 Min/+ mice.³⁰

Yamada *et al.*³⁴ found that microadenomas, which resemble the flat ACF, formed in the colon of untreated B6 Min/+ mice had lost the remaining nonmutated *Apc* allele, suggesting that loss of heterozygosity, and consequently APC function, leads to development of these microadenomas. However, loss of heterozygosity in the *Apc* gene did not appear to be sufficient to allow for progression from microadenoma to tumor.^{34,35} It appears that microadenomas required an additional alteration, such as the addition of the inflammatory stimulus dextran sulfate (DSS),³⁵ or the colon carcinogen AOM,¹⁹ to progress to tumors. In contrast, flat ACF in the A/J Min/+ mouse spontaneously progressed to tumors without the addition of carcinogenic agents, suggesting that the additional stochastic event needed for tumor formation in the A/J Min/+ mouse model arises with time. This time-related event that promotes tumor formation in the A/J Min/+ mouse may potentially be caused by increased inflammation occurring in older animals; it has been suggested that both a change in redox status as well as a dysregulation of the immune system that occurs during aging may lead to increased inflammation with age.³⁶ However, in this study, pronounced inflammatory cell infiltration was not detected. Additionally, the average diameter of lesions in the colon of 34-week-old A/J Min/+ mice was 5.0 mm, while

Oyama *et al.*³⁵ observed that, even at 35 weeks, no spontaneously formed lesions were greater than 0.3 mm in diameter.

The genetic background appears to have an effect on both lifespan and tumor formation of Min/+ mice. The Min/+ trait has been introgressed on various inbred genetic backgrounds, including BTBR, AKR and FVB.^{37–39} Min/+ trait on a BTBR genetic background resulted in over 600 small intestinal lesions and 12 colonic lesions, while, on the other end of the spectrum, AKR Min/+ mice developed on average four lesions in the small intestine and zero colonic lesions.^{37,40} BTBR Min/+ mice also had a short lifespan of no >84 days due to the enormous number of lesions present in the small intestine, while AKR Min/+ mice could live for up to 336 days. The conventional B6 Min/+ mouse seldom lives past 120 days and develop an average of 30 small intestinal tumors, and <1 colonic tumor.^{10,19,30,41} In contrast, the novel A/J Min/+ mouse presented with a greater number of tumors in the colon, with the majority of these colonic tumors occurring in older animals, but did not exhibit an increase in small intestinal tumors. Furthermore, this mouse had a longer lifespan; in this study, the oldest mouse reached 420 days before showing signs of declining health, requiring termination.

Most tumors in the B6 Min/+ mouse are benign adenomas that rarely progress to cancer, which may be due to the limited 120-day lifespan of this mouse.^{10,38} Another model for colonic tumor development, the Apc^{+/Min-FCCC} mouse, lives much longer than the conventional Min/+ mouse, and has a maximum lifespan of 241 days. However, even with the extended lifespan, colonic adenomas in this mouse do not progress to cancer, unless a stimulus such as DSS is administered.^{42,43} Halberg *et al.*²¹ crossed B6 Min/+ males with C57BR/cdcJ females producing Min/+ hybrids with a mean lifespan of 232 days. However, these F1 hybrids exhibited a considerable reduction in number of intestinal tumors, with, on average, only 19 tumors recorded in the entire intestinal tract. In contrast to the Apc^{+/Min-FCCC} mouse, 56% of the tumors in the F1 Min/+ hybrids were identified as invasive adenocarcinomas.²¹ In the novel A/J Min/+ mouse model, benign adenomas in both the colon and the small intestine progressed to carcinomas with age. A 100% incidence of intestinal carcinomas was found in mice older than 30 weeks. The longer lifespan of the A/J Min/+ mouse likely allowed for the progression of lesions from adenomas to carcinomas.

The first observed incidence of colon carcinoma was seen in a 41-week-old A/J Min/+ mouse, which in mice, according to Flurkey *et al.*²⁷ equals approximately 38 human years. FAP patients develop cancer at a median age of 42 years.²

In the A/J Min/+ mouse, the average colonic to small intestinal lesion count ratio, when lesions of all sizes are scored, was found to be 1.1:1. Even though the A/J Min/+ mouse does not develop tumors solely in the colon, but also shows a similar tumor load in the small intestine, the ratio of colonic to small intestinal lesions is closer to the ratio observed in human FAP (>1:1) than that of the B6 Min/+ mouse (<1:40).⁴⁴ In human CRC, nuclear accumulation of β -catenin has been found to occur early, and is consistent throughout the adenoma–carcinoma sequence.⁴⁵ In comparison, the novel A/J Min/+ mouse model shows β -catenin accumulation in monocryptal lesions as well as tumors. The novel A/J Min/+ mouse model more closely resembles the PIRC (Polyposis In the Rat Colon) rat model for colorectal cancer, in that this rat also develops a greater number of lesions in the colon.⁴⁴ Femia *et al.*⁴⁶ found that the number of mucin-depleted foci, which are comparable to the flat ACF, and macroscopic tumors in the PIRC rat colon increased with age. This is similar to what was observed for the A/J Min/+ mouse.

In summary, we have studied long-term spontaneous intestinal tumorigenesis in the novel A/J Min/+ mouse to explore whether it may be a more appropriate model for colorectal cancer than existing murine FAP models. We found that this novel mouse presented with a substantial increase in colonic tumors, and that these lesions showed Wnt signaling activation. Furthermore, we found that past a certain age, both colonic and small intestinal adenomas progressed to carcinomas. This potential for carcinoma formation may be due to the increased lifespan of this mouse when compared to conventional models where carcinomas have not been detected. Taken together, these findings suggest the novel A/J Min/+ mouse model as a relevant model for initiation, promotion and progression of colorectal cancer.

Acknowledgements

The authors thank C.W. Johnsen for excellent assistance with the mice, and P. Mokhova, S. Lunner and M.K.A. Ådland for excellent technical assistance with histological preparations.

References

- Ferlay J, Soerjomataram I, Ervik M, et al. GLOBOCAN 2012 v1.0, cancer incidence and mortality worldwide: IARC CancerBase No. 11 [Internet]. 2013. Available at: <http://globocan.iarc.fr> (accessed May 21, 2015).
- Kinzler KW, Vogelstein B. Lessons from hereditary colorectal cancer. *Cell* 1996;87:159–70.
- Fodde R. The APC gene in colorectal cancer. *Eur J Cancer* 2002;38:867–71.
- Fodde R, Smits R. Disease model: familial adenomatous polyposis. *Trends Mol Med* 2001;7:369–73.
- Fodde R, Smits R, Clevers H. APC, signal transduction and genetic instability in colorectal cancer. *Nat Rev Cancer* 2001;1:55–67.
- Fodde R, Tomlinson I. Nuclear β -catenin expression and Wnt signalling: in defence. *J Pathol* 2010;221:239–41.
- Fearnhead NS, Britton MP, Bodmer WF, et al. The ABC of APC. *Hum Mol Genet* 2001;10:721–33.
- Ilyas M, Straub J, Tomlinson IPM, et al. Genetic pathways in colorectal and other cancers. *Eur J Cancer* 1999;35:335–51.
- Kelloff GJ, Schilsky RL, Alberts DS, et al. Colorectal adenomas: a prototype for the use of surrogate end points in the development of cancer prevention drugs. *Clin Cancer Res* 2004;10:3908–18.
- Moser AR, Pitot HC, Dove WF. A dominant mutation that predisposes to multiple intestinal neoplasia in the mouse. *Science* 1990;247:322–4.
- Paulsen JE. Modulation by dietary factors in murine FAP models. *Toxicol Lett* 2000;112–113:403–9.

12. Van Es JH, Giles RH, Clevers HC. The many faces of the tumor suppressor gene APC. *Exp Cell Res* 2001;264:126–34.
13. Su LK, Kinzler KW, Vogelstein B, et al. Multiple intestinal neoplasia caused by a mutation in the murine homolog of the APC gene. *Science* 1992; 256:668–70.
14. Srivastava S, Verma M, Henson DE. Biomarkers for early detection of colon cancer. *Clin Cancer Res* 2001;7:1118–26.
15. Bird RP. Observation and quantification of aberrant crypts in the murine colon treated with a colon carcinogen: preliminary findings. *Cancer Lett* 1987;37:147–51.
16. Bird RP, Good CK. The significance of aberrant crypt foci in understanding the pathogenesis of colon cancer. *Toxicol Lett* 2000;112–113: 395–402.
17. Paulsen JE, Namork E, Steffensen IL, et al. Identification and quantification of aberrant crypt foci in the colon of Min mice—a murine model of familial adenomatous polyposis. *Scand J Gastroenterol* 2000;35:534–9.
18. Paulsen JE, Løberg EM, Ølstorn HB, et al. Flat dysplastic aberrant crypt foci are related to tumorigenesis in the colon of azoxymethane-treated rat in the colon of azoxymethane-treated rat. *Cancer Res* 2005;65:121–9.
19. Paulsen JE, Steffensen IL, Løberg EM, et al. Qualitative and quantitative relationship between dysplastic aberrant crypt foci and tumorigenesis in the Min/+ mouse colon. *Cancer Res* 2001;61: 5010–15.
20. Mekada K, Abe K, Murakami A, et al. Genetic differences among C57BL/6 substrains. *Exp Anim* 2009;58:141–9.
21. Halberg RB, Waggoner J, Rasmussen K, et al. Long-lived Min mice develop advanced intestinal cancers through a genetically conservative pathway. *Cancer Res* 2009;69:5768–75.
22. Hinoi T, Akyol A, Theisen BK, et al. Mouse model of colonic adenoma-carcinoma progression based on somatic Apc inactivation. *Cancer Res* 2007;67:9721–30.
23. Rosenberg DW, Giardina C, Tanaka T. Mouse models for the study of colon carcinogenesis. *Carcinogenesis* 2009;30:183–96.
24. Glickman LT, Suissa S, Fleischer DM. Proliferative characteristics of chronic crypt cells in C57BL/6J and A/J mice as predictors of subsequent tumor formation. *Cancer Res* 1987;47:4766–70.
25. Papanikolaou A. Sequential and morphological analyses of aberrant crypt foci formation in mice of differing susceptibility to azoxymethane-induced colon carcinogenesis. *Carcinogenesis* 2000;21:1567–72.
26. Ølstorn HB. The effect of acrylamide and glycidamide on intestinal carcinogenesis in mice. Ph.D thesis, University of Oslo: Norwegian Institute of Public Health, 2009. 63 pp. ISSN 1501-7710, nr. 825.
27. Flurkey K, Currer JM, Harrison DE. Mouse models in ageing research. In: Fox JG, Barthold S, Davison M, Newcomer CE, Quimby FW, Smith A, eds. The mouse in biomedical research: normative biology, husbandry, and models. Burlington, MA: Academic Press, 2006. 637–72.
28. Sødring M, Oostindjer M, Egelandsdal B, et al. Effects of hemin and nitrite on intestinal tumorigenesis in the A/J Min/+ mouse model. *PLoS One* 2015;10:e0122880.
29. Moolenbeek C, Ruitenberg EJ. The "Swiss roll": a simple technique for histological studies of the rodent intestine. *Lab Anim* 1981;15:57–9.
30. Paulsen JE, Elvsaas IK, Steffensen IL, et al. A fish oil derived concentrate enriched in eicosapentaenoic and docosahexaenoic acid as ethyl ester suppresses the formation and growth of intestinal polyps in the Min mouse. *Carcinogenesis* 1997;18: 1905–10.
31. Amos-Landgraf JM, Heijmans J, Wielenga MCB, et al. Sex disparity in colonic adenomagenesis involves promotion by male hormones, not protection by female hormones. *Proc Natl Acad Sci USA* 2014;111:16514–19.
32. Paulsen JE, Steffensen I-L, Namork E, et al. Age-dependent susceptibility to azoxymethane-induced and spontaneous tumorigenesis in the Min/+ mouse. *Anticancer Res* 2003;23:259–65.
33. Steffensen I-L, Schut HAJ, Paulsen JE, et al. Intestinal tumorigenesis in multiple intestinal neoplasia mice induced by the food mutagen 2-amino-1-methyl-6-phenylimidazo[4,5-b]pyridine: perinatal susceptibility, regional variation, and correlation with DNA adducts. *Cancer Res* 2001; 61:8689–96.
34. Yamada Y, Hata K, Hirose Y, et al. Microadenomatous lesions involving loss of Apc heterozygosity in the colon of adult Apc(Min/+) mice. *Cancer Res* 2002;62:6367–70.
35. Oyama T, Yamada Y, Hata K, et al. Further upregulation of beta-catenin/Tcf transcription is involved in the development of macroscopic tumors in the colon of ApcMin/+ mice. *Carcinogenesis* 2008;29:666–72.
36. Chung HY, Cesari M, Anton S, et al. Molecular inflammation: underpinnings of aging and age-related diseases. *Ageing Res Rev* 2009;8:18–30.
37. Kwong LN, Dove WF. APC and its modifiers in colon cancer. *Adv Exp Med Biol* 2009;656:85–106.
38. Moser AR, Dove WRF, Roth KA, et al. The Min (multiple intestinal neoplasia) mutation: its effect on gut epithelial cell differentiation and interaction with a modifier system. *J Cell Biol* 1992;116: 1517–26.
39. Svendsen C, Alexander J, Knutsen HK, et al. The min mouse on FVB background: susceptibility to spontaneous and carcinogen-induced intestinal tumorigenesis. *Anticancer Res* 2011;31: 785–8.
40. Kwong LN, Shedlovsky A, Biehl BS, et al. Identification of Mom7, a novel modifier of Apc(Min/+) on mouse chromosome 18. *Genetics* 2007;176: 1237–44.
41. Paulsen JE, Steffensen IL, Andreassen A, et al. Neonatal exposure to the food mutagen 2-amino-1-methyl-6-phenylimidazo[4,5-b]pyridine via breast milk or directly induces intestinal tumors in multiple intestinal neoplasia mice. *Carcinogenesis* 1999;20:1277–82.
42. Cooper HS, Chang W-CL, Coudry R, et al. Generation of a unique strain of multiple intestinal neoplasia (Apc(+)/Min-FCCC) mice with significantly increased numbers of colorectal adenomas. *Mol Carcinog* 2005;44:31–41.
43. Cooper HS, Everley L, Chang WC, et al. The role of mutant Apc in the development of dysplasia and cancer in the mouse model of dextran sulfate sodium-induced colitis. *Gastroenterology* 2001; 121:1407–16.
44. Amos-Landgraf JM, Kwong LN, Kendziorski CM, et al. A target-selected Apc-mutant rat kindred enhances the modeling of familial human colon cancer. *Proc Natl Acad Sci USA* 2007;104: 4036–41.
45. Iwamoto M. Expression of beta-catenin and full-length APC protein in normal and neoplastic colonic tissues. *Carcinogenesis* 2000;21:1935–40.
46. Femia A, Pietro Luceri C, Soares PV, et al. Multiple mucin depleted foci, high proliferation and low apoptotic response in the onset of colon carcinogenesis of the PIRC rat, mutated in Apc. *Int J Cancer* 2015;136:E488–E495.



II

Detection and characterization of flat aberrant crypt foci (flat ACF) in the novel A/J Min/+ mouse

MARIANNE SØDRING¹, GJERMUND GUNNES², and JAN ERIK PAULSEN^{1*}

¹Norwegian University of Life Sciences, Department of Food Safety and Infection Biology, Oslo, Norway

²Norwegian University of Life Sciences, Department of Basic Sciences and Aquatic Medicine, Oslo, Norway

Abstract. *Background: Flat aberrant crypt foci (flat ACF) and mucin depleted foci (MDF) have previously been described as preneoplastic colonic lesions. We used the novel A/J Min/+ mouse model, which demonstrates extensive spontaneous colon carcinogenesis, to refine the method of detection of flat ACF, and to further characterize and define them as early lesions by histological examination and comparison with MDF. Materials and Methods: Colons were stained with methylene blue (MB) for flat ACF detection and restained with HID-AB for MDF detection. Results: Optimal flat ACF recognition required at least 24 hours of storage post MB staining and adherence to a set of characteristics. The fraction of flat ACF corresponding with MDF was 93%. Flat ACF/MDF displayed the same picture of severe dysplasia, lack of mucus and goblet cells and accumulation of cytoplasmic β -catenin. Conclusion: The easily detectable flat ACF are reliable surface biomarkers of Apc-driven colon carcinogenesis.*

Introduction

To date, a variety of preneoplastic lesions thought to be the initial step in colon carcinogenesis have been characterized, including aberrant crypt foci (ACF), flat aberrant crypt foci (flat ACF), and mucin-depleted foci (MDF) (1–4).

Aberrant crypt foci (ACF) were originally described by Bird in 1987 in the colon of mice treated with carcinogens, and are identified by their characteristic morphology of enlarged crypts, thickened epithelial lining, irregular lumens, increased pericryptal space, and elevation from the mucosa (1, 5). The MDF was first described by Caderni *et al.* in 2003 (4), in the colon of azoxymethane (AOM)-treated rats, and was found to show dysplastic properties similar to those observed in colonic tumors. This lesion is first and foremost characterized by no- or scarce production of mucins. Other features of this lesion includes distorted cryptal lumens that are smaller than surrounding crypts, elevation from the mucosa, and crypt multiplicity of more than 3 crypts (4, 6). Furthermore, the MDF also shows both β -catenin accumulation and Apc mutations, two traits present in colonic tumors, further emphasizing the MDF as a preneoplastic lesion for colon carcinogenesis (7, 8).

The multiple intestinal neoplasia (Min/+) mouse is, like humans with the familial adenomatous polyposis (FAP) syndrome, heterozygous for a mutation in the tumour suppressor gene *Apc*. This mutation leads to the development of numerous neoplastic intestinal polyps. Inactivation of *Apc* with β -catenin accumulation mimics Wnt signalling pathway stimulation (reviewed in: 10–12). Unlike human FAP, conventional C57BL/6J (B6) Min/+ mice develop tumors predominantly in the small intestine. Even though the incidence of colonic tumors is very low in this mouse, preneoplastic

Correspondence to: Jan Erik Paulsen, Norwegian University of Life Sciences, Department of Food Safety and Infection Biology, PO Box 8146 Dep., 0033 Oslo, Norway. Fax: +47 6496 5001; Email: jan.paulsen@nmbu.no

Keywords: Colorectal cancer, A/J Min/+ mouse, flat ACF, MDF

colonic lesions called flat ACF were found in the colons of young B6 Min/+ mice; however, no ACF were detected (3). Flat ACF differed from the 'classic' ACF described by Bird as they were not elevated from the mucosa, and they were undetectable without methylene blue (MB) staining and transillumination. Later studies in azoxymethane (AOM) treated B6 Min/+ mice and rats revealed that only the flat ACF, not the classic ACF, demonstrated a continuous development from monocryptal stage to tumor (2, 12). In AOM treated B6 Min/+ mice scored for flat ACF, MDF and classic ACF, a 57% correspondence between flat ACF and MDF was observed. Approximately 50% of the non-coincident lesions were identified as classic ACF, and the rest were not identified (13).

Our novel Min/+ mouse on an A/J genetic background provides a better model for colorectal cancer as these mice spontaneously develop a considerable number of colonic lesions that demonstrate a continuous growth from the monocryptal stage to adenoma and, with time, carcinoma (14). The flat ACF is seldom chosen when colonic lesions are to be scored, mainly due to a notion that this particular lesion is difficult to detect (15).

The objectives of the present study were to: i) refine the method of detection for flat ACF using the sensitive A/J Min/+ mouse; ii) further characterize the flat ACF and define them as early lesions of colon carcinogenesis by histological examination and comparison with MDF.

Materials and methods

A/J Min/+ mice. Intestines collected from A/J Min/+ mice bred at the Department of Experimental Biomedicine at the Norwegian University of Life Sciences, Campus Adamstuen were used for the study. All animals were housed in Makrolon Type III open top plastic cages in a room with a 12-hour light/dark cycle, 55-65% humidity and 20-22°C. Water and feed were given ad libitum. All animals

were fed the standard rodent diet RM1 (SDS Special Diet Services, Witham, UK) for the duration of the study. Mice were sacrificed by cervical dislocation. This study was conducted in strict accordance with The Norwegian Regulation on Animal Experimentation, and approved by the Institutional Animal Care and Use Committee at the Norwegian University of Life Sciences, Campus Adamstuen.

Methylene Blue (MB) staining and scoring of flat ACF. The colon was excised from anus to cecum, rinsed in, and flushed with, ice-cold phosphate buffered saline solution (PBS) to remove any intestinal contents, before being slit open longitudinally. Next, the colon was fixed flat between two PBS-soaked filter papers held together with staples. The flat-fixed colon was then stored in 10% neutral buffered formalin for at least 24 hours before staining. Once fixated, the colon was removed from the filter paper. Any remaining fat on the muscularis side of the colon was carefully removed with a pair of forceps, before the colon was stained for 8-10 seconds in a glass beaker containing a 0.2% methylene blue (MB) (M9140, Sigma-Aldrich, St. Louis, MO) dissolved in 10% neutral buffered formalin solution. After no more than 10 seconds, the colon was transferred to a new beaker filled with 10% formalin, rinsed of excess MB, before again being transferred to another beaker containing 10% formalin for a second rinse. Next, the colon was moved to an individual 50 ml Falcon® polypropylene tube filled with either 10% formalin or 70% ethanol for at least 24 hours. This last step is of importance because the flat ACF is barely visible until after at least 24 hours post methylene blue staining (see Figure 1a). To examine the MB-stained intestine, the colon was placed in a Nunc® OmniTray single-well plate (Thermo Fisher Scientific, Waltham, MA). This plate was divided into segments by carving vertical lines, each 1 cm thick, down the length of the plate. Additionally, one horizontal line spanning the plate was drawn down the center of the plate, thus dividing the plate into a top and bottom section. This grid was used to map

the location of all colonic lesions. The colon, with the mucosal side down, was fixed under a glass microscope slide to ease scoring. To examine the colon for flat ACF, surface microscopy and transillumination using an inverted microscope (CKX41, Olympus Inc., Hamburg, Germany) equipped with a digital color camera (DP25, Olympus Inc.) was used. Morphological appearance and surface location of each lesion were documented with an image and grid coordinates.

To be considered a flat ACF, a lesion must fulfill certain specific criteria. It must i) turn a bright blue/green color after MB staining, a coloration distinguishable from normal crypts which stain a more subdued brownish-green, ii) have enlarged crypts with compressed luminal openings, iii) show elongated pit patterns, which gives it a gyrus-like appearance. One additional feature of the flat ACF is usually, but now always, present: the majority of the lesions lay flat against the surrounding epithelium in the colon; however, a small number of lesions may appear somewhat polypoid. To be considered a flat ACF, the first three criteria must be met, while flatness, albeit the lesion's name suggesting so, is not required. Although flat ACF can be detected from the monocryptal stage, in order to compare this lesion to the MDF, only flat ACF containing more than 3 crypts were scored for the comparison analysis; thus, all lesions between 4 and 30 crypts were scored.

High-Iron Diamine Alcian Blue (HID-AB) staining and scoring of MDF. After scoring the MB-stained colon for flat ACF, the same colon was stained with the HID-AB mucin stain to look for MDF. High-Iron Diamine stains sulfomucins a dark brown, while alcian blue stains sialomucins blue (16). Other than the amount of diamines used, the staining procedure was as described by Caderni *et al.* (17). Briefly, the MB-stained colons were rinsed in distilled water for 5 minutes before staining with a HID solution made with 45 mg N-N'-dimethyl-m-phenylenediamine (219223, Sigma-Aldrich, St.

Louis, MO) and 55 mg of N-N'-dimethyl-p-phenylenediamine (D4139, Sigma-Aldrich, St. Louis, MO) dissolved in 50 ml of distilled water, with 1.4 ml of 60% ferric chloride. Each colon was stained for no less than 18 hours at room temperature, , rinsed three times in distilled water, and stained for 30 min with 1% alcian blue (A1357, Sigma-Aldrich, St. Louis, MO) in 3% acetic acid. Next, colons were rinsed in 80% ethanol three times followed by a rinse in distilled water, and stored in 10% formalin or 70% ethanol. HID-AB stained colons were examined like the MB stained intestines, and morphological appearance and surface location of each MDF was documented with an image and grid coordinates, which was later compared to the corresponding information gathered from the MB stained colon. All MDF larger than 3 crypts, and smaller than 30 crypts, were scored for comparison with flat ACF.

Histological examination. After scoring the MB and HID-AB stained intestines, histological cross-sections were prepared. The HID-AB stained intestines were cut into 1 cm segments from distal to proximal end and embedded in paraffin with the muscle side down, before histological cross sections (2-3 μ m) cut in parallel with the mucosal surface, were made. The sections were stained with hematoxylin and eosin (HE). A set of intestines only stained with MB were also used. These intestines were prepared with a modification of the Swiss roll technique (18). Briefly; the longitudinally cut, flat-fixed colon was rolled lengthwise, from proximal to distal end with the mucosa facing inward, using a pair of curved dissecting forceps. To hold the roll together, a pin was pushed carefully through it. The prepared Swiss rolls were embedded in paraffin before histological sections (2-3 μ m) were made. Each section was then manually stained with both MB and HID-AB. The sections were stained with MB and HID-AB to observe how histological sections of flat ACF and MDF stain as compared to whole colon staining. For MB staining: the histological sections were stained for 10 seconds in the same MB solution used to

stain the full colon, followed by two 10% formalin rinses before overnight storage in 10% formalin. For HID-AB staining: the sections were stained in the equivalent HID solution as used for the colon whole mount for no less than 18 hours, and subsequently rinsed in dH₂O prior to a dip in alcian blue. Next, the sections were rinsed in dH₂O again, and counterstained for 5 minutes with nuclear fast red to achieve the pink coloration seen in the whole mount sample scored for MDF. Finally the sections were rinsed in dH₂O, before mounting from xylene.

Immunohistochemistry. Swiss rolls were also subjected to β -catenin staining to show Wnt signaling activation. Paraffin sections were deparaffinized and rehydrated, before endogenous peroxidase quenching with 3.0% H₂O₂. Antigen retrieval was performed in Tris/EDTA (pH 9.1). Sections were blocked using the Mouse on Mouse (M.O.M) kit (Vector Laboratories, Burlingame, CA), before incubation with a primary monoclonal antibody against β -catenin (Purified mouse anti- β -catenin, C19220; Transduction Laboratories, Lexington, KY) at a 1:2,500 dilution. Sections were incubated in M.O.M. biotinylated anti-mouse IgG reagent followed by addition of the avidin-biotinylated peroxidase complex. Antibody binding was detected with DAB substrate according to the manufacturer's protocol (34065, Thermo Scientific Pierce, Waltham, MA). Sections were counterstained with hematoxylin, and mounted from xylene.

Results

Detection of flat ACF. Flat ACF were easily identified when the colons were prepared as described in detail above. Critical steps for detection were: flushing through the colon with

ice cold PBS to remove luminal content; longitudinal bisection of the colon before careful flattening on a smooth, PBS-soaked surface; transferring the wet, flat colon preparation to filter paper and placing another wet filter paper on top, securing with staples; fixing flat between the filter papers in formalin for at least 24 hours. Testing showed that staining with MB for no more than 8-10 seconds, followed by at least 24 hours of storage before surface examination, produced optimal lesion coloration. When adhering to these time requirements, flat ACF appeared as blue-green structures that differed from the surrounding tissues which stained a brownish-green color (Figure 1a). In addition to coloration, compressed crypt openings exhibiting gyrus-like pit patterns (see Figure 1a and 1b) were considered critical features for flat ACF detection. Furthermore, the majority of flat ACF exhibited a flat structure compared with the surrounding mucosa, even at a relatively large size (Figure 1b, right); however, sometimes these lesions could have a polypoid appearance, even when small in size (Figure 1b, middle). Polypoid flat ACF were differentiated from classic ACF by their gyrus-like pit pattern.

Correspondence between flat ACF and MDF.

Ten colons from A/J Min/+ mice ranging from 10 to 32 weeks old were examined after staining with two distinct staining methods to detect the early colonic lesions flat ACF and MDF. A total of 107 lesions were scored. Of these, 106 were scored as flat ACF and 100 were scored as MDF: 99 lesions were scored as flat ACF in MB and as MDF in HID-AB, with a fraction of correspondence of 92.5% (Figure 1b and d). A total of 7 lesions (6.5 %) were scored as flat ACF in the MB stained intestine, but did not fulfil the criteria of an MDF after HID-AB

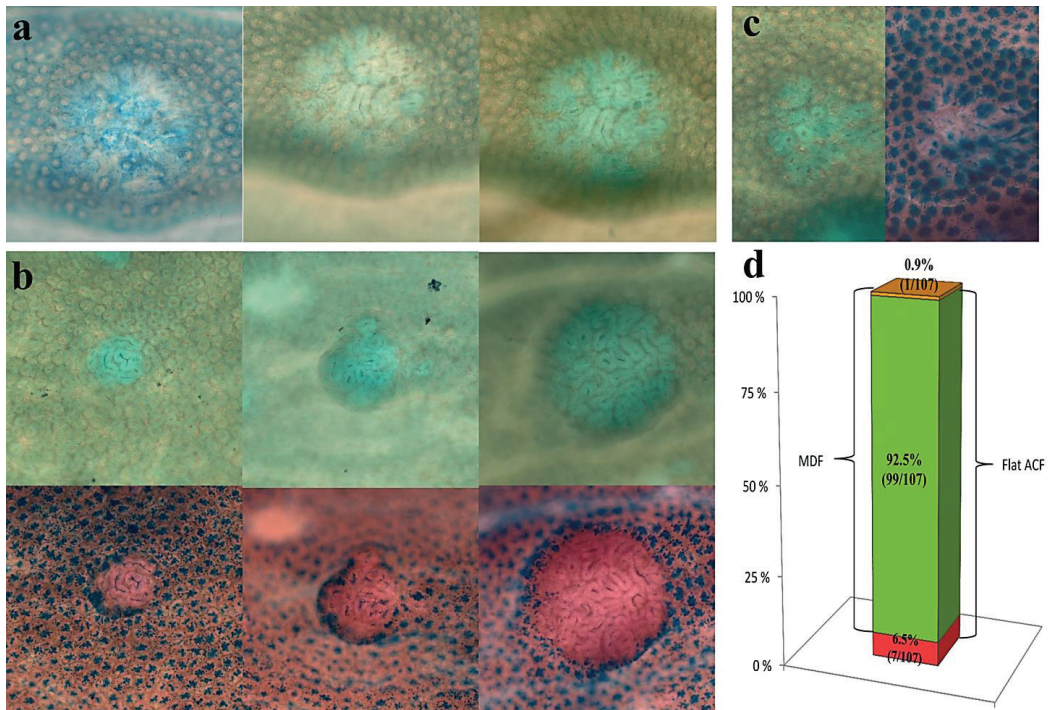


Figure 1. Representative examples of morphological features of colonic lesions spontaneously formed in the A/J Min/+ mouse. Images a (right), and b (top) are good examples of flat ACF fulfilling the criteria of coloration, crypt size, compressed luminal openings, and gyrus-like pit patterns. (a) Illustrates the importance of allowing sufficient time to pass after staining the colon with methylene blue prior to scoring : coloration of a large flat ACF after 10 minutes (left), 3 hours (middle), and 24 hours (right). (b) Coinciding lesions identified as flat ACF with MB staining (top) and as MDF with HID-AB staining (bottom). The middle image shows a polypoid flat ACF/MDF that is slightly elevated from the mucosa. (c) A non-corresponding lesion scored as a flat ACF, but not as an MDF. This lesions may have been a collection of smaller flat ACF in close proximity (rather than one large lesions), with healthy, mucin-producing crypts interspersed in between, masking mucin depletion in the adjacent lesions. (d) Histogram showing the percent of flat ACF scored in MB-stained colons corresponding with MDF scored in HID-AB-stained colons (green box), percent of flat ACF not scored as MDF in HID-AB (red box), and percent of MDF not corresponding with flat ACF in MB (orange box). Values in parentheses show the number of lesions in each category. All magnifications are x100

staining. Also, 0.9% of lesions that were identified as MDF in the HID-AB stained colon were not scored as flat ACF in the MB stained intestine (Figure 1d). The non-corresponding lesions were either not detected, or did not fulfill criteria for the specified lesion (Figure 1c).

Histological characterization of corresponding flat ACF and MDF. After surface examination, histological cross-sections were made to determine the pathological status of the lesions. All the flat ACF/MDF examined exhibited the same picture of severe dysplasia as shown in Figure 2a-c. Longitudinal sections made from Swiss rolls demonstrated that small and large

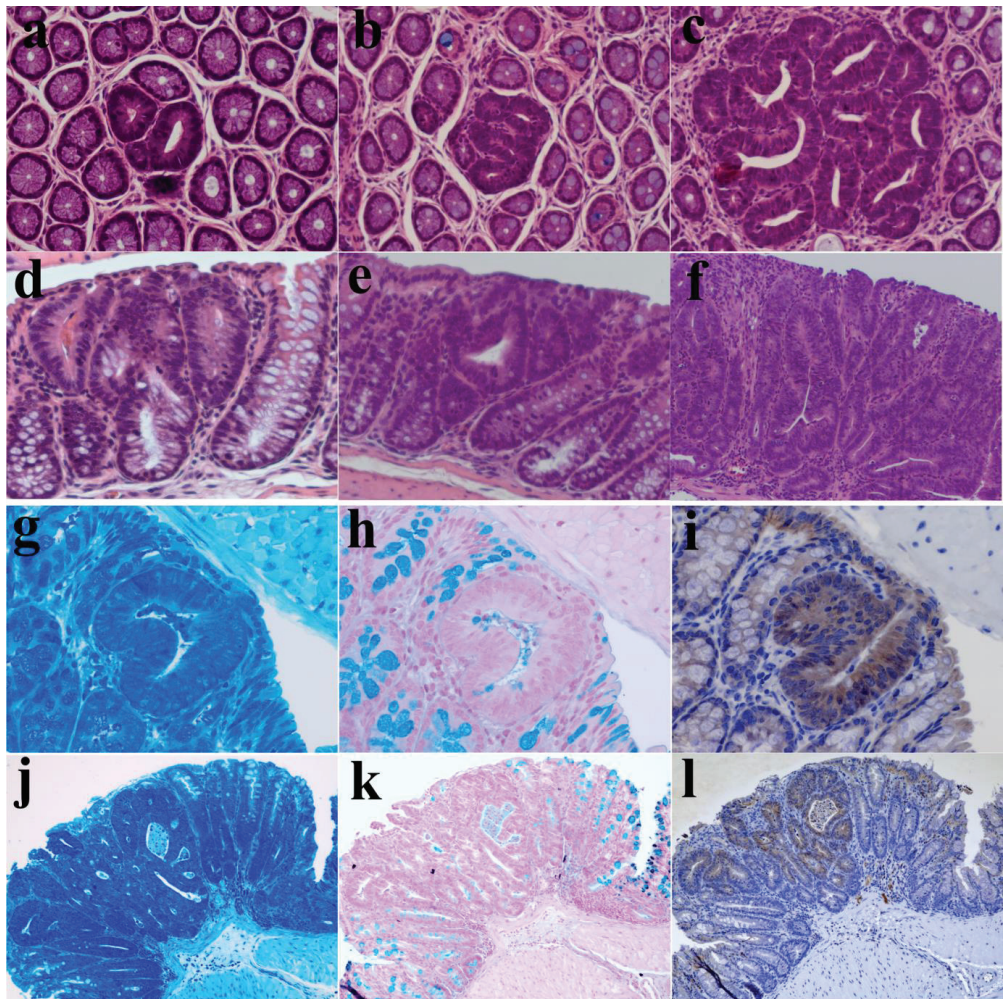


Figure 2. Representative examples of histological features of colonic lesions spontaneously formed in the A/J Min/+ mouse. (a – c) Cross-sections of HE-stained flat ACF of different sizes. Longitudinal sections of HE-stained Swiss rolls showing small flat ACF (d and e), and a tumor (f); note that both small and large lesions (a – e, f) display the same degree of dysplasia. Longitudinal sections of Swiss rolls stained with (g and j) methylene blue (MB), (h and k) high-iron diamine alcian blue (HID-AB) counterstained with nuclear fast red, and (i and l) β -catenin immunohistochemistry. (g – i) shows a 1-2 crypt flat ACF/MDF, while (j – l) shows a large flat ACF/MDF. HID-AB staining (h and k) clearly allowed for detection of the dysplastic lesions by indicating loss of goblet cells and mucus production, while MB staining (g and j) merely stained the dysplastic crypts a darker blue than normal crypts. β -catenin accumulation (i and l) was observed in sections coinciding with the MB and HID-AB lesions, indicating that both show Wnt signaling pathway activation. Magnifications (a – e), and (g – i): x400; Magnifications (f), and (j – l): x100

lesions always displayed the same degree of dysplasia (Figure 2d-f). Serial sections from Swiss rolls were stained with MB, HID-AB and β -catenin in order to define characteristic features of these lesions. While HID-AB staining clearly allowed for detection of the dysplastic status of the lesions by indicating loss of goblet cells and mucus production (Figure 2h and k), MB staining did not do anything other than stain the dysplastic crypts a darker blue than normal crypts (Figure 2g and j). Swiss roll immunohistochemistry showed β -catenin accumulation in sections coinciding with MB and HID-AB lesions, indicating Wnt signaling pathway activation in both lesions (Figure 2i and l).

Non-corresponding flat ACF and MDF. The one lesion identified as MDF, but not scored as flat ACF, was obviously overlooked since it displayed all characteristics of a flat ACF, in particular compressed pit pattern. The 7 lesions that were scored as flat ACF, but not identified as MDF (see Figure 1c), were attempted to be identified in cross sections without success.

Discussion

In the present work, we used the novel A/J Min/+ mouse model, which demonstrates extensive spontaneous initiation, promotion, and progression of colorectal cancer (14), to refine the method of detection of flat ACF, and to further characterize and define them as early lesions of colon carcinogenesis.

Although flat ACF have been recognized as suitable preneoplastic colonic lesions (19–21), few other groups have used them in experimental studies. This is apparently due to difficulties with technical or methodological aspects of flat ACF detection; consequently, the present work aimed at providing more detailed and refined methods of detection. Of particular importance were the time requirements during MB staining: the colons should not be stained more than 8–10 seconds; after which the colons must be stored in 10% formalin or 70% ethanol for at least 24 hours. After 24 hours, the flat

ACF had retained more methylene blue than the surrounding normal epithelium, which then allowed for a color distinction between dysplastic and healthy crypts (see Figure 1a). The reason for this is unknown, but Ochiai *et al.* (22) suggests that dysplastic tissue may be more resilient to decolorization after treatment with methanol than normal tissue. This may also potentially be true for decolorization in formalin or 70% ethanol, which is used in the method described here. Other than showing slightly darker coloring in dysplastic crypts, staining histological sections of flat ACF with MB did not provide any additional information to explain why a color difference is produced. Since other structures, such as lymphoid aggregates, may attain similar coloration as flat ACF, an additional feature for flat ACF detection was defined: to be considered a flat ACF, the lesions must contain compressed crypt openings with gyrus-like pit patterns. The majority of flat ACF did not protrude above the surrounding mucosa; however, a few lesions did appear slightly polypoid. By examining pit patterns, these polypoid flat ACF could be distinguished from classic ACF, a type of lesions which accounts for only 0.4% of the preneoplastic lesions in this model (14).

We found a high correspondence (93%) between flat ACF and MDF, and histological characterization of the lesions strongly suggested that these surface biomarkers indeed represent the same dysplastic lesions formed in APC-driven colon carcinogenesis. Hence, the A/J Min/+ mouse model resembles the Pirc rat (23). Of the non-corresponding lesions, one MDF was not scored as a flat ACF. However, this lesion was presumably a flat ACF since the MDF clearly showed all characteristics required for classification as a flat ACF. There were also seven lesions that were scored as flat ACF but not as MDF. Why these lesions were scored as flat ACF while failing to fulfill the criteria for MDF is uncertain. Although the A/J Min/+ mouse only has a very small fraction of classic ACF (14), one explanation may be that some of these non-coincidental lesions were in fact

classic ACF, which do not exhibit complete mucin depletion (4). Another potential explanation is that the flat ACF scored may have been a collection of smaller flat ACF in close proximity (rather than one large lesion), with healthy, mucin-producing crypts interspersed between these smaller flat ACF, masking mucin depletion in the adjacent lesions (see Figure 1c). It is also possible that non-coincidental lesions represent something that has yet to be described. Unfortunately, preparing histological cross-sections of this small fraction of lesions was unsuccessful.

In AOM treated B6 Min/+ mice, the correspondence between flat ACF and MDF has previously been determined to be only 57% (13), in contrast to 93% in the present study. The discrepancy between these two studies may be due to additional tumor causing mechanisms in AOM treated Min/+ mice that are not present in the spontaneous tumorigenesis of the A/J Min/+ mouse. In the AOM-treated B6 Min/+ mouse (13), some MDF were scored as classic ACF, while in the A/J Min/+ mouse, classic ACF are rarely observed (14). In the study by Femia et al (13), some of the lesions scored in the MB stained colon may have actually been polypoid flat ACF wrongly scored as classic ACF. As the present work clearly shows, flat ACF may appear polypoid (see figure 1b, middle). Here, when these polypoid flat ACF were restained with HID-AB, mucin depletion was unmistakable.

In conclusion, flat ACF can easily be detected by surface examination of MB-stained colons from the A/J Min/+ mouse, which demonstrates extensive spontaneous colon carcinogenesis. The virtually complete overlap between flat ACF and MDF, as well as their comparable histological characteristics, suggests that these structures indeed represent the same early, dysplastic colonic lesion. Consequently, flat ACF are reliable surface biomarkers of APC-driven colon carcinogenesis.

References

- 1 Bird RP: Observation and quantification of aberrant crypts in the murine colon treated with a colon carcinogen: preliminary findings. *Cancer Lett* 37: 147–51, 1987.
- 2 Paulsen JE, Løberg EM, Ølstørn HB, Knutsen H, Steffensen I and Alexander J: Flat Dysplastic Aberrant Crypt Foci Are Related to Tumorigenesis in the Colon of Azoxymethane-Treated Rat in the Colon of Azoxymethane-Treated Rat. *Cancer Res*: 121–129, 2005.
- 3 Paulsen JE, Namork E, Steffensen IL, Eide TJ and Alexander J: Identification and quantification of aberrant crypt foci in the colon of Min mice--a murine model of familial adenomatous polyposis. *Scand J Gastroenterol* 35: 534–539, 2000.
- 4 Caderni G, Femia A Pietro, Giannini A, Favuzza A, Luceri C, Salvadori M and Dolara P: Identification of Mucin-depleted Foci in the Unsectioned Colon of Azoxymethane-treated Rats: Correlation with Carcinogenesis. *Cancer Res* 63: 2388–2392, 2003.
- 5 Bird RP and Good CK: The significance of aberrant crypt foci in understanding the pathogenesis of colon cancer. *Toxicol Lett* 112-113: 395–402, 2000.
- 6 Femia A Pietro, Dolara P and Caderni G: Mucin-depleted foci (MDF) in the colon of rats treated with azoxymethane (AOM) are useful biomarkers for colon carcinogenesis. *Carcinogenesis* 25: 277–81, 2004.
- 7 Femia A Pietro, Bendinelli B, Giannini A, Salvadori M, Pinzani P, Dolara P and Caderni G: Mucin-depleted foci have beta-catenin gene mutations, altered expression of its protein, and are dose- and time-dependent in the colon of 1,2-dimethylhydrazine-treated rats. *Int J Cancer* 116: 9–15, 2005.
- 8 Femia A Pietro, Dolara P, Giannini A, Salvadori M, Biggeri A and Caderni G: Frequent mutation of Apc gene in rat colon tumors and mucin-depleted foci, preneoplastic lesions in experimental colon carcinogenesis. *Cancer Res* 67: 445–9, 2007.
- 9 Paulsen JE: Modulation by dietary factors in murine FAP models. *Toxicol Lett* 112-113: 403–409, 2000.
- 10 Kwong LN and Dove WF: APC and its modifiers in colon cancer. *Adv Exp Med Biol* 656: 85–106, 2009.
- 11 McCart AE, Vickaryous NK and Silver A: Apc mice: models, modifiers and mutants. *Pathol Res Pract* 204: 479–90, 2008.
- 12 Paulsen JE, Steffensen IL, Løberg EM, Husøy T, Namork E and Alexander J: Qualitative and quantitative relationship between dysplastic aberrant crypt foci and tumorigenesis in the Min/+ mouse colon. *Cancer Res* 61: 5010–5015, 2001.
- 13 Femia A Pietro, Paulsen JE, Dolara P, Alexander J and Caderni G: Correspondence between flat aberrant crypt foci and mucin-depleted foci in rodent colon carcinogenesis. *Anticancer Res* 28: 3771–5, 2008.
- 14 Sødning M, Gunnes G and Paulsen JE: Spontaneous initiation, promotion, and progression of colorectal cancer in the novel A/J Min/+ mouse. *Int J Cancer* 138: 1936–46, 2016.
- 15 Corpet DE: ACF, MDF, BCAC: Pre-Cancerous Lesions? Available from: <http://tumor.free.fr/ACF-BCAC-MDF.html> [last accessed February 23, 2016].
- 16 Usman A, AH N, Naseem N and Ullah E: Mucin Histochemistry in Tumours of Colon, Ovaries and Lung. *J Cytol Histol* 03: 3–6, 2012.
- 17 Caderni G, Giannini A, Lancioni L, Luceri C, Biggeri A and Dolara P: Characterisation of aberrant crypt foci in carcinogen-treated rats: association with intestinal carcinogenesis. *Br J*

- Cancer *71*: 763–9, 1995.
- 18 Moolenbeek C and Ruitenberg EJ: The “Swiss roll”: a simple technique for histological studies of the rodent intestine. *Lab Anim* *15*: 57–9, 1981.
- 19 Suzui M, Morioka T and Yoshimi N: Colon Preneoplastic Lesions in Animal Models. *J Toxicol Pathol* *26*: 335–341, 2013.
- 20 Rosenberg DW, Giardina C and Tanaka T: Mouse models for the study of colon carcinogenesis. *Carcinogenesis* *30*: 183–96, 2009.
- 21 Wargovich MJ, Brown VR and Morris J: Aberrant crypt foci: the case for inclusion as a biomarker for colon cancer. *Cancers (Basel)* *2*: 1705–16, 2010.
- 22 Ochiai M, Watanabe M, Nakanishi M, Taguchi A, Sugimura T and Nakagama H: Differential staining of dysplastic aberrant crypt foci in the colon facilitates prediction of carcinogenic potentials of chemicals in rats. *Cancer Lett* *220*: 67–74, 2005.
- 23 Femia A Pietro, Luceri C, Soares PV, Lodovici M and Caderni G: Multiple mucin depleted foci, high proliferation and low apoptotic response in the onset of colon carcinogenesis of the PIRC rat, mutated in *Apc*. *Int J Cancer* *136*: E488–95, 2015.



III

RESEARCH ARTICLE

Effects of Hemin and Nitrite on Intestinal Tumorigenesis in the A/J Min/+ Mouse Model

Marianne Sødning^{1*}, Marije Oostindjer², Bjørg Egeland², Jan Erik Paulsen¹

1 Norwegian University of Life Sciences, Department of Food Safety and Infection Biology, PO Box 8146 Dep., 0033, Oslo, Norway, **2** Norwegian University of Life Sciences, Department of Chemistry, Biotechnology and Food Science, PO Box 5003, 1432, Ås, Norway

* marianne.sodring@nmbu.no

Abstract

Red and processed meats are considered risk factors for colorectal cancer (CRC); however, the underlying mechanisms are still unclear. One cause for the potential link between CRC and meat is the heme iron in red meat. Two pathways by which heme and CRC promotion may be linked have been suggested: fat peroxidation and N-nitrosation. In the present work we have used the novel A/J Min/+ mouse model to test the effects of dietary hemin (a model of red meat), and hemin in combination with nitrite (a model of processed meat) on intestinal tumorigenesis. Mice were fed a low Ca²⁺ and vitamin D semi-synthetic diet with added hemin and/or nitrite for 8 weeks post weaning, before termination followed by excision and examination of the intestinal tract. Our results indicate that dietary hemin decreased the number of colonic lesions in the A/J Min/+ mouse. However, our results also showed that the opposite occurred in the small intestine, where dietary hemin appeared to stimulate tumor growth. Furthermore, we find that nitrite, which did not have an effect in the colon, appeared to have a suppressive effect on tumor growth in the small intestine.

Introduction

Colorectal cancer (CRC) is the third most common cancer worldwide, and accounts for a large number of deaths each year [1]. Although the cause of sporadic CRC is not clear, it appears that food and nutrition is closely related with both causation and prevention of this type of cancer [2]. Intake of red and processed meat has been linked to an increased risk of colorectal cancer; however, it is still unclear exactly how these are connected. The relationship between red meat and CRC is complex, and may depend on other variables besides the meat itself; heme iron or nitrite in meat, harmful intestinal microbiota, abnormally functioning digestive system, or an unbalanced diet composition [3,4]. Research suggests that heme iron in the meat may be the culprit, which may explain why the link between CRC and red meat is stronger than the link between CRC and intake of white meat, which is low in heme iron [5,6]. Two pathways by which heme and CRC promotion may be linked have been suggested: fat peroxidation which produces aldehydes capable of forming mutagenic adducts with DNA, and N-nitrosation which may result in the formation of N-nitroso-specific DNA adducts. The former pathway



OPEN ACCESS

Citation: Sødning M, Oostindjer M, Egeland B, Paulsen JE (2015) Effects of Hemin and Nitrite on Intestinal Tumorigenesis in the A/J Min/+ Mouse Model. PLoS ONE 10(4): e0122880. doi:10.1371/journal.pone.0122880

Academic Editor: François Blachier, National Institute of Agronomic Research, FRANCE

Received: November 18, 2014

Accepted: February 24, 2015

Published: April 2, 2015

Copyright: © 2015 Sødning et al. This is an open access article distributed under the terms of the [Creative Commons Attribution License](https://creativecommons.org/licenses/by/4.0/), which permits unrestricted use, distribution, and reproduction in any medium, provided the original author and source are credited.

Data Availability Statement: All relevant data are within the paper and its supporting information files.

Funding: The authors have no support or funding to report.

Competing Interests: The authors have declared that no competing interests exist.

may explain CRC promotion by fresh, red meat, while the latter may clarify CRC promotion by nitrite-cured (processed) meat [7]. Heme iron is believed to catalyze the endogenous formation of N-nitroso compounds (NOCs) in the colon, many of which are known carcinogens [6,8]. In processed meat, added nitrate and nitrite may also contribute to exogenous formation of NOCs within the meat. Furthermore, nitrite cured meat combines heme iron and nitrite in the digestive tract producing more endogenous NOCs than fresh meat, which may account for the hypothesis that processed meat is more closely related to CRC promotion than fresh meat [2,9].

Development of colorectal cancer is a multistep process involving tumor initiation, promotion, and progression. In humans, most colorectal cancers progress very slowly; it may take 5–20 years from early colonic lesions to develop into benign adenomatous polyps, and another 5–15 years for those adenomas to develop into a malignant carcinoma [10,11]. Most cases of colorectal cancer appear to be caused by somatic mutations, but a small number of cases are the result of germ-line mutations in the tumor-suppressor gene adenomatous polyposis coli (APC) which causes an inherited condition called familial adenomatous polyposis (FAP) [12,13]. FAP is characterized by the development of multiple adenomas in the colon, and occurs when an individual that has inherited one mutated *APC* allele experiences loss of heterozygosity. Inactivation of the second *APC* allele causes decreased degradation of β -catenin and activation of the canonical Wnt signaling pathway, which in turn leads to dysplasia [14–16]. In individuals who do not have FAP, approximately 80% of sporadic colon cancer cases still appear to be related to mutations in the *APC* gene where one allele mutates first, followed by mutation in, or loss of, the second allele [17].

The APC multiple intestinal neoplasia (Min/+) mouse (*Mus musculus*) is one of the most widely used murine models for human FAP. The Min mouse has a heterozygous truncation mutation at codon 850 of the tumor suppressor gene *APC*. This mutation is analogous to the mutation seen in the human *APC* gene, and results in the spontaneous formation of several neoplastic lesions in the mouse intestines [16,18–20]. FAP patients usually develop hundreds to thousands of adenomas in the colon and rectum, while the conventional Min/+ mouse, bred on a C57BL/6J genetic background, mainly develops adenomas in the small intestine and only a few in the colon [13,21]. A new Min/+ mouse strain, established at the Norwegian Institute of Public Health, develops a much higher number colonic lesions as compared to the C57BL/6J Min/+ mouse, and may therefore be more suited as a model for human CRC [22]. These early colonic lesions are known as flat aberrant crypt foci (flat ACF), and are visible as enlarged crypts with compressed pit patterns, which are not elevated from the mucosa, and are only visible with methylene-blue staining and transillumination. The flat ACF exhibits a continuous development from the monocryptal stage to adenoma. The adenoma, a benign lesion that may develop into a malignant adenocarcinoma, resembles the flat ACF, but contains a larger number of aberrant crypts, and is usually elevated from the mucosa [23].

The objective of the present study was to investigate the potential involvement of dietary heme and dietary nitrite on the development of colorectal cancer in the A/J Min/+ mouse model.

Materials and Methods

Ethics Statement

Experiments were conducted in accordance with The Norwegian Regulation of Animal Experimentation, and approved by the Norwegian Animal Research Authority (application ID: 5556). All animals were sacrificed by cervical dislocation.

Animals

The A/J Min/+ mouse was produced at the Norwegian Institute of Public Health after backcrossing the Min/+ trait onto an A/J genetic background for more than 12 generations to secure their status as inbred [22]. This mouse was transferred to the Norwegian University of Life Sciences, Campus Adamstuen, where it has been maintained for several generations. The mice are maintained as an inbred colony, with brother-sister breeding as the chosen breeding-pair configuration when possible. New A/J blood is regularly added to the colony by backcrossing A/J +/+ females purchased from Jackson Laboratory (The Jackson Laboratory, Bar Harbor, ME) with resident A/J Min/+ mice in order to uphold the A/J Min/+ mouse line. All animals involved in the present study were bred at the experimental animal facilities at the Norwegian University of Life Sciences, Campus Adamstuen.

A/J Min/+ males were mated with A/J +/+ females, and the resulting Min/+ pups from each litter were used for the experiment. In total, 80 Min/+ offspring were used (1:1 ratio of males to females). All animals, both parents and offspring, were housed in Makrolon Type III open top plastic cages in a room with a 12-hour light/dark cycle, 55–65% humidity and 20–22°C. Water and feed were given *ad libitum*. Once born, the litter remained in the parental cage until weaned at 19–21 days, after which the pups were separated from the parental cage. Only mice with the APC mutation were used for the experiments, and to correctly determine the genotype of each mouse, ear tissue was collected at time of weaning. The ear tissue was subsequently processed to extract DNA for polymerase chain reaction. Allele-specific PCR was used to genotype the mice using three primers; MAPC MT (5'-TGAGAAAGACAGAAGTA-3'), MAPC 15 (5'-TTCCAATTTGGCATAAGGC-3'), and MAPC 9 (5'-GCCATCCCTT-CACGTTAG-3'). The PCR product from a Min allele is 327bp long, while the PCR product from a wild-type allele (+) is 618bp long [24].

Diets and experimental study design

Four experimental diets were designed: Hemin (model of red meat), Hemin+Nitrite (model of processed meat), Nitrite, and Control. The amount of hemin added to the diet was chosen based on demonstrated effectiveness in previous studies [25–28]. The Hemin+Nitrite and the Nitrite diet contained 2.8μmol/g of sodium nitrite (NaNO₂). To balance the iron and sodium contents of the diets, each diet received the appropriate amount of iron (FeCl₃) and/or sodium (NaCl): 0.5μmol/g and 2.8μmol/g respectively. Each experimental diet was on a semi-synthetic AIN-93M basis, with reduced calcium (15μmol/g) and no added vitamin D (0IU/g) (SDS special diet services, Witham, UK). To achieve low vitamin D, the milk protein casein, usually present in the AIN-93M diet, was exchanged for Hamlet soy protein for all four diets. The semi-synthetic AIN-93M diet base contained 4% fat and 73% carbohydrates. Both the Hemin and the Hemin+Nitrite diets contained 0.5μmol/g hemin, a ferric form of heme iron with a chloride ligand. Once genotyped, the A/J min/+ mice were randomly assigned to four experimental groups to test effects of the four diets on intestinal tumorigenesis: Hemin (n = 21, 11 females and 10 males), Hemin+Nitrite (n = 20, 10 females and 10 males), Nitrite (n = 20, 10 females and 10 males), and Control (n = 19, 10 females and 9 males). The animals were fed the experimental diets for eight weeks, from weaning at 3 weeks until 11 weeks, when the experiment was terminated.

AIN-93M versus RM1

To demonstrate the dynamics of the novel A/J Min/+ mouse model, a parallel group of 15 A/J Min/+ mice fed the standard rodent diet, RM1, was included in the study. RM1 is a natural ingredient diet containing wheat, wheatfeed, barley, whey powder, soya oil, soya protein

concentrate, and de-hulled extracted toasted soya. In contrast, the semi-synthetic AIN-93M diet used in this study contained Hamlet soy protein, corn starch, cellulose, sucrose, and soya oil. Both diets are supplemented with vitamins and minerals. Proximal analyses of both diets, based on values provided by the manufacturer (SDS special diet services, Witham, UK), are presented in [S1 Table](#). Lesion development in 11 week ($n = 9$) and 25 week ($n = 6$) old RM1-fed A/J Min/+ mice was then compared to 11 week old mice fed the AIN-93M Control diet ($n = 19$).

Scoring of small intestinal and colonic lesions

Mice were terminated by cervical dislocation at 11 weeks before the small and large intestines were excised from anus to stomach, rinsed in, and flushed with, ice-cold phosphate buffered saline solution (PBS), before being slit open longitudinally. The small intestines were divided into three parts; proximal, middle, and distal, while the colon remained intact. Both small and large intestines were then fixed flat between PBS-soaked filter papers. The flat fixed intestines were stored in 10% neutral buffered formalin for no less than 24 hours. Once fixated, the intestines were stained for 10–15 seconds with 0.2% methylene blue dissolved in the same formalin solution. The intestines were rinsed in fresh formalin to remove excess methylene blue stain, and stored in 10% neutral buffered formalin for another 24 hours, prior to examination by transillumination in an inverse light microscope. All examinations were done by an observer blind to the treatment of each sample. Surface microscopy was used to detect tumors as well as the early colonic lesions, flat ACF. The latter can be recognized by the difference in color as compared to normal epithelia; flat ACF stain a brighter blue/green while normal crypts a more subdued brownish-green. Furthermore, the flat ACF has enlarged crypts, lays flat against the surrounding epithelium, and has compressed luminal opening which give the lesion a gyrus-like appearance. The tumor resembles the flat ACF, but contains 30 or more aberrant crypts, and is usually elevated from the mucosa ([S1 Fig](#)). To describe the distribution of flat ACF and tumors, the recorded lesions were grouped into lesion size classes. The smallest colonic lesions observed ranged in size from 0.002 to 0.008 mm², therefore this was chosen as the first size class. The remaining lesions were grouped into four additional size classes based on a suitable logarithmic scale with a base of 8: 0.009 to 0.064 mm², 0.065 to 0.512 mm², 0.513 to 4.096 mm², and lesions greater than 4.097 mm².

Statistics

All results are expressed as mean values with 95% confidence intervals. All comparisons were performed two-tailed with a significance level of 5%. To test for differences between effects of the four diets, a two-way Analysis of Variance (ANOVA), with gender as a covariate, was used. Some gender differences were noticed, but no interactions between diet and gender were found, so the effects seen in the different diet groups were never dependent on gender. Thus, gender was pooled for further analysis. To test for differences between Hemin+ and Hemin-, and Nitrite+ and Nitrite-, a two-way ANOVA, was performed. If significant results were obtained in the two-way ANOVAs, the Holm-Sidak pairwise multiple comparisons post hoc test was used.

Results

To determine the tumorigenic potential of the dietary interventions the following variables were scored: number of small intestinal and colonic tumors, number flat ACF in the colon, lesion size (mm²) and load (total area of the lesions).

Body weight

Mice were fed specialized diets for 8 weeks, from weaning at week 3 till termination at week 11. After 8 weeks on the diets, there was a significant difference in body weight for animals in the four diet groups. Significant differences were also detected between males and females within each diet, however, no interaction between gender and diet was observed (Table 1). The Holms-Sidak post hoc test showed that animals in the Hemin+Nitrite group had a significantly lower body weight at termination than animals in both the Nitrite and the Control diet groups. However, there was no significant difference in the body weight of animals in the Hemin + Nitrite group when compared to those in the Hemin group. The animals fed Hemin were also significantly lighter than the control animals, but no such difference was observed when these animals were compared to animals fed nitrite alone. There was no significant difference in body weight detected in animals in the Nitrite diet group as compared to control animals.

Colon

In the colon, two types of lesions were observed; flat ACF and tumors (Fig 1 and S1 Fig). The number of flat ACF observed in the colon of mice fed diets Hemin or Hemin+Nitrite was significantly lower than in mice fed Nitrite or Control. The size of flat ACF did not differ between mice fed the four different diets. Nevertheless, a tendency for slightly smaller flat ACFs was seen in both Hemin and Hemin+Nitrite fed animals, although not significant. The total area of flat ACF per mouse (flat ACF load) was significantly lower in mice fed Hemin or Hemin+Nitrite than in mice fed Nitrite or Control. When compared with flat ACF, the mice had few colonic tumors. Interestingly, the patterns of tumor number ($p = 0.090$), tumor size and tumor load ($p = 0.075$) observed in animals fed the four experimental diets were similar to those observed for flat ACF. However, the differences in tumor scores did not achieve statistical significance.

In previous studies, a continuous development from the monocryptal flat ACF to the stage of adenoma has been demonstrated; all lesions were characterized by severe dysplasia, altered control of β -catenin and rapid growth [29]. Hence, we present size distributions of pooled flat

Table 1. Average body weight of animals in a diet group, recorded after termination at 11 weeks.

Diet	Gender	N	Body weight
Control ^a	Female	10	20.8 [20.1–21.5]
	Male	9	25.2 [23.8–26.6]
	Total	19	22.9 [21.6–24.2]
Hemin ^{bc}	Female	11	19.6 [18.3–20.8]
	Male	10	22.0 [20.7–23.3]
	Total	21	20.7 [19.7–21.7]
Hemin+Nitrite ^c	Female	10	18.2 [17.2–19.2]
	Male	10	21.4 [20.4–22.4]
	Total	20	19.8 [18.8–20.8]
Nitrite ^{ab}	Female	10	20.3 [18.9–21.6]
	Male	10	23.4 [22.3–24.4]
	Total	20	21.8 [20.7–22.9]

All values are presented as mean [95% confidence interval]. Treatment means with a different superscript are significantly different at $p < 0.05$. Two-way ANOVA p-values: Diet $p < 0.001$; Gender $p < 0.001$; Diet X Gender $p = 0.410$.

doi:10.1371/journal.pone.0122880.t001

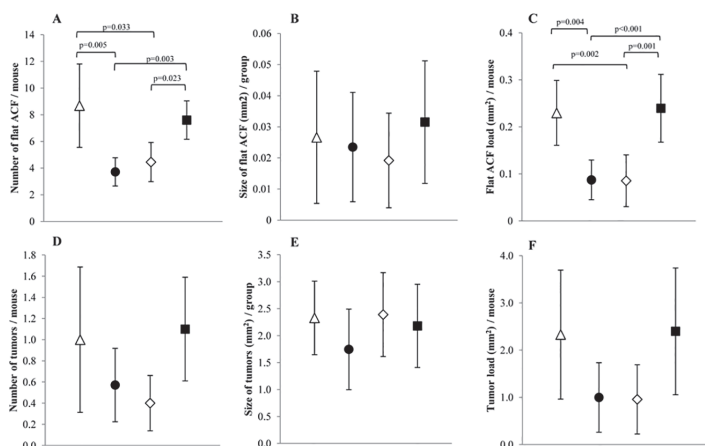


Fig 1. Colonic lesion development in A/J Min/+ mice fed four different diets; (△) Control; (●) Hemin; (○) Hemin+Nitrite; (■) Nitrite. A-C shows data for flat ACF, while D-F presents data for colonic tumors. A and D) Number of lesions, B and E) size of lesions, C and F) flat ACF load and tumor load, respectively. Values represent the mean, error bars show the 95% confidence interval. Horizontal bars indicate significant difference between the groups.

doi:10.1371/journal.pone.0122880.g001

ACF and tumors to illustrate the effects of the dietary interventions (Fig 2). As expected, Hemin, or Hemin+Nitrite caused a shift towards smaller lesion sizes and fewer lesions compared with Nitrite or Control (Fig 2A). This suppressive effect was apparently due to the presence of hemin in the diet, as illustrated by the size distributions (Fig 2B) of these lesions in mice fed Hemin⁺ (pooled Hemin and Hemin+Nitrite) compared with mice fed Hemin⁻ (pooled Nitrite and Control). The Two-Way ANOVA (Table 2) showed that hemin in the diet (Hemin⁺) caused a statistically significant reduction in the formation of flat ACF and tumors as well as in the growth of flat ACF. Typically, the load of flat ACF and tumors was reduced by approximately 60% ($p < 0.001$ and $p = 0.019$, respectively). When comparing mice fed Nitrite⁺ (pooled Nitrite and Hemin+Nitrite) to mice fed Nitrite⁻ (pooled Control and Hemin), no significant difference was observed (Table 2), indicating that nitrite in the diet did not have an effect in the colon of the A/J Min/+ mice.

Small intestine

The size of small intestinal tumors was reduced in animals in the Nitrite group compared with animals in the Hemin, Hemin+Nitrite, or Control groups (Fig 3). However, the number of tumors, or tumor load did not differ significantly among animals fed the four diets. The mean sizes (Fig 3B), as well as the size distributions of the small intestinal tumors from animals (Fig 4A) fed these diets suggest that dietary hemin might stimulate tumor growth in the small intestines. This is further illustrated by the size distribution of small intestinal tumors from animals fed Hemin⁺ and Hemin⁻ (Fig 4B) and their differences in calculated tumor size ($P < 0.001$; Table 2). Also a suggestive increase ($P = 0.084$) in tumor load (mm²/mouse) was observed in mice fed Hemin⁺ as compared with mice fed Hemin⁻ (Table 2). In contrast, the mean size of tumors in mice fed Nitrite⁺ significantly decreased when compared to mice fed Nitrite⁻, suggesting that dietary nitrite may cause a suppressive effect on tumor growth in the small intestine (Table 2).

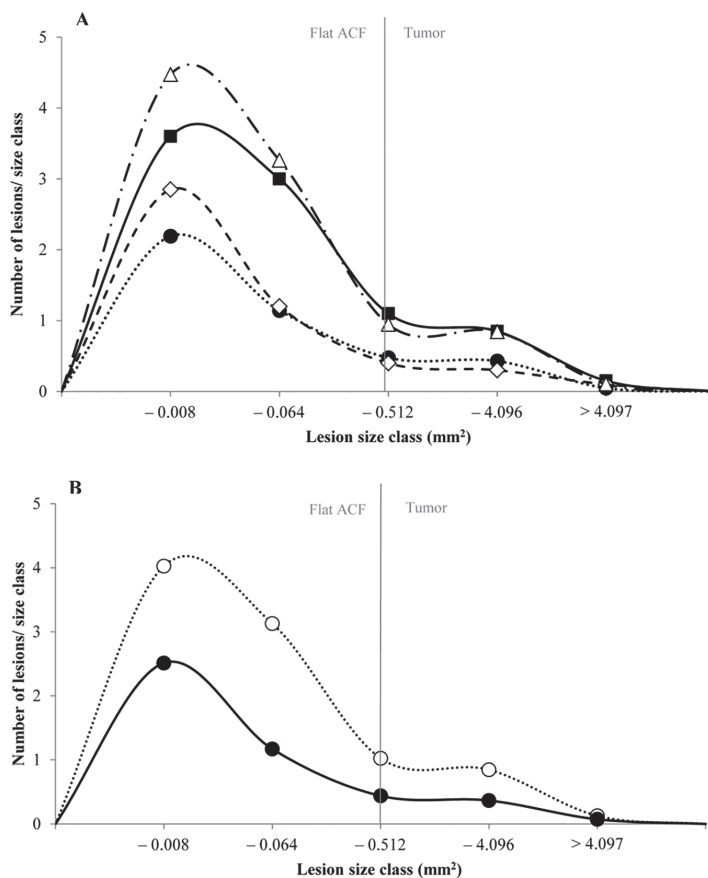


Fig 2. Size distribution of flat ACF and tumors in the colon of A/J Min/+ mice. A) mice fed four different diets, (△) Control; (●) Hemin; (○) Hemin+Nitrite; (□) Nitrite, and B) mice fed diets with or without hemin, (●) Hemin⁺; (○) Hemin⁻. The smallest size class contained lesions with 1–4 crypts. One crypt had an area of 0.002mm². In the colon, lesions are considered tumors if they contain more than 30 crypts/lesion (approximately 0.4mm²).

doi:10.1371/journal.pone.0122880.g002

Comparison of control diet and basic maintenance diet

The tumorigenesis induced by the Control (modified AIN-93) diet was compared with the tumorigenesis induced by the standard maintenance diet RM1 (Fig 5). In the colon, the RM1 diet yielded significantly more flat ACF ($p < 0.001$) and more tumors than the Control diet, demonstrating that dietary components actually may stimulate the A/J Min/+ mouse model used (positive control). Furthermore, the size distribution data showed that flat ACF increased their size from week 11 to week 25, indicating a progression from early lesion to tumor. In the small intestine, animals fed RM1 for 11 weeks had a larger amount of lesions than 11 week old AIN-93M-fed animals. However, the AIN-93M lesions were significantly larger than those seen in RM1 animals of the same age ($p < 0.001$). RM1-fed animals terminated at week 25 had a

Table 2. Number of lesions, lesions size, and lesion load in the colon and small intestine of A/J Min/+ mice fed a diet with or without hemin (Hemin⁺: Hemin and Hemin+Nitrite; Hemin⁻: Nitrite and Control), or a diet with or without nitrite (Nitrite⁺: Nitrite and Hemin+Nitrite; Nitrite⁻: Hemin and Control).

Colon		Number of lesions/mouse		Lesion size (mm ² /group)		Load (mm ² /mouse)	
		Flat ACF	Tumor	Flat ACF	Tumor	Flat ACF	Tumor
Hemin	Hemin ⁺	4.07 [3.18–4.97]	0.49 [0.27–0.71]	0.02 [0.01–0.03]	2.00 [1.47–2.54]	0.09 [0.05–0.12]	0.98 [0.46–1.49]
	Hemin ⁻	8.13 [6.45–9.81]	1.05 [0.64–1.46]	0.03 [0.01–0.04]	2.25 [1.74–2.76]	0.24 [0.19–0.28]	2.36 [1.42–3.31]
	P-value	<0.001	= 0.020	= 0.023	= 0.598	<0.001	= 0.019
Nitrite	Nitrite ⁺	6.03 [4.90–7.15]	0.75 [0.45–1.05]	0.03 [0.01–0.04]	2.24 [1.70–2.77]	0.16 [0.11–0.21]	1.68 [0.89–2.46]
	Nitrite ⁻	6.08 [4.33–7.82]	0.78 [0.40–1.15]	0.03 [0.01–0.04]	2.10 [1.60–2.60]	0.16 [0.11–0.20]	1.63 [0.86–2.40]
	P-value	= 0.418	= 0.881	= 0.831	= 0.559	= 0.930	= 0.942
Hemin X Nitrite	P-value	= 0.918	= 0.570	= 0.140	= 0.279	= 0.646	= 0.819
Small intestine							
Hemin	Hemin ⁺		22.05 [19.46–24.64]		0.63 [0.45–0.80]		13.80 [11.32–16.28]
	Hemin ⁻		20.43 [18.36–22.51]		0.50 [0.38–0.63]		10.31 [9.05–11.57]
	P-value		= 0.346		<0.001		ns (p = 0.084)
Nitrite	Nitrite ⁺		21.33 [18.98–23.67]		0.54 [0.40–0.67]		11.41 [9.58–13.24]
	Nitrite ⁻		21.20 [18.80–23.60]		0.60 [0.43–0.77]		12.79 [10.52–15.06]
	P-value		= 0.898		= 0.024		= 0.456
Hemin X Nitrite	P-value		= 0.208		= 0.055		= 0.999

Data is presented as mean [95% confidence interval]. Significant results are shown in bold text

doi:10.1371/journal.pone.0122880.t002

comparable number of lesions to those observed in the 11 week old mice, but the lesions in the 25 week old mice were significantly larger (p<0.001).

Discussion

In the present experiment, the A/J Min/+ mouse was used to test the effect of dietary hemin (a model of red meat), and hemin in combination with nitrite (a model of processed meat) on intestinal tumorigenesis. Surprisingly, we found that mice fed hemin, either in combination with nitrite or not, experienced a significant decrease in both number and load of the early colonic lesions; flat ACF. Hemin thus appeared to suppress growth of flat ACF in the colon of A/J Min/+ mice. The iron(III) chloride added to the Control and Nitrite diets to balance for the heme iron in the Hemin and Hemin+Nitrite diets could potentially account for the differences observed in mice fed diets with or without hemin, however, from the literature it seems that

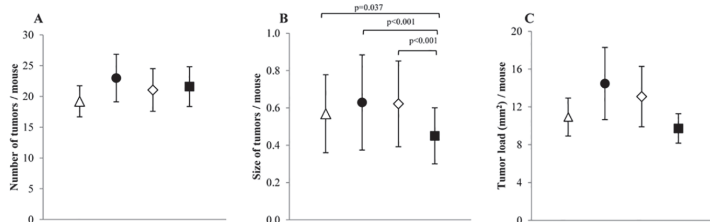


Fig 3. Small intestinal lesion development in A/J Min/+ mice fed four different diets; (△) Control; (●) Hemin; (◊) Hemin+Nitrite; (◻) Nitrite. A) number of tumors, B) tumor size, and C) tumor load in the small intestine. Values represent the mean, error bars show the 95% confidence interval. Horizontal bars indicate significant difference between the groups.

doi:10.1371/journal.pone.0122880.g003

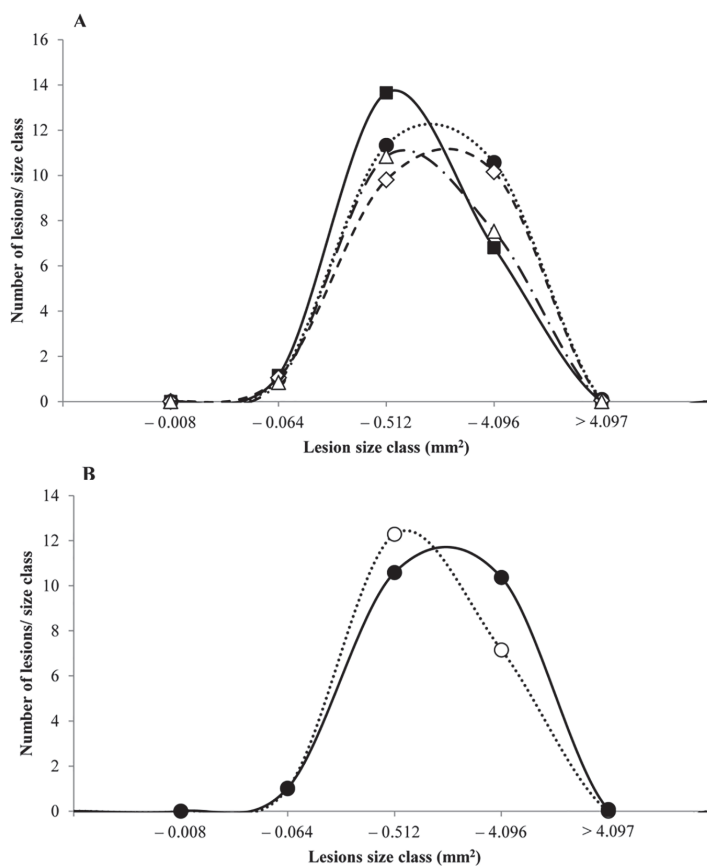


Fig 4. Size distribution of tumors in the small intestine of A/J Min/+ mice. A) mice fed four different diets, (△) Control; (●) Hemin; (○) Hemin+Nitrite; (□) Nitrite, and B) mice fed diets with or without hemin, (●) Hemin⁺; (○) Hemin⁻. The smallest size class contained lesions with 1–4 crypts.

doi:10.1371/journal.pone.0122880.g004

the free iron concentration added to the non-hemin diets was too low to explain these tumors [30–34]. The decrease in number and load of flat ACF in A/J Min/+ mice fed hemin was mirrored for colonic tumors as well, albeit not significantly. We also saw a tendency for hemin-fed animals to have smaller colonic lesions than animals not fed hemin. Winter *et al.* [35] found that mice fed 0.2 μmol/g hemin showed an increase in proliferation when fed hemin for 3 weeks. Furthermore, they saw that apoptosis was inhibited in animals fed hemin for 6 months, and also that long term hemin-feeding increased DNA adducts in the colon. However, they did not see any increase in colonic neoplasms. This is similar to what we found in the present study.

Why hemin-fed A/J Min/+ mice in this study did not show an increase in colonic lesions is uncertain. It has previously been shown that anti-inflammatory drugs decrease the number of tumors in C57BL/6J Min/+ mice [36,37]. Thus, it could be speculated that the effects observed in the present study may, in some way, be connected to inflammation. Zhong *et al.* [38] found that, in a DSS-induced murine model for colitis, hemin decreased colonic inflammation, as

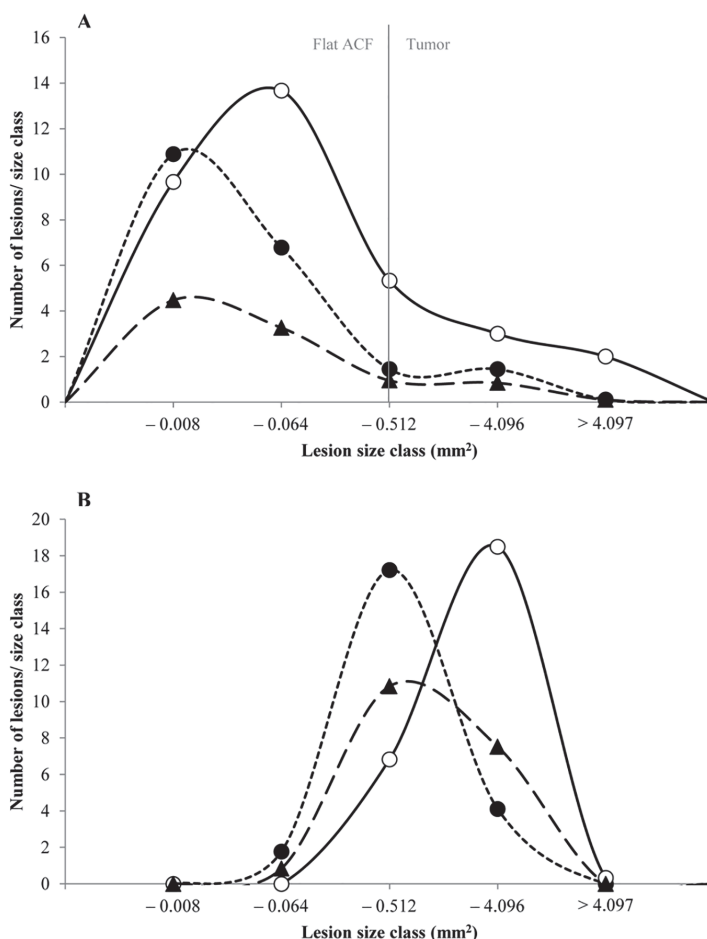


Fig 5. Size distribution of colonic and small intestinal lesions of A/J Min/+ mice fed two different rodent diets. A) flat ACF and tumors in the colon, and B) tumors in the small intestine of animals fed (◐) AIN-93M for 11 weeks, (●) RM1 for 11 weeks, or (○) RM1 for 25 weeks. The smallest size class contained lesions with 1–4 crypts. One crypt had an area of 0.002mm². In the colon, lesions are considered tumors if they contain more than 30 crypts/lesion (approximately 0.4mm²).

doi:10.1371/journal.pone.0122880.g005

well as reduced expression of the proinflammatory cytokine interleukin-17 (IL-17), which has been implicated in CRC [38–40]. The observed effect in the colon of hemin-fed A/J Min/+ mice in the present study may therefore be the result of a potential indirect anti-inflammatory effect of hemin.

In many animal studies investigating the effect of red and processed meat, fat is added to better resemble a westernized diet. One potential reason for the observed decrease in tumorigenic effect of dietary hemin in the colon of mice in this study is the low fat content in the diet. In the present study, no additional fat was added to the diet as our main objective was the potential effect of hemin; our special diets only contained the fat supplied in the base-diet

AIN-93M which is 4% soy oil [41]. Intake of polyunsaturated fatty acids together with heme iron may lead to formation of peroxy radical species in the intestinal tract, and consequently colorectal cancer [42]. Heme catalyzes the formation of reactive oxygen species (ROS), which leads to elevated levels of lipid peroxidation end-products such as malondialdehyde (MDA) and 4-hydroxynonenal (4-HNE), both of which are known risk factors for various diseases, including chronic inflammation and various cancers [7,43–45].

Jyssennagger *et al.* [25] found that heme has two separate effects on colonic epithelium; an acute reactive oxygen species stress and a delayed cytotoxicity stress. The delayed effects of heme caused cytotoxicity, hyperproliferation, and hyperplasia in the colon. Acute ROS stress induced the formation of lipid peroxidation products, and was evident shortly after heme intake, but no indication that ROS stress directly causes colonic hyperproliferation was found. However, intake of heme may lead to the formation of a cytotoxic heme factor (CHF), a compound thought to be formed when reactive lipid peroxides covalently bind to the protoporphyrin ring of the heme [46]. Cytotoxic heme factor formation is highly dependent on the presence of lipid peroxides, and, when enough accumulates in the colon, the cytotoxicity of the luminal contents increases, which in turn damages the colonic mucosa, and leads to hyperproliferation and hyperplasia [25]. In the present study, we observed a decrease in colonic lesions in animals fed hemin, and although this differs from other studies, it may possibly be because we did not add extra fat to the diet to bring about heme-induced ROS, and consequently formation and accumulation of cytotoxic heme factor.

Most studies investigating the effect of dietary heme add an additional amount of fat to the experimental diet, often 40% fat, to simulate the amount of a typical westernized diet, and these studies observe an increased risk of CRC [25–27,47–49]. However, there are a few studies in which less than 40% fat has been added to the experimental diet, and these studies show a somewhat similar tendency to what is seen in the present study. For example, neither Pence *et al.* [50] nor Lai *et al.* [51] observed an increase in colonic tumors in carcinogen-treated rats fed beef with a fat content of 5% and 6.35%, respectively. Pierre *et al.* [28] found that rats fed diets with 0.5 $\mu\text{mol/g}$ hemin, in combination with 5% safflower oil, did not differ significantly from the control animals in the number of lesions recorded. The aforementioned, in combination with the results from the present study, may suggest that heme iron, which has been shown to be a CRC risk factor, may in fact require other dietary factors such as dietary fat, to be present, to cause cancer.

In contrast to results observed in the colon of the A/J Min/+ mice, lesions in the small intestine of animals fed hemin (Hemin⁺: Hemin and Hemin+Nitrite), were on average larger than lesions observed in animals not fed hemin (Hemin⁻: Nitrite and Control), which correlates with previous research with rodent models showing an increased risk of CRC with intake of dietary heme [26,48,52], however most of these studies are mainly conducted in the colon. In addition, we found that mice fed diets containing nitrite experienced a decrease in the size of small intestinal lesions, indicating a potential protective effect of nitrite on small intestinal tumor promotion. It is unclear why nitrite seemed to have a protective effect in the small intestine of A/J Min/+ mice, but it may be due to nitric oxide (NO) derived from dietary nitrite in the feed. NO is a signaling molecule that can regulate a variety of biological processes, and it has been suggested that dietary nitrite may have an anti-inflammatory effect [53,54]. NO may also possibly increase the amount of small intestinal mucus, which could likely explain the protective effect observed; the mucous layer in the intestine plays many important roles, including being the first line of defense against detrimental factors from the outside environment, such as those from foods [55,56]. Van Hecke *et al.* [57] found that nitrite-cured pork meat inhibited both lipid and protein oxidation in *in vitro* digestion studies; however, at higher fat contents (20%), this inhibitory effect was less evident [57]. Also, Chenni *et al.* [9] found that nitrite

given via drinking water reduced heme-induced lipid peroxidation in the colon of rats; however, this effect was not observed to be significant at lower doses.

During this study, a parallel group of A/J Min/+ mice were fed the standard rodent diet, RM1. These mice were included purely as a positive control to be compared to the control animals fed the AIN-93M special diet, and thus to demonstrate the effectiveness of the novel A/J Min/+ mouse model. The results indicate that animals fed RM1 had both larger and a higher number of colonic lesions than animals fed the AIN-93M control diet, which is consistent with previous results seen in C57BL/6J Min/+ mice, and likely attributed to compositional differences in these two diets, such as fiber, fat, and carbohydrate content [58].

After 8 weeks on the special diet, mice fed hemin or hemin in combination with nitrite had a significantly lower body weight at termination than those fed the control diet. Similar decrease in body weight has been observed previously in animals fed heme [26,35]. Even though we did not observe an increase in colonic lesions in animals fed hemin, the decreased body weight may indicate that there was a toxic effect of heme.

In conclusion, our results showed that dietary hemin decreased the number of colonic lesions in the A/J Min/+ mouse, an effect contrary to what was expected. However, the present study also revealed that dietary hemin had an opposite effect in the small intestine, where it appeared to stimulate tumor growth. Furthermore, our results showed that dietary nitrite had no effect in the colon of the A/J Min/+ mice, but a suppressive effect on CRC promotion in the small intestine.

Supporting Information

S1 Data. Number, load, and size of colonic and small intestinal lesions.

(XLSX)

S1 Fig. Colonic lesions of the A/J Min/+ mouse. Both A) flat ACF, and B) tumor, were observed at 10X magnification in an inverse light microscope.

(TIF)

S1 Table. Proximate analysis of AIN-93M Control diet and standard maintenance diet RM1.

(DOCX)

Author Contributions

Conceived and designed the experiments: MS MO BE JEP. Performed the experiments: MS. Analyzed the data: MS. Contributed reagents/materials/analysis tools: JEP. Wrote the paper: MS. Critically reviewed the manuscript: MO BE JEP.

References

1. Ferlay J, Soerjomataram I, Ervik M, Dikshit R, Eser S, Mathers C, et al. GLOBOCAN 2012 v1.0, Cancer Incidence and Mortality Worldwide: IARC CancerBase No. 11 [Internet]. 2013 [cited 21 Mar 2014]. Available: <http://globocan.iarc.fr>
2. World Cancer Research Fund, American Institute for Cancer Research. Food, Nutrition, Physical Activity, and the Prevention of Cancer: a Global Perspective. Washington DC; 2007.
3. Oostindjer M, Alexander J, Amdam GV, Andersen G, Bryan NS, Chen D, et al. The role of red and processed meat in colorectal cancer development: A review, based on findings from a workshop. Meat Sci. 2014; 97: 583–596. doi: [10.1016/j.meatsci.2014.02.011](https://doi.org/10.1016/j.meatsci.2014.02.011) PMID: [24769880](https://pubmed.ncbi.nlm.nih.gov/24769880/)
4. Demeyer D, Mertens B, De Smet S, Ulens M. Mechanisms linking Colorectal Cancer to the Consumption of (Processed) Red Meat: a review. Crit Rev Food Sci Nutr. 2014; In Press.

5. Santarelli RL, Pierre F, Corpet DE. Processed meat and colorectal cancer: a review of epidemiologic and experimental evidence. *Nutr Cancer*. 2008; 60: 131–44. doi: [10.1080/01635580701684872](https://doi.org/10.1080/01635580701684872) PMID: [18444144](https://pubmed.ncbi.nlm.nih.gov/18444144/)
6. Bastide NM, Pierre FHF, Corpet DE. Heme iron from meat and risk of colorectal cancer: a meta-analysis and a review of the mechanisms involved. *Cancer Prev Res*. 2011; 4: 177–84. doi: [10.1158/1940-6207.CAPR-10-0113](https://doi.org/10.1158/1940-6207.CAPR-10-0113) PMID: [21209396](https://pubmed.ncbi.nlm.nih.gov/21209396/)
7. Corpet DE. Red meat and colon cancer: should we become vegetarians, or can we make meat safer? *Meat Sci*. 2011; 89: 310–6. doi: [10.1016/j.meatsci.2011.04.009](https://doi.org/10.1016/j.meatsci.2011.04.009) PMID: [21558046](https://pubmed.ncbi.nlm.nih.gov/21558046/)
8. Cross AJ, Pollock JRA, Bingham SA. Haem, not protein or inorganic iron, is responsible for endogenous intestinal N-nitrosation arising from red meat. *Cancer Res*. 2003; 63: 2358–60. PMID: [12750250](https://pubmed.ncbi.nlm.nih.gov/12750250/)
9. Chenni FZ, Taché S, Naud N, Guéraud F, Hobbs DA, Kunhle GGC, et al. Heme-induced biomarkers associated with red meat promotion of colon cancer are not modulated by the intake of nitrite. *Nutr Cancer*. 2013; 65: 227–33. doi: [10.1080/01635581.2013.749291](https://doi.org/10.1080/01635581.2013.749291) PMID: [23441609](https://pubmed.ncbi.nlm.nih.gov/23441609/)
10. Ilyas M, Straub J, Tomlinson IPM, Bodmer WF. Genetic pathways in colorectal and other cancers. *Eur J Cancer*. 1999; 35: 335–351. PMID: [10448282](https://pubmed.ncbi.nlm.nih.gov/10448282/)
11. Kelloff GJ, Schilsky RL, Alberts DS, Day RW, Guyton KZ, Pearce HL, et al. Colorectal adenomas: a prototype for the use of surrogate end points in the development of cancer prevention drugs. *Clin Cancer Res*. 2004; 10: 3908–18. PMID: [15173100](https://pubmed.ncbi.nlm.nih.gov/15173100/)
12. Fodde R. The APC gene in colorectal cancer. *Eur J Cancer*. 2002; 38: 867–871. PMID: [11978510](https://pubmed.ncbi.nlm.nih.gov/11978510/)
13. Half E, Bercovich D, Rozen P. Familial adenomatous polyposis. *Orphanet J Rare Dis*. 2009; 4: 22. doi: [10.1186/1750-1172-4-22](https://doi.org/10.1186/1750-1172-4-22) PMID: [19822006](https://pubmed.ncbi.nlm.nih.gov/19822006/)
14. Fodde R, Smits R, Clevers H. APC, signal transduction and genetic instability in colorectal cancer. *Nat Rev Cancer*. Nature Publishing Group; 2001; 1: 55–67. PMID: [11900252](https://pubmed.ncbi.nlm.nih.gov/11900252/)
15. Fodde R, Tomlinson I. Nuclear beta-catenin expression and Wnt signalling: in defence of the dogma. *J Pathol*. 2010; 221: 239–41. doi: [10.1002/path.2718](https://doi.org/10.1002/path.2718) PMID: [20527017](https://pubmed.ncbi.nlm.nih.gov/20527017/)
16. Paulsen JE. Modulation by dietary factors in murine FAP models. *Toxicol Lett*. 2000; 112–113: 403–409.
17. Fearnhead NS, Britton MP, Bodmer WF, Hospital JR, Ox O. The ABC of APC. *Hum Mol Genet*. 2001; 10.
18. Van Es JH, Giles RH, Clevers HC. The many faces of the tumor suppressor gene APC. *Exp Cell Res*. 2001; 264: 126–34. PMID: [11237529](https://pubmed.ncbi.nlm.nih.gov/11237529/)
19. Su LK, Kinzler KW, Vogelstein B, Preisinger AC, Moser AR, Luongo C, et al. Multiple intestinal neoplasia caused by a mutation in the murine homolog of the APC gene. *Science* (80-). 1992; 256: 668–670.
20. Fodde R, Smits R. Disease model: familial adenomatous polyposis. *Trends Mol Med*. 2001; 7: 369–373. PMID: [11516998](https://pubmed.ncbi.nlm.nih.gov/11516998/)
21. Taketo MM, Edelmann W. Mouse models of colon cancer. *Gastroenterology*. 2009; 136: 780–98. PMID: [19263594](https://pubmed.ncbi.nlm.nih.gov/19263594/)
22. Ølstørn HB. The effect of acrylamide and glycidamide on intestinal carcinogenesis in mice. University of Oslo. 2009.
23. Paulsen JE, Løberg EM, Ølstørn HB, Knutsen H, Steffensen I, Alexander J. Flat Dysplastic Aberrant Crypt Foci Are Related to Tumorigenesis in the Colon of Azoxymethane-Treated Rat in the Colon of Azoxymethane-Treated Rat. *Cancer Res*. 2005; 121–129.
24. Dietrich WF, Lander ES, Smith JS, Moser A R, Gould K a, Luongo C, et al. Genetic identification of Mom-1, a major modifier locus affecting Min-induced intestinal neoplasia in the mouse. *Cell*. 1993; 75: 631–9. PMID: [8242739](https://pubmed.ncbi.nlm.nih.gov/8242739/)
25. Ijssennagger N, Rijnierse A, de Wit NJW, Boekschoten M V, Dekker J, Schonewille A, et al. Dietary heme induces acute oxidative stress, but delayed cytotoxicity and compensatory hyperproliferation in mouse colon. *Carcinogenesis*. 2013; 34: 1628–35. doi: [10.1093/carcin/bgt084](https://doi.org/10.1093/carcin/bgt084) PMID: [23455377](https://pubmed.ncbi.nlm.nih.gov/23455377/)
26. Ijssennagger N, Rijnierse A, de Wit N, Jonker-Termont D, Dekker J, Müller M, et al. Dietary haem stimulates epithelial cell turnover by downregulating feedback inhibitors of proliferation in murine colon. *Gut*. 2012; 61: 1041–9. doi: [10.1136/gutjnl-2011-300239](https://doi.org/10.1136/gutjnl-2011-300239) PMID: [21948946](https://pubmed.ncbi.nlm.nih.gov/21948946/)
27. Ijssennagger N, Derrien M, van Doorn GM, Rijnierse A, van den Bogert B, Müller M, et al. Dietary heme alters microbiota and mucosa of mouse colon without functional changes in host-microbe cross-talk. *PLoS One*. 2012; 7: e49868. doi: [10.1371/journal.pone.0049868](https://doi.org/10.1371/journal.pone.0049868) PMID: [23239972](https://pubmed.ncbi.nlm.nih.gov/23239972/)
28. Pierre F, Taché S, Petit CR, Van der Meer R, Corpet DE. Meat and cancer: haemoglobin and haemin in a low-calcium diet promote colorectal carcinogenesis at the aberrant crypt stage in rats. *Carcinogenesis*. 2003; 24: 1683–90. PMID: [12896910](https://pubmed.ncbi.nlm.nih.gov/12896910/)

29. Paulsen JE, Steffensen IL, Løberg EM, Husøy T, Namork E, Alexander J. Qualitative and quantitative relationship between dysplastic aberrant crypt foci and tumorigenesis in the Min/+ mouse colon. *Cancer Res.* 2001; 61: 5010–5015. PMID: [11431334](#)
30. Xue X, Taylor M, Anderson E, Hao C, Qu A, Greenson JK, et al. Hypoxia-inducible factor-2 α activation promotes colorectal cancer progression by dysregulating iron homeostasis. *Cancer Res.* 2012; 72: 2285–93. doi: [10.1158/0008-5472.CAN-11-3836](#) PMID: [22419665](#)
31. Radulescu S, Brookes MJ, Salgueiro P, Ridgway RA, McGhee E, Anderson K, et al. Luminal iron levels govern intestinal tumorigenesis after Apc loss in vivo. *Cell Rep.* 2012; 2: 270–82. doi: [10.1016/j.celrep.2012.07.003](#) PMID: [22884366](#)
32. Rimbach G, Markant A, Most E, Pallauf J. Liver and colon oxidant status in growing rats fed increasing levels of dietary iron. *J Trace Elem Med Biol.* 1997; 11: 99–104. PMID: [9285890](#)
33. Chin J, Carpenter CE. Effects of dietary fat type and iron level on in vivo lipid peroxidation in rat colon. *Nutr Res.* 1997; 17: 1381–1389.
34. Stimson J, Fischer JG. Iron intake affects lipid peroxidation and glutathione peroxidase activity of distal colonic mucosa. *Nutr Res.* 1997; 17: 1683–1691.
35. Winter J, Young GP, Hu Y, Gratz SW, Conlon MA, Le Leu RK. Accumulation of promutagenic DNA adducts in the mouse distal colon after consumption of heme does not induce colonic neoplasms in the western diet model of spontaneous colorectal cancer. *Mol Nutr Food Res.* 2014; 58: 550–8. doi: [10.1002/mnfr.201300430](#) PMID: [24115497](#)
36. Jacoby RF, Marshall DJ, Newton MA, Novakovic K, Tutsch K, Cole CE, et al. Chemoprevention of Spontaneous Intestinal Adenomas in the Apc Min Mouse Model by the Nonsteroidal Anti-inflammatory Drug Piroxicam. *Cancer Res.* 1996; 56: 710–714. PMID: [8631000](#)
37. Barnes CJ, Lee M. Chemoprevention of spontaneous intestinal adenomas in the adenomatous polyposis coli Min mouse model with aspirin. *Gastroenterology.* 1998; 114: 873–877. PMID: [9558273](#)
38. Zhong W, Xia Z, Hinrichs D, Rosenbaum JT, Wegmann KW, Meyrowitz J, et al. Hemin exerts multiple protective mechanisms and attenuates dextran sulfate sodium-induced colitis. *J Pediatr Gastroenterol Nutr.* 2010; 50: 132–9. doi: [10.1097/MPG.0b013e3181c61591](#) PMID: [20081544](#)
39. Wu D, Wu P, Huang Q, Liu Y, Ye J, Huang J. Interleukin-17: a promoter in colorectal cancer progression. *Clin Dev Immunol.* 2013; 2013: 436307. doi: [10.1155/2013/436307](#) PMID: [24382972](#)
40. Chae W-J, Gibson TF, Zelterman D, Hao L, Henegariu O, Bothwell ALM. Ablation of IL-17A abrogates progression of spontaneous intestinal tumorigenesis. *Proc Natl Acad Sci U S A.* 2010; 107: 5540–4. doi: [10.1073/pnas.0912675107](#) PMID: [20212110](#)
41. Reeves PG. Components of the AIN-93 diets as improvements in the AIN-76A diet. *J Nutr.* 1997; 127: 838S–841S. PMID: [9164249](#)
42. Sawa T, Akaike T, Kida K, Fukushima Y, Takagi K, Maeda H. Lipid peroxyl radicals from oxidized oils and heme-iron: implication of a high-fat diet in colon carcinogenesis. *Cancer Epidemiol Biomarkers Prev.* 1998; 7: 1007–1012. PMID: [9829709](#)
43. Pierre F, Tache S, Guéraud F, Ferole AL, Jourdan M-L, Petit C. Apc mutation induces resistance of colonic cells to lipoperoxide-triggered apoptosis induced by faecal water from haem-fed rats. *Carcinogenesis.* 2007; 28: 321–7. PMID: [16885197](#)
44. Negre-Salvayre A, Coatrieux C, Ingueneau C, Salvayre R. Advanced lipid peroxidation end products in oxidative damage to proteins. Potential role in diseases and therapeutic prospects for the inhibitors. *Br J Pharmacol.* 2008; 153: 6–20. PMID: [17643134](#)
45. Kanner J. Dietary advanced lipid oxidation endproducts are risk factors to human health. *Mol Nutr Food Res.* 2007; 51: 1094–101. PMID: [17854006](#)
46. Sesink ALA, Termont DSML, Kleibeuker JH, Van der Meer R. Red Meat and Colon Cancer: The Cytotoxic and Hyperproliferative Effects of Dietary Heme. *Cancer Res.* 1999; 59: 5704–5709. PMID: [10582688](#)
47. Ijssennagger N, de Wit N, Müller M, van der Meer R. Dietary heme-mediated PPAR α activation does not affect the heme-induced epithelial hyperproliferation and hyperplasia in mouse colon. Veitia RA, editor. *PLoS One.* Public Library of Science; 2012; 7: e43260. doi: [10.1371/journal.pone.0043260](#) PMID: [22905243](#)
48. De Vogel J, Van-Eck WB, Sesink ALA, Jonker-Termont DSML, Kleibeuker J, van der Meer R. Dietary heme injures surface epithelium resulting in hyperproliferation, inhibition of apoptosis and crypt hyperplasia in rat colon. *Carcinogenesis.* 2008; 29: 398–403. doi: [10.1093/carcin/bgm278](#) PMID: [18174249](#)
49. Sesink AL, Termont DS, Kleibeuker JH, Van Der Meer R. Red meat and colon cancer: dietary haem, but not fat, has cytotoxic and hyperproliferative effects on rat colonic epithelium. *Carcinogenesis.* 2000; 21: 1909–15. PMID: [11023550](#)

50. Pence BC, Butler MJ, Dunn DM, Miller MF, Zhao C, Landers M. Non-promoting effects of lean beef in the rat colon carcinogenesis model. *Carcinogenesis*. 1995; 16: 1157–60. PMID: [7767979](#)
51. Lai C, Dunn DM, Miller MF, Pence BC. Non-promoting effects of iron from beef in the rat colon carcinogenesis model. *Cancer Lett*. 1997; 112: 87–91. PMID: [9029173](#)
52. De Vogel J, Jonker-Termont DSML, van Lieshout EMM, Katan MB, van der Meer R. Green vegetables, red meat and colon cancer: chlorophyll prevents the cytotoxic and hyperproliferative effects of haem in rat colon. *Carcinogenesis*. 2005; 26: 387–93. PMID: [15550456](#)
53. Ignarro LJ. Nitric oxide. A novel signal transduction mechanism for transcellular communication. *Hypertension*. 1990; 16: 477–83. PMID: [1977698](#)
54. Weitzberg E, Lundberg JO. Novel aspects of dietary nitrate and human health. *Annu Rev Nutr*. 2013; 33: 129–59. doi: [10.1146/annurev-nutr-071812-161159](#) PMID: [23642194](#)
55. Kim YS, Ho SB. Intestinal goblet cells and mucins in health and disease: recent insights and progress. *Curr Gastroenterol Rep*. 2010; 12: 319–30. doi: [10.1007/s11894-010-0131-2](#) PMID: [20703838](#)
56. Petersson J, Phillipson M, Jansson E a, Patzak A, Lundberg JO, Holm L. Dietary nitrate increases gastric mucosal blood flow and mucosal defense. *Am J Physiol Gastrointest Liver Physiol*. 2007; 292: G718–24. PMID: [17082222](#)
57. Van Hecke T, Vossen E, Vanden Bussche J, Raes K, Vanhaecke L, De Smet S. Fat content and nitrite-curing influence the formation of oxidation products and NOC-specific DNA adducts during in vitro digestion of meat. *PLoS One*. 2014; 9: e101122. doi: [10.1371/journal.pone.0101122](#) PMID: [24978825](#)
58. Svendsen C, Alexander J, Paulsen JE, Knutsen HK, Hjertholm H, Brantsæter AL, et al. The impact of commercial rodent diets on the induction of tumours and flat aberrant crypt foci in the intestine of multiple intestinal neoplasia mice. *Lab Anim*. 2012; 46: 207–14. doi: [10.1258/la.2012.011055](#) PMID: [22522416](#)